**MSc thesis in Geo-Engineering**

# Application of the Heat Flow Cone Penetration Test to measure the thermal conductivity of offshore soils

Leon Vrielink

November 2022

A thesis submitted to the Delft University of Technology in partial fulfillment of the requirements for the degree of Master of Science in Geo-Engineering.

Committee: Dr. Ir. P.J. Vardon (TU Delft)
Dr. A.D. Daniilidis (TU Delft)
Dr. Ir. M. Murali (Fugro)

# Abstract

Interpretation of the thermal properties of soils is an important challenge in the field of geo-engineering, for example for the development of geothermal energy solutions and for the design of electricity cable routes used for offshore wind farms. Of the thermal properties, the thermal conductivity is of most interest to find, as this determines the long-term thermal response of the soil. The soil volumetric heat capacity is of secondary interest, as this mainly influences the short-term thermal response. To find the thermal properties of offshore soils, a new in-situ test is being developed, called the heat flow cone penetration test (HF-CPT). The HF-CPT consists of a module that can be attached to a cone penetration test (CPT) which contains a heating element and temperature sensors. In this test, the penetration trough the soil is stopped at a required depth, the heating element is then activated, and the thermal response of the probe is measured. This thesis presents an interpretation method that can predict the thermal conductivity of soils based on the thermal response of the HF-CPT. The interpretation method is validated by conducting laboratory tests in four different materials: moist sand, saturated sand, kaolin clay and a water-agar mixture. The interpretation method consists of an inverse analysis on a finite element method forward numerical model. The forward model is shown to accurately simulate the thermal behaviour of the HF-CPT, when correct values of thermal conductivity and volumetric heat capacity are used. The interpretation method used a regularization of the inversion method to overcome a high sensitivity to the volumetric heat capacity. With the regularized inversion method, excellent agreement between single thermal needle probe results is found with the laboratory tests conducted in saturated sand, kaolin clay and the water-agar mixture. The inversion method is suitable for offshore testing, as the runtime of the method is short (less then 0.2 seconds per test) and the storage space is low (128 kB). The method gives an accurate prediction for testing duration of 300 seconds, which is fast when compared to other in-situ tests to measure the thermal conductivity of the soil. With this interpretation method, the HF-CPT can become a successful new in-situ test to determine the thermal conductivity of offshore soils. This way, the thesis contributes to the implementation of geothermal energy solutions and offshore cable routes for wind farms.

# Acknowledgements

For the past 9 months, from February until November 2022, I have been working on my thesis which I now present to you. In this period, I greatly enjoyed going to the office at Fugro in Nootdorp and performing laboratory tests at the university in Delft. I am extremely grateful for the input of the many people I met during my thesis at both Fugro and the university. Due to these people, I was able to keep my motivation and drive for my thesis high.

There are some people I would like to mention specifically, as they played a mayor role during my thesis project. First of all, I would like to thank my committee, Phil Vardon, Alex Daniilidis and Maddy Murali, for the great guidance throughout my thesis. It was a pleasure to work under your supervision. Secondly, my thanks go out to Joek Peuchen. Your sharp feedback during my thesis meetings helped me keep focus on the goal that I was trying to achieve. Thanks also go out to Vsevolod Kovalenko for being my personal mathematical consultant, and providing an important breakthrough during my thesis. High praise goes out to Nico Parasie and Stan Krohof. I enjoyed the many stand-up meetings we had as the "HF-CPT team" and look forward to continue the collaboration to further develop the test for offshore practice.

Finally, my thesis period would not have been as pleasant without the support from Maaike. Thank you for always being there for me, and never getting tired of me not being able to stop thinking about my thesis. Due to you, I was always able to stay positive during my thesis period.

# Contents

# List of Figures

# List of Tables

# Acronyms

# 1. Introduction

Interpretation of the thermal properties of soils is an important challenge in the field of geo-engineering. As the efforts towards finding sustainable energy solutions in the world increase, the interest in geothermal energy solutions has grown. For geothermal energy solutions like ground source heat systems, knowledge of the thermal conductivity and volumetric heat capacity of the soil is of major importance. Next to this, knowledge of the thermal properties plays a role in the development of offshore wind farms. The thermal properties of the soil give important information about the most efficient location and conductor diameter of the electricity cables of wind farms. This master thesis focuses on finding the thermal properties for offshore purposes, as this environment brings extra challenges that need to be considered.

Two soil properties are important in determining the heat flow trough the soil: volumetric heat capacity and thermal conductivity. For the development of offshore wind farms, the long-term thermal response determines the placement and conductor diameter of the power cables. For the two thermal properties, the volumetric heat capacity only influences the transient effects of the heat flow though the soil, while the thermal conductivity determines the steady state thermal response (Zhang & Wang, 2017). This makes the thermal conductivity the leading thermal property for the development of offshore wind farms. The focus of this thesis therefore lays on finding the thermal conductivity, with finding the volumetric heat capacity as an optional goal.

Multiple methods are used in practice for the measurement of thermal conductivity of soils. For example, laboratory tests like the thermal needle probe test and the hot disk test are commonly used (Maglic et al., 1992). However, a disadvantage of performing laboratory tests for offshore soils is the sample disturbance that occurs when transporting the sample, affecting the thermal properties found. Especially disturbance due to leakage of water is an issue, as the thermal conductivity greatly depends on the water content (de Vries & Usbeck, 2018). Another disadvantage to laboratory testing for offshore soils is that the acquirement and the transportation of soil samples to the laboratory is relatively expensive and time consuming (Akrouch et al., 2016).

The thermal conductivity can also be measured with in-situ tests. With in-situ tests, the problem with sample disturbance is no longer an issue. A wildly used in-situ test is the thermal response test, which uses a borehole and a thermal loop. A disadvantage of this test is relatively long testing duration of at least 50 hours. This is undesirable for offshore purposes, as offshore soil testing is expensive in comparison to land testing (de Vries & Usbeck, 2018). In-situ push in thermal needle probe tests are also available, for example one that can be used with a Cone Penetration Test (CPT) rig, replacing the CPT cone with a thermal needle probe. The disadvantage to these tests is that they are fragile, and only applicable in relatively soft soils close to the seabed. In harder soils, the needle easily breaks or gets lost in the soil (Fugro, 2021).

In order to overcome these challenges, a new type of in-situ test was proposed by Akrouch et al. (2016): the Thermal Cone Penetration Test (T-CPT). This test was then improved and validated in the field by Vardon et al. (2018). The T-CPT is a cone penetration test with a temperature sensor in the cone tip. Under normal circumstances, the cone in the CPT heats up due to the soil friction. If the cone penetrometer is stopped, the dissipation of heat generated on the cone tip is measured. In this way, the thermal conductivity in the soil is found. But, as Lines et al. (2017) mentioned in the early stages of the T-CPT development, when the cone penetrates soft soils, the heating of the cone is not always sufficient to perform a reliable thermal dissipation test. This makes the measurement of the thermal conductivity in certain soft soils impossible.

In order to overcome the issue of the cone penetrometer not heating up in soft soils, a new type of in-situ test, based on the T-CPT, is proposed. This new test is a detachable module for the CPT that includes a heating element and a temperature sensor. The name of this test is the Heat Flow Cone Penetration Test (HF-CPT). This test is currently in the design phase at Fugro. In this test, the CPT is stopped during penetration and then the heating element is activated. By measuring the temperature increase of the HF-CPT module, the thermal conductivity is found. For this master thesis, data of the HF-CPT is analysed to examine if the test can be used in practice to find the thermal conductivity of offshore soils. The research question that is answered during the thesis is:

*Which method is suitable for the interpretation of the thermal conductivity of offshore soils from heat flow cone penetration test data?*

The method must be relatively simple to conduct and give reliable results for a wide range of offshore soil types. As the test is designed to find the thermal conductivity in an offshore environment and offshore soil investigation is expensive, it is important that the test duration is kept to a minimum, while still gaining reliable results.

# 2. Literature Study

## 2.1. Thermal properties of soils

In this section, the properties that determine the thermal response of soils are explained. Two soil properties are important in describing the heat flow trough the soil: volumetric heat capacity and thermal conductivity.

Volumetric heat capacity is a property that indicates how much energy is needed to raise the temperature of a unit volume of soil by 1° Celsius (Farouki, 1986). The volumetric heat capacity relates to the specific heat capacity and density as follows (Farouki, 1986):

$$C = \rho \cdot c_p \tag{2.1}$$

where

$C$ is the volumetric heat capacity [J/(m$^3$K)]
$\rho$ is the density [kg/m$^3$]
$c_p$ is the specific heat capacity [J/(kgK)]

The second thermal property discussed in this chapter is the thermal conductivity. The thermal conductivity of a soil is the amount of heat passing trough a soil cross section under a temperature gradient (Farouki, 1986). Soil thermal conductivity is influenced by many different factors, including mineralogy, particle size and shape, water content, density and temperature. Water content has a relatively large influence on thermal conductivity compared to the other factors. (Zhang & Wang, 2017).

The volumetric heat capacity, $C$, and thermal conductivity, $k$, are respectively expressed by an arithmetic (Equation 2.2) and geometric mean (Equation 2.3) (Vardon & Peuchen, 2020).

$$C_{soil} = (1-n)\sum_i (f_{solid,i} \cdot C_{solid,i}) + n \cdot S \cdot C_{water} + n(1-S)C_{air} \tag{2.2}$$

$$k_{soil} = (\prod_i k_{solid,i}^{(1-n)k_{solid,i}}) k_{water}^{nS} \cdot k_{air}^{n(1-S)} \tag{2.3}$$

where

$n$ is the porosity [-]
$S$ is the saturation [-]
$f_{solid,i}$ is the fraction by volume of solid component i [-]

The thermal property values for relevant soil components are shown in Table 2.1. The effect of air on the volumetric heat capacity of the soil is negligible due to the low volumetric heat capacity value of air. For saturated soils (saturation close to one) the last part of Equation 2.3 tends to one and is also neglected (Vardon & Peuchen, 2020).

Table 2.1.: Thermal properties of soil components at 20 °C and atmospheric pressure (adapted from Vardon and Peuchen (2020)).

| Soil component | Thermal conductivity [W/(mK)] | Volumetric heat capacity [MJ/($m^3$K)] |
|---|---|---|
| Water (pure) | 0.6 | 4.140 |
| Air | 0.026 | 0.012 |
| Clay mineral | 2.9 | 2.120 |
| Sand (quartz) | 8.4 | 1.940 |

## 2.2. Heat flow equation

In this section, the equations that are used for determining the heat flow though a soil are described. The final equation described in this section, the one-dimensional axisymmetric heat conduction equation (Equation 2.10), forms the basis for both the both the thermal needle probe test and the T-CPT interpretation. Therefore, the derivation of this equation is of interest.

Heat flows trough a soil due to three different mechanisms: conduction, convection and radiation. The effect of radiation in soils is negligible (Carslaw & Jaeger, 1959). Convection in soil only plays an important role if there are groundwater flow conditions (Akrouch et al., 2016). This makes the conduction the only important mechanism in soils without groundwater flow conditions.

Fourier's law (Equation 2.4) is commonly used to calculate conductive heat flow.

$$q = -k \cdot \nabla T \tag{2.4}$$

where

$q$ is the vector of heat flow [W/m$^2$]
$k$ is the thermal conductivity [W/(mK)]
$\nabla T$ is the gradient of the temperature [K/m]

The heat balance of a soil element is described by the following equation (Carslaw & Jaeger, 1959):

$$C\frac{\delta T}{\delta t} + \nabla q = 0 \tag{2.5}$$

where

$C$ is the volumetric heat capacity [J/(m$^3$ K)]
$T$ is the temperature [K]
$t$ is the time [s]

When the properties of the soil are homogeneous and the thermal conductivity does not depend on the heat of the soil, Equation 2.4 and 2.5 are combined to form the general heat conduction equation (Carslaw & Jaeger, 1959):

$$\frac{1}{D}\frac{\delta T}{\delta t} = \nabla^2 T \tag{2.6}$$

with

$$D = \frac{k}{C} \tag{2.7}$$

where

$D$ is the thermal diffusivity [$m^2/s$]

Equation 2.6 is written in Cartesian coordinates as (Carslaw & Jaeger, 1959):

$$\frac{1}{D}\frac{\delta T}{\delta t} = \frac{\delta^2 T}{\delta x^2} + \frac{\delta^2 T}{\delta y^2} + \frac{\delta^2 T}{\delta z^2} \tag{2.8}$$

Equation 2.6 can also be written in cylindrical coordinates as (Carslaw & Jaeger, 1959):

$$\frac{1}{D}\frac{\delta T}{\delta t} = \frac{\delta^2 T}{\delta r^2} + \frac{1}{r}\frac{\delta T}{\delta r} + \frac{1}{r^2}\frac{\delta^2 T}{\delta \theta^2} + \frac{\delta^2 T}{\delta z^2} \tag{2.9}$$

If the heat flow is assumed to be constant in the $z$ and $\theta$ direction, Equation 2.9 can be written as an one-dimensional axisymmetric equation where the heat conduction is only dependent on r (Carslaw & Jaeger, 1959):

$$\frac{1}{D}\frac{\delta T}{\delta t} = \frac{\delta^2 T}{\delta r^2} + \frac{1}{r}\frac{\delta T}{\delta r} \tag{2.10}$$

## 2.3. Thermal cone penetration test

Is this section, a description of the T-CPT is given, which is an in-situ tool to find the thermal conductivity of the soil. A derivation of the interpretation method of the T-CPT is also given.

### 2.3.1. Description thermal cone penetration test

The T-CPT is an in-situ test to find the thermal conductivity proposed by Akrouch et al. (2016) and improved by Vardon et al. (2018). This test is an addition to the CPT, which finds the cone tip resistance, sleeve friction and, dependent on the cone type, pore-pressures of the soil. On the cone tip of the CPT, a temperature sensor is installed (Figure 2.1, right). When performing a CPT, heat is generated on the cone tip of the penetrometer. The penetration is stopped during testing and the dissipation of heat through the soil is measured. In this way, the thermal conductivity of the soil is found. (Vardon et al., 2019).

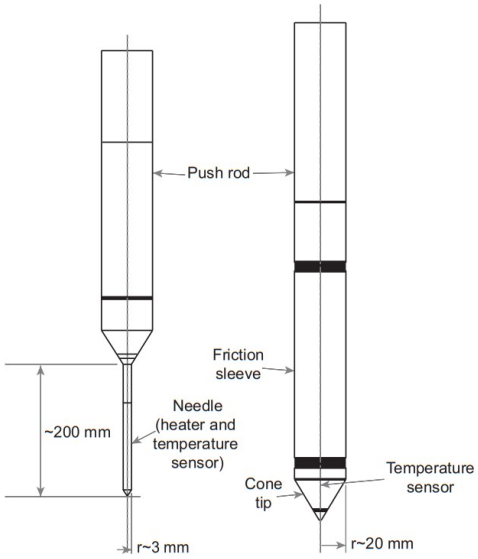


Figure 2.1.: Thermal needle probe (left) and temperature cone penetration test (right) (Vardon et al., 2019).

### 2.3.2. Calculation method thermal cone penetration test

To find the thermal conductivity due to the dissipation of heat, Vardon et al. (2018) consider three different solutions for Equation 2.10:

- Instantaneous heat release along a line inside an infinite medium.
- Instantaneous heat release along the surface of a cylinder inside an infinite medium.
- Perfectly conducting cylinder inside an infinite medium.

It is shown that all three solutions lead to the same outcome for large timescales (Vardon et al. (2019), Appendix A). The solution for instantaneous heat release along a line inside an infinite medium is described by the following equation (Carslaw & Jaeger, 1959):

$$T - T_0 = \frac{Q}{4\pi k t} \exp\left(-\frac{Cr^2}{4kt}\right) \tag{2.11}$$

where

$T_o$ is the initial temperature [K]
$Q$ is the heat release per unit of length [W/m]

For a large timescale (500 to 1000 seconds) and a small radius, the term inside the exponent tends to zero and the equation is rewritten to (Vardon et al., 2018):

$$k = f_{TC} \frac{Q}{4\pi t (T - T_0)} \tag{2.12}$$

where

$f_{TC}$ is a newly introduced calibration factor for the T-CPT cone [-]. This factor takes into account the type of penetrometer used and is found by conducting a numerical study.

The heat release per length is defined as (Vardon et al., 2018):

$$Q = (T_{max} - T_0) c_{p,steel} \cdot \rho_{steel} \cdot A_{cone} \tag{2.13}$$

where

$T_{max}$ is the maximum recorded temperature [K]
$c_{p,steel}$ is the specific heat capacity of steel [J/(m$^3$K)]
$\rho_{steel}$ is the density of steel [kg/m$^3$]
$A_{cone}$ is the cross sectional area of the CPT cone [m$^2$]

The initial temperature is found by waiting until the temperature in the cone is constant. This, however, takes a long time. As a long waiting time is undesirable for offshore soil investigation, Vardon et al. (2018) propose the following relation to estimate the initial temperature, which does not require waiting for the temperature in the cone to be constant:

$$T_0 = \frac{t_1 T_1 - t_2 T_2}{t_1 - t_2} \tag{2.14}$$

The thermal conductivity can also be found by a graphical method which is derived from the same equations. An example of the graphical method is shown in Vardon et al. (2018).

## 2.4. Thermal needle probe test

Is this section, a description of the thermal needle probe test is given. This test is both used in laboratories and in-situ to find the thermal conductivity of the soil. Similar to the HF-CPT, this test contains a heating element with temperaturte sensors. A derivation of the interpretation method of the thermal needle probe test is also given.

### 2.4.1. Description thermal needle probe test

The thermal needle probe test is a widely used laboratory test to find the thermal conductivity of the soil (ASTM, 2014). The thermal needle probe test is available as an in-situ test (Figure 2.1, left) and also as a laboratory test (Figure 2.2). This test consists of a thin needle probe which can be inserted into the soil. This needle probe consists of both a heating element and a temperature sensor. When the probe is inserted into the soil, the probe is heated and the temperature of the probe is recorded. With the temperature data of the probe, the thermal conductivity of the soil is found. After the heating, an additional cooling phase can be added to the test to improve the accuracy of the test. During this cooling phase, the temperature dissipation of the probe is measured.

Figure 2.2.: Laboratory thermal needle probe test sensor (METER Group, 2021).

### 2.4.2. Calculation method thermal needle probe test

Both the thermal needle probe and the HF-CPT interpret the thermal conductivity of soils by applying a transient heat source to the soil and monitoring the temperature change. Therefore, it is of interest to examine the way the thermal conductivity is found with a thermal needle probe test.

When using a thermal needle probe, the thermal conductivity is found from a solution for the one-dimensional axisymmetric heat conduction (Equation 2.10): the infinite line heat source. This solution assumes that there is an infinite line with a constant heat input at $r = 0$. As the length of the probe is significantly larger than the diameter of the probe, this solution is valid (Shiozawa & Campbell, 1990). The solution for an infinite line heat source is described by the following equation (Carslaw & Jaeger, 1959):

$$T - T_0 = -\frac{Q}{4\pi k} Ei(-\frac{Cr^2}{4kt}) \tag{2.15}$$

Where $Ei()$ is the exponential integral function, defined as (Carslaw & Jaeger, 1959):

$$-Ei(-x) = \int_x^\infty \frac{\exp(-u)}{u} du \tag{2.16}$$

When the term inside the exponential integral is small, as is the case for the small diameter of a thermal needle probe, $Ei$ is estimated with the following series (Carslaw & Jaeger, 1959):

$$-Ei(-x) = -\gamma + -\ln(x) + x - \frac{1}{4}x^2 + ... \tag{2.17}$$

Where:

$\gamma$ is the Euler's constant, which has a value of approximately 0.5772 [-]

For large values of t ($t > \frac{5Cr^2}{k}$), the x term in Equation 2.17 is small and the terms after $\ln(x)$ are neglected in this equation. Equation 2.15 is in this case rewritten to (Carslaw & Jaeger, 1959):

$$T - T_0 = \frac{Q}{4\pi k} \left( -\gamma - \ln(\frac{Cr^2}{4kt}) \right) \tag{2.18}$$

This is further rewritten to (Carslaw & Jaeger, 1959):

$$T - T_0 = \frac{Q}{4\pi k} \left( -\gamma - \ln(\frac{Cr^2}{4k}) + \ln(t) \right) \tag{2.19}$$

Note that $-\gamma$ and $\ln(\frac{Cr^2}{4k})$ are constants that are independent of time. When taking the gradient of $(T - T_0)$ against $\ln(t)$, these parts are zero and the thermal conductivity is found with the following equation (ASTM, 2014):

$$k = f_{NP} \frac{Q}{4\pi S} \tag{2.20}$$

Where:

$f_{NP}$ is an newly introduced calibration factor for the thermal needle probe [-]. Information on deriving this factor is shown in ASTM (2014).

$S$ is the gradient of the measured temperature against $\ln(t)$, occurring at a long timescale

## 2.5. Other analytical solutions

In addition to the infinite line heat source solution (Equation 2.15), there are other analytical solutions of Equation 2.10 that are relevant when examining a method to find the thermal conductivity with the HF-CPT. As the HF-CPT has a significantly larger radius in comparison with the thermal needle probe test, a solution that considers a cylindrical instead of a line heat source can be more representative. Two cylindrical solutions are described in this section.

### 2.5.1. Infinite hollow cylindrical heat source

The first analytical solution of Equation 2.10 discussed is the infinite hollow cylindrical heat source. This solution assumes an infinite cylindrical heat source with a constant heat and a constant radius $r_c$. On the outside of the cylinder, a soil with constant thermal properties is present. On the inside of the cylinder no material is present, hence the name hollow. The infinite hollow cylindrical heat source solution is described by the following equation (Carslaw & Jaeger, 1959):

$$T - T_0 = \frac{Q}{\pi^2 k r_c} \left( \int_0^\infty \left[ -\exp(-\frac{u^2 tk}{C}) - 1 \right] \frac{J_o(ur)Y_1(ur_c) - Y_0(ur)J_1(ur_c)}{u^2 \left[ J_1^2(ur_c) + Y_1^2(ur_c) \right]} du \right) ; (r \geq r_c) \tag{2.21}$$

Where:

| | |
|---|---|
| $J_0()$ & $J_1()$ | are the Bessel functions of the first kind of order zero and one, respectively |
| $Y_0()$ & $Y_1()$ | are the Bessel functions of the second kind of order zero and one, respectively |
| $r_c$ | is the radius of the cylindrical heat source [m] |

### 2.5.2. Infinite solid cylindrical heat source

The second cylindrical solution of Equation 2.10 discussed is the infinite solid cylindrical heat source. The same infinite cylindrical heat source as solution 2.21 is assumed, but now the inside of the cylinder is filled with the same soil as present on the outside of the cylinder. The infinite solid cylindrical heat source solution is described by the following equation (Man et al., 2010):

$$T - T_0 = -\frac{Q}{4\pi k} \int_0^\pi \frac{1}{\pi} Ei \left( -\frac{(r^2 + r_c^2 - 2rr_c \cos u)C}{4kt} \right) du \tag{2.22}$$

## 2.6. G-Functions

Another possible way of finding the thermal properties with the HF-CPT is by using a (semi-)numerical solution. A possible solution that is examined in this thesis is deriving a g-function from numerical simulations. in this section, multiple possible types of g-functions are described.

G-functions, also called thermal response functions, are functions that describe the relationship between the normalized temperature and other dimensionless parameters, such as the Fourier number. The normalized temperature is expressed as:

$$\theta = \frac{2\pi k}{Q} \Delta T \tag{2.23}$$

Where:

$\theta$ is the normalized temperature [-]

The Fourier number is expressed as:

$$Fo = \frac{kt}{Cr_c^2} \tag{2.24}$$

$Fo$ is the Fourier number [-]

The g-functions were originally designed by Eskilson (1987) for the design of borehole configurations. Man et al. (2010) and Loveridge and Powrie (2013) describe the following form of a g-function that is dependent on the Fourier number:

$$T - T_0 = \frac{Q}{2\pi k} G(Fo) \tag{2.25}$$

Where:

$G(Fo)$ is the g-function, which is dependent on the Fourier number [-]

All solutions of the one-dimensional axisymmetric heat conduction equation (Equation 2.10) mentioned in Section 2.4.2 and 2.5 can be expressed as g-functions in this form (Cimmino et al., 2013). In literature, another form of a g-function that is derived by curve fitting from numerical simulation is described (Bernier (2001), Man et al. (2010) & Loveridge and Powrie (2013)). These g-functions have the general form of:

$$\ln(G(Fo)) = a + b\ln(Fo) + c\ln^2(Fo) + d\ln^3(Fo) + e\ln^4(Fo) + f\ln^5(Fo) \tag{2.26}$$

Where:

$a$, $b$, $c$, $d$, $e$ & $f$ are factors that are found by curve fitting from numerical simulations [-]

The original g-Functions derived by Eskilson (1987), have a more complicated form. These g-functions are based on a different set of dimensionless parameters. Eskilsons g-functions are described as (Rees, 2016):

$$T - T_0 = \frac{Q}{2\pi k} G(t/t_s, r_b/H, B/H, D/H) \tag{2.27}$$

With:

$$t_s = \frac{H^2 C}{9k} \tag{2.28}$$

Where:

$G(...)$ is the g-function, which is dependent on various dimensionless parameters [-]
$t_s$ is the steady state time [s]
$r_b$ is the radius of the borehole [m]
$H$ is the height of the borehole [m]
$B$ is the borehole to borehole spacing ($\infty$ for a single borehole) [m]
$D$ is the length from the top of the borehole to the surface level [m]

The latter two dimensionless factors, $B/H$ & $D/H$, are not relevant for the HF-CPT. As there is only one heat source that needs to be accounted for, the term for the borehole spacing does not need to be used. It is assumed that the depth of the heat source is large enough that no significant boundary effects due to the surface level are occurring. Because of this, the term for the height of the borehole to the surface level is irrelevant for the HF-CPT.
The term $r_b/H$ describes the ratio between the length and radius of the heat source and is relevant to examine. This ratio has a relatively large value for the HF-CPT in comparison to a borehole or thermal needle probe test. However, note that this ratio is not a variable for the actual HF-CPT, as both the height and diameter are constants in the test.
The term $t/t_s$ is a similar term as the Fourier number. The main difference is that the Fourier number is dependent on the radius of the heat source, while $t/t_s$ is dependent on the height of the heat source. But, as both these values are constant for the actual HF-CPT, the time is the only variable in both parameters.

## 2.7. Other heat flow cone penetration tests and analysis methods

This section considers similar research on the development of a HF-CPT. In total, there are three different studies published that consider the usage of a heating element in a CPT to find the thermal conductivity. Next to this, a similar in-situ test, called push heat, is currently being developed by Fielax.

### 2.7.1. PSO Algorithm, Mo et al. (2021)

First of all, Mo et al. (2021) proposed to use a combination of a numerical model and a Particle Swarm Optimization (PSO) algorithm to find the thermal conductivity and the specific heat capacity for a T-CPT with a heating element. Both the heating and cooling data of the probe are considered to interpret the thermal conductivity and specific heat capacity of the soil. The numerical model is based on the one-dimensional asymmetric heat transfer equation (Equation 2.10). This means that the model only considers heat transfer in the radial direction. The numerical model is based on the assumption that the inside of the cylindrical heating element is filled with perfectly conductive steel and the outside consists of a uniform soil, with perfect thermal contact between the soil and the steel.

This numerical model is used to generate data for a PSO algorithm that is able to identify the thermal conductivity and specific heat capacity of the soil when thermal response data is put into the algorithm. When using data generated by a numerical model, the PSO algorithm finds the correct values for the thermal conductivity and the specific heat capacity. However, the model was not validated by field or laboratory test data.

### 2.7.2. Laboratory tests long heating element, Liu et al. (2022)

Liu et al. (2022) conducted a study with a T-CPT that contains a heating element of 100 cm. Because of the large length of the heater, a one-dimensional analysis of the heat flow trough the soil is considered. The equations for the T-CPT method proposed by Vardon et al. (2018) (Section 2.3.2) are used to find the thermal conductivity of the soil. The T-CPT was tested in a large size model tank filled with sand. The test started with a heating phase where the heating element is powered with 100W for 5 minutes. After this, a cooling phase of 20 minutes was performed. Only the data from the cooling phase was used for the prediction of the thermal conductivity. The thermal conductivity value that was found with the T-CPT was within a 10% error margin of thermal needle probe test results conducted in the same soil. In-situ land tests were also conducted with the T-CPT. These tests resulted a higher found thermal conductivity value when compared to thermal needle tests on undisturbed samples.

### 2.7.3. Discrete element method model, Mo et al. (2022)

Mo et al. (2022) conducted a study that combines physical testing with a HF-CPT and a simulation of this HF-CPT with a Discrete Element Method (DEM) model. For the physical model, the HF-CPT is pushed into a cubic cast filled with sand. No information on the power level used during the test and length of the heating element is supplied in the paper. Analysing the test results with the method proposed by Vardon et al. (2018) resulted in an average overestimation of the thermal conductivity value of 10% when compared to results of hot disk tests in the same sand. A DEM model is proposed able to simulate the stresses that occur in the soil during penetration and the thermal response of the soil when conduction a thermal response test. Then, using again the method of proposed by Vardon et al. (2018) a thermal conductivity value was found with a 4.5% overestimation when compared to the value used as input for the model.

### 2.7.4. Fielax push heat system, de Vries and Usbeck (2018)

The Fielax push heat system combines a heat-flow probe system and a mini-CPT. The heat flow probe system consists of a 1.4 cm diameter and 3 to 5 m long string with temperature sensors and heater elements attached to the outside of a steel coring tube. The probe and steel tube are pushed into the seabed by either a gravity type or vibrocorer type setup. The data obtained by the probe is interpreted with an inversion scheme based on the one-dimensional axisymmetric heat flow equation (Equation 2.10) (Hartmann & Villinger, 2002). A one-dimensional axisymmetric approximation is justified due to the relatively large length and small diameter of the probe. Instead of connecting the heat flow probe to a steel coring tube, developments have been made to implement the probe into a mini-CPT system, which has roughly the same diameter as the probe. The testing procedure is as follows: The mini-CPT is first penetrated to the seabed; When the desired depth is reached, the probe is stopped and the heat generated by the soil friction dissipates; The cooling of the probe due to soil friction is measured for approximately 20 minutes; After this, the probe is shortly heated with a heat pulse and the cooling of the probe is again measured for approximately 20 minutes. The total time taken by the heat flow measurement is approximately 40 minutes. Due to the length of the rod, which is stated to have a maximum length of 6 meters, measurements with the Fielax push heat system is limited to measuring the top 6 meters of the seabed.

### 2.7.5. Comparison heat flow cone penetration test methods

The methods described in this section have in common that they all assume a one-dimensional heat flow trough the soil. As the heating element of the HF-CPT considered in this thesis has a relative short length and large diameter, it is important to find out if this assumption is valid for this HF-CPT. The test procedure used for all studies is a combination of heating and cooling of the probe with Liu et al. (2022) describing a total test duration of 25 minutes and de Vries and Usbeck (2018) describing a total test duration of 40 minutes. The test duration of the HF-CPT test proposed in this thesis should be in this range or, preferably, be less than this range. An overview of the similar research considering the usage of a heating element in a CPT to find the thermal conductivity is shown in Table 2.2.

Table 2.2.: Overview of similar research considering the usage of a heating element in a cone penetration test to find the thermal conductivity.

| Source | Mo et al. (2021) | Liu et al. (2022) | Mo et al. (2022) | de Vries and Usbeck (2018) |
|---|---|---|---|---|
| Section | 2.7.1 | 2.7.2 | 2.7.3 | 2.7.4 |
| Heater length | Unknown | 1 m | Unknown | 6 m |
| Heating data used for interpretation | ✓ | ✗ | ✓ | ✓ |
| Cooling data used for interpretation | ✓ | ✓ | ✓ | ✓ |
| Finds thermal conductivity | ✓ | ✓ | ✓ | ✓ |
| Finds heat capacity | ✓ | ✗ | ✗ | ✓ |
| Practical tests performed | ✗ | ✓ | ✓ | ✓ |
| Total test duration | - | 25 minutes | 160 minutes | 40 minutes |

## 2.8. Conclusion

Heat mainly flows trough soils with conductive heat transfer. The process of conductive heat transfer is described by the general heat conduction equation (Equation 2.6). This equation can be written as a one-dimensional axisymmetric heat conduction equation (Equation 2.10). The solutions of this equation form the basis for various interpretation methods of tests to find the thermal conductivity, including the T-CPT (Section 2.3.2), thermal needle probe (Section 2.4.2) and other heat flow cone penetration tests (Section 2.7). Other than the analytical solutions used for the analysis of the tests mentioned, two possibly suitable solutions for the interpretation of the HF-CPT are described in Section 2.5. It is expected that these solutions more accurately represent the heat transfer of the HF-CPT, as a cylindrical heat source is assumed. All solutions mentioned assume one-dimensional heat transfer though the soil. It is important to examine if this assumption is valid for the HF-CPT, as the heating element of the probe has a relatively large diameter and short length. If this assumption is not valid, an interpretation method based on numerical solutions can be used for interpretation. One of the methods that can be suitable is the usage of g-functions derived from numerical simulations (Section 2.6).

# 3. Research Questions

The main research question of the thesis is:

*Which method is suitable for the interpretation of the thermal conductivity of offshore soils from heat flow cone penetration test data?*

In this chapter, the series of research questions that help solve the main research question are described.

## 3.1. Predicting the thermal response of the heat flow cone penetrometer with a forward model

To construct an interpretation method, a suitable forward model needs to be found. A forward model should be able to accurately predict the thermal response of the heat flow cone penetrometer with the thermal properties of the soil as an input. The first research question is:

*Which forward model is suitable for the interpretation of the heat flow cone penetration test data?*

This research question is answered by analysing the suitability of three different types of forward models. The results of the forward models are compared to laboratory tests performed with HF-CPT probes. The following three types of forward models are analysed:

- Numerical solution found with finite element modelling.
- Analytical solution of the asymmetric heat conduction equation (Equation 2.10).
- Semi-analytical solution of interpolating a g-function from numerical analysis.

## 3.2. Interpreting laboratory test data with an inversion method

When a suitable forward model is found, this model is used in an inverse analysis. An inversion method is constructed that can interpret the thermal properties of the soil using test data of the HF-CPT as input. The second research question is:

*Can the inversion method combined with the suitable forward model accurately predict the thermal properties of the materials used in laboratory tests with the heat flow cone penetration test?*

This research question is answered by proposing an inversion method that can interpret the thermal properties of the soil using test data of the HF-CPT. This model is validated by conducting laboratory tests with the heat flow cone penetrometer.

## 3.3. Addressing practical design considerations for offshore testing

If the numerical solution is validated, there are other considerations that need to be addressed before offshore tests with the HF-CPT can be performed. The third research question is:

*Which practical design conditions need to be addressed before the test procedure of an offshore heat flow cone penetration test can be determined?*

One of the design considerations that needs to be addressed is the effect of the heating of the probe on the inversion method due to the soil friction. It is examined if the testing procedure should be adapted if this occurs. Another consideration is the probing depth of the soil, with determines the amount of soil volume examined by the test. A longer test duration might be needed to reach a certain amount of probing depth. A final advice on the testing procedure, which must be reliable and performed in a short testing duration, is described.

Considering these three research questions, a comprehensive answer to the main research question is obtained.

# 4. Objectives and methods

## 4.1. Laboratory testing

In order to validate the interpretation method presented in this thesis, laboratory tests with the HF-CPT prototype were performed from July 15, 2022 to August 5, 2022 at the Delft University of Technology. This section explains the objective and methods of the experiments.

### 4.1.1. Objective

The objective of the tests was to validate the interpretation method developed to find the thermal conductivity and volumetric heat capacity of offshore soils with the HF-CPT. In these laboratory tests, a HF-CPT prototype was placed in a cast filled with a specific reference material. The probe was heated and the temperature change of the probe was recorded. To ensure that there was no undesired influence of the outside environment on the data recorded with the HF-CPT, the tests were performed in a climate-controlled room. The probe and the materials had the same temperature at the start of the test. In order to validate the interpretation method, it is beneficial to do tests on multiple reference materials with a wide range of thermal properties. The reference materials used were as uniform as possible. In order to determine if the interpretation method gave accurate predictions, the thermal properties of the reference materials were examined with separate laboratory tests. In this way, the results of the interpretation method were validated by checking if the thermal conductivity and heat capacity values were within the expected range found for the reference materials. The repeatability of the tests was also examined.

### 4.1.2. Methods

#### Test setup

An overview of the test setup is shown in Figure 4.1. The casts used for the test consisted of 35L volume buckets. The buckets were significantly large to ensure no boundary effects due to the cast size were of influence on the test results (Appendix A). In order to prevent the evaporation of water from the reference materials, plastic film was used to cover up the casts. The HF-CPT prototype probes used in the test do not contain CPT sensors to measure the soil stress, but instead use a dummy cone tip, thus they are further referred to as 'test probe' (Figure 4.2). The test probes contained four temperature sensors located in the middle of the heating element in the axial direction. An additional temperature sensor was present at the same height in the core of the test probe outside of the heating element. The temperature sensors inside the probes have an accuracy of 0.02 K. Test were performed with various power levels from 4.9 to 21.7 W (Table 5.3). All tests consisted of a heating phase of 1800 seconds (30 minutes) and a cooling phase of the same duration.

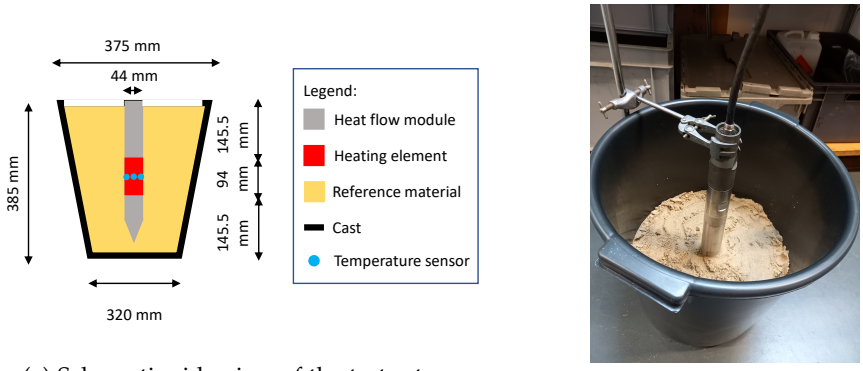


(a) Schematic side view of the test setup.

(b) Test setup.

Figure 4.1.: Overview of the test setup.

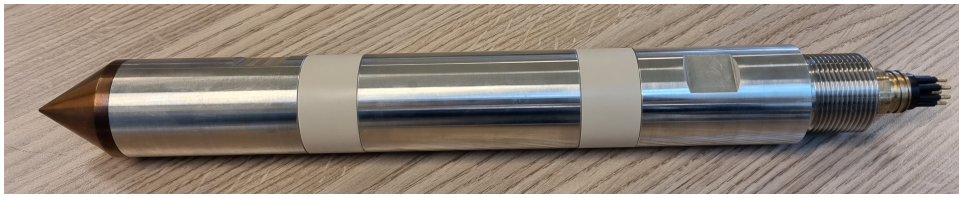

Figure 4.2.: Test probe used for the heat flow cone penetration laboratory tests.

The test probe was not pushed into the material during construction, as this would induce unwanted boundary effects due to soil disturbance, depending on the size of the cast. Instead, the reference materials were formed uniformly around the test probe. All cast were prepared and tested in a climate room, which had a constant temperature of 292.65 K and a relative humidity of 68%. Between building the cast and testing with the probe, a waiting period at least 24 hours was taken. This period was taken to ensure the material and test probe were at same constant temperature before testing. A detailed explanation of the building of the cast per reference material is described. The following four reference materials were used for the test:

- Moist sand
- Saturated sand
- Kaolin clay
- Water mixed with agar

**Moist sand**

The moist sand used for the test was not air or oven dried, causing for some small amount water to be still present in the soil, hence the name 'moist'. The average water content of the soil was approximately 5%. In order to ensure a uniform density throughout the test sample, the sample was built up in layers of approximately 5 cm in height. Each layer was densified using a proctor hammer. After the first layer of sand was placed in the cast, the test probe was installed in the middle of the cast, held in place by a laboratory probe stand (Figure 4.1b). The next soil layers were carefully installed around the probe, ensuring good thermal contact between the probe and the soil.

**Saturated sand**

For the saturated sand sample, the same sand type as for the moist sand tests was used. Similar to the moist sand tests, the sample was built up in layers of approximately 5 cm in height. Per layer, water was added to flood the sand. After this, the layer was densified using a proctor hammer. This resulted in a water content of the soil of approximately 27 %. The same technique as the moist sands

test of placing the test probe with a laboratory stand after the first layer was used. Note that the technique of flooding the soil does not ensure full saturation of the sand, as small gas particles can be present throughout the sample.

#### Kaolin clay

A mixture of kaolin clay powder and water was used to form the kaolin clay samples. In order to ensure the kaolin clay can easily be moulded around the test probe, the kaolin clay was mixed with a soil mixer to have a water content of 80%, which is higher than the liquid limit of $\sim$ 65% (Murali, 2015). A 5 cm sand layer was put at the bottom of the cast as a drainage layer. On top of this layer, the test probe was installed with a laboratory probe stand. The kaolin clay was then carefully added around the probe in layers of approximately 5 cm, ensuring good thermal contact between the probe and the soil. On top of the last kaolin clay layer, a 5 cm sand layer was added. This sand layer was added to compress the clay and remove the possible air gaps in the kaolin clay.

#### Water mixed with agar

A mixture of water and agar was used as the fourth reference material. The mixture was prepared to form a jelly like structure according to appendix A2.2 of ASTM (2014). This mixture prevents the free convection of water while still maintaining the known thermal values of water and is widely used as a calibration material of thermal needle probes (ASTM, 2014). In order to prepare the sample, water was heated and 5g agar per 1L water was added while stirring. This mixture was bought to a boil for 5 minutes and then cooled to approximately 40 °C. After the test probe was placed at the required location in the cast with a laboratory probe stand, the hot liquid mixture was poured in the cast. This liquid hardened after cooling, resulting in a solid jelly like structure (Figure 4.3d).

(a) Moist sand test setup. (b) Saturated sand test setup. (c) Kaolin clay test setup. (d) Water test setup.

Figure 4.3.: Overview of the test setup for different reference materials.

### Reference material tests

#### Single Laboratory Thermal Needle probe

To find the thermal conductivity of the reference materials, laboratory thermal needle probe tests were conducted with a TEMPOS Thermal Properties Analyzer TR3 single thermal needle probe according to the ASTM (2014) standard. The thermal needle probe has an accuracy of $\sim$ 10% for the thermal conductivity measurement (METER Group, 2018). Before testing, a verification of the thermal needle probe was performed in glycerine, which has a known thermal conductivity value of 0.286 W/(mK). For each test cast, at least three thermal needle probe tests were performed. These thermal needle probe tests were performed at different locations in the casts. As the top layer of the reference materials can be affected by evaporation of water from the soil, a 3 cm soil layer was locally removed before the needle was pushed in the material.

### Dual Laboratory Thermal Needle probe

To find the volumetric heat capacity of the reference materials, laboratory thermal needle probe tests with the TEMPOS Thermal Properties Analyzer SH3 dual thermal needle probe were conducted. Similar to the thermal conductivity measurement, the thermal needle probe has an accuracy of $\sim 10\%$ for the volumetric heat capacity (METER Group, 2018). Before conducting the test, a verification of the thermal needle was performed in a block of delrin of which the thermal properties are known. Similar to the single thermal needle probe test, at least three tests were performed at different locations of the cast, removing 3 cm of the top soil.

### Hot disk

In situ hot disk tests were performed to find both the thermal conductivity and volumetric heat capacity of the reference materials. These tests were performed with the Hot Disk TPS 2200 device with a 4922 kapton sensor which has a radius of 14.16 mm. In order to use the hot disk sensor in-situ, the sensor was loaded vertically into the material, after making a narrow and deep trench with a spackle knife (Figure 4.4). For the kaolin clay and saturated sand test, the trench was compressed slightly after the sensor is loaded into the trench to ensure perfect contact between the sensor and the reference material. The method of inserting the sensor can disturb the material, but has the benefit of performing the test in the same cast as the test probes. At least four hot disk tests per reference materials were performed.

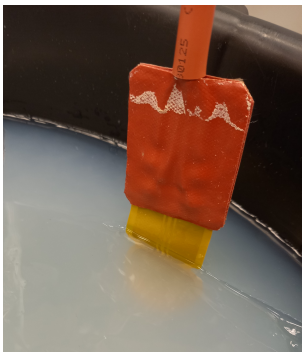

Figure 4.4.: Hot disk sensor vertically installed in the water test setup.

### Density measurements

During the preparation of the casts, multiple samples of the reference materials were taken by pushing a metal ring with a known volume into the soil inside the casts. The samples were then weighed in order to find the bulk density of the materials. After this, the samples were oven dried for at least 24 hours and weighed again in order to find the dry density of the materials. With this information, the water content of the materials was also determined. Three different samples were taken per cast during the preparation. During the dismantling of the cast, two extra tests were performed. It must be noted that this testing procedure can have some inconsistencies due to the soil disturbance that occurs when pushing the ring into the soil and due to the possible loss of water when retrieving the soil inside the ring from the cast.

## 4.2. Interpretation of heat flow cone penetration test data

### 4.2.1. Objective

The main objective of the interpretation method developed is to find the thermal conductivity of the soil from offshore HF-CPT data. The second objective is to also find the volumetric heat capacity of the soil. This method should give reliable and consistent results for a wide range of offshore soil types. Due to the relatively high cost of offshore soil investigation, the method should be able to interpret the data for a relatively short testing duration, preferably within 20 minutes.

### 4.2.2. Methods

The interpretation method consists of two parts: a forward model and an inverse analysis. The forward model can accurately predict the thermal response of the HF-CPT probe when the thermal properties of the soil are used as an input. This model can than be used for an inverse analysis to predict the thermal properties of the soil when the HF-CPT probe thermal data is used as an input. A schematic overview of the froward model and inverse analysis is shown in Figure 4.5

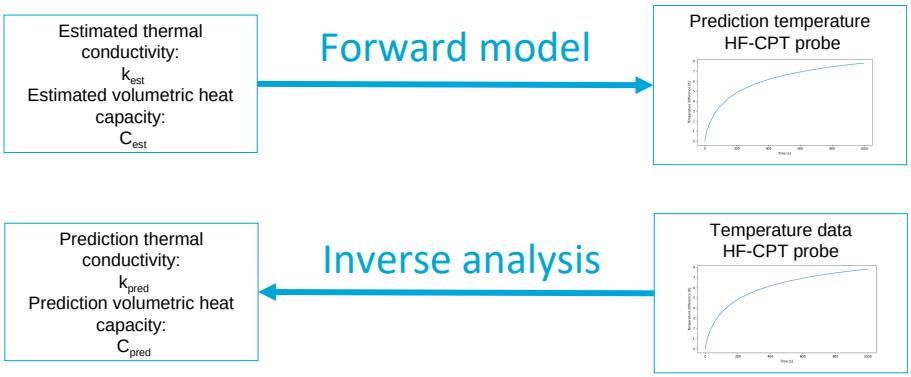


Figure 4.5.: Schematic overview of a forward model (top figure) and an inverse analysis (bottom figure).

#### Forward model

A forward model needs to be constructed that accurately predicts the thermal response of the probe with the thermal parameters of the soil as an input. The following three types of forward models were considered in the thesis:

- Numerical solution found with finite element modelling.
- Analytical solution of the asymmetric heat conduction equation (Equation 2.10).
- Semi-analytical solution of interpolating a g-function from numerical analysis.

A numerical solution made with finite element modelling software is widely used to predict the behaviour of heat transfer for similar problems (Akrouch et al. (2016),Vardon et al. (2018), Mo et al. (2021) & Liu et al. (2022)). In this thesis, the numerical model was constructed in COMSOL Multiphysics. The model was based on the geometry of the HF-CPT. This finite element model predicts the conductive heat transfer occurring between the HF-CPT and the soil by solving the general heat conduction differential equation (Equation 2.6). Due to the axisymmetric geometry of the probe, the model was constructed in a radial coordinate system. Due to the relatively small length and large diameter of the heating element compared to other in-situ tests, it is unknown if the heat transfer in

the soil only occurs in the radial direction. Therefore, the COMSOL model was constructed in a two-dimensional axisymmetric coordinate system. The results of the numerical model were compared to the results found by the HF-CPT laboratory tests to examine if a numerical solution is suitable as a forward model.

Analytical solutions of the asymmetric heat conduction equation (Equation 2.10) are used as a forward model for similar in-situ thermal test like the T-CPT (Section 2.3.2) and the thermal needle probe (Section 2.4.2). To find if an analytical solution can accurately represent the behaviour of the probe, and can thus be used as a forward model, the results gained with the HF-CPT laboratory tests were compared with three analytical solutions of the axisymmetric heat conduction equation:

- Solution for an infinite line heat source (Equation 2.15)
- Solution for a hollow infinite cylindrical heat source (Equation 2.21)
- Solution for a solid infinite cylindrical heat source (Equation 2.22)

The first analytical solution, the infinite line heat source, is also used for the interpretation of the thermal needle probe test. However, due to the relatively large diameter of the HF-CPT heating element compared to the thermal needle probe, this solution might not be the best representation of the behaviour of the HF-CPT. The latter two solutions, the hollow and solid infinite cylindrical heat source, might give a more accurate result as these solutions assume the heat source to be cylindrical. However, due to the relatively small ratio of the diameter over the length of the heating element, a one-dimensional approach might not accurately represent the behaviour of the probe.

If the numerical model can accurately predict the thermal behaviour of the soil, it might be possible to derive a g-function from the numerical results that can predict the behaviour of the HF-CPT (Section 2.6). The possibility of deriving a g-function was examined by transposing the results of the numerical model to a dimensionless coordinate system based on the normalized temperature and Fourier number. If transposing the data for various input parameters of the model results in a similar outcome, a single g-function can be interpolated in the form of Equation 2.26. In order to examine this, a parametric study was performed. In this parametric study, a single input parameter of the numerical model was changed while the other input parameters were kept constant. The following three parameters were examined: heater power level, thermal conductivity of the soil and volumetric heat capacity of the soil. The thermal conductivity and the volumetric heat capacity values examined were chosen to represent the expected range found for offshore soils.

#### Inverse analysis

When a suitable forward model is found, this model is used in an inverse analysis. An inversion method was constructed during this thesis. The goal of the inversion method is to find the thermal properties of the soil when data acquired with the HF-CPT is used as an input.

When either an analytical solution or a single g-function is used as the forward model, the following procedure is performed to construct the inversion method. First, an error function is defined. This function quantifies the difference between the data acquired with the HF-CPT and the prediction of the forward model for a specific thermal conductivity and volumetric heat capacity value. This error function can than be minimized with an optimization procedure in order to find the soil thermal properties for which the least difference between the forward model and the data acquired with the HF-CPT is found.

When the numerical solution is used, the error function must be constructed in a different way. An error function that directly runs the numerical model is not suitable, as minimizing this error function would require the numerical model to be run multiple times, which is time-consuming. Instead, a solution space is constructed that contains the numerical model results for a range of thermal values. This solution space is then interpolated to find the forward result used in the error function. This error function is minimized in order to find the thermal properties that best matches the data acquired with the HF-CPT.

# 5. Laboratory Test Results

In this chapter, the results of the laboratory tests with the HF-CPT dummy probe and the reference material test results are presented and analysed.

## 5.1. Reference material test results

The reference material tests on the water agar mixture were in agreement with the expected thermal values of water. The results of the reference material tests for the other materials are shown in Table 5.1. No in-situ hot disk tests were performed on the moist sand samples due to the unavailability of the device during these material tests. For the saturated sand tests, the hot disk test and the single thermal needle probe test were in agreement with the found value for the thermal conductivity. For the kaolin clay test, the hot disk test resulted in a significantly lower thermal conductivity value than the single thermal needle probe results. A possible explanation of this discrepancy is the disturbance of the kaolin clay that occurred when performing the hot disk test. Because of this, the single thermal needle probe result is assumed to be more reliable for the kaolin clay test. When an assumption is made on the particle density of the soil, the volumetric heat capacity can be estimated with Equation 2.2 (Table 5.2). For the moist sand and kaolin clay tests, the estimated value aligns with the dual thermal needle test results. For the saturated sand tests the estimated value aligns with the hot disk test result.

Table 5.1.: Results of various test performed on the reference materials.

| | Moist sand | | Staurated Sand | | Kaolin Clay | |
|---|---|---|---|---|---|---|
| | Mean | Std | Mean | Std | Mean | Std |
| Single thermal needle probe | | | | | | |
| Thermal conductivity [W/(mK)] | 1.105 | 0.095 | 2.083 | 0.053 | 1.331 | 0.090 |
| Dual thermal needle probe | | | | | | |
| Volumetric heat capacity [MJ/(m$^3$K)] | 1.316 | 0.037 | 2.608 | 0.137 | 3.363 | 0.234 |
| Hot disk test | | | | | | |
| Thermal conductivity [W/(mK)] | - | - | 2.087 | 0.076 | 1.1706 | 0.067 |
| Volumetric heat capacity [MJ/(m$^3$K)] | - | - | 2.840 | 0.340 | 2.842 | 0.216 |
| Bulk density [kg/m$^3$] | 1484 | 45.56 | 2003 | 60.52 | 1463 | 99.35 |
| Dry density [kg/m$^3$] | 1416 | 43.78 | 1590 | 45.67 | 805.7 | 56.41 |
| Water content [-] | 0.049 | 0.003 | 0.260 | 0.012 | 0.817 | 0.040 |

Table 5.2.: Estimated volumetric heat per reference material capacity based on an assumed particle density and measurements of the dry and wet densities of the materials.

| | Moist sand | Saturated sand | Kaolin Clay |
|---|---|---|---|
| Assumed particle density [kg/m$^3$] | 2660 | 2660 | 2650 |
| Saturation [-] | 0.15 | 1.00 | 0.95 |
| Porosity [-] | 0.47 | 0.40 | 0.70 |
| Volumetric heat capacity [MJ/(m$^3$K)] | 1.32 | 2.87 | 3.38 |

## 5.2. Overview of the tests performed with the test probe

In total, 32 tests were conducted with the heat flow cone penetration test probes. Test were performed with varying heater power levels. All tests consisted of a heating phase of 1800 seconds (30 minutes) and a cooling phase of the same duration. An overview of all tests performed are shown in Table 5.3.

Table 5.3.: Overview of the tests performed with the test probe.

| Moist Sand | | Saturated sand | | Water | | Kaolin | |
|---|---|---|---|---|---|---|---|
| Testname | Power [W] | Testname | Power [W] | Testname | Power [W] | Testname | Power [W] |
| ds_08072022_91 | 21.7 | ws_15072022_91 | 20.4 | wa_21072022_91 | 5.6 | kc_03082022_91 | 20.3 |
| ds_08072022_92 | 19.4 | ws_15072022_92 | 19.5 | wa_22072022_91 | 5.6 | kc_03082022_92 | 19.2 |
| ds_08072022_94 | 19.9 | ws_15072022_94 | 18.7 | wa_22072022_92 | 4.9 | kc_03082022_94 | 18.6 |
| ds_13072022_91 | 21.8 | ws_18072022_91 | 20.4 | | | kc_04082022_91 | 20.3 |
| ds_13072022_92 | 19.3 | ws_18072022_92 | 19.3 | | | kc_04082022_92 | 19.3 |
| ds_13072022_94 | 18.6 | ws_18072022_94 | 18.7 | | | kc_04082022_94 | 18.6 |
| ds_14072022_91 | 10.0 | ws_19072022_91 | 10.0 | | | kc_05082022_91 | 10.0 |
| ds_14072022_92 | 9.2 | ws_19072022_92 | 9.1 | | | kc_05082022_92 | 9.1 |
| ds_14072022_94 | 8.6 | ws_19072022_94 | 8.6 | | | kc_05082022_94 | 8.6 |
| | | ws_20072022_92 | 9.2 | | | | |
| | | ws_20072022_94 | 8.7 | | | | |

## 5.3. Test probe results

The results of the heating test per reference material are shown in Figure 5.1 to 5.4. The tests were performed with various heating power levels (Table 5.3). The difference in power level between tests can be normalized with the following equation.

$$\Delta T_{norm} = \Delta T_{test} * \frac{Q_{ref}}{Q_{test}} \tag{5.1}$$

where

| | |
|---|---|
| $\Delta T_{norm}$ | is the normalized temperature difference [K] |
| $\Delta T_{test}$ | is the found temperature difference of the test [K] |
| $Q_{ref}$ | is reference the power level used for normalization [W] |
| $Q_{test}$ | is the power level of the test [W] |

In Figure 5.1 to 5.4, the temperature difference of the tests were normalized to a reference power level of 20 W.

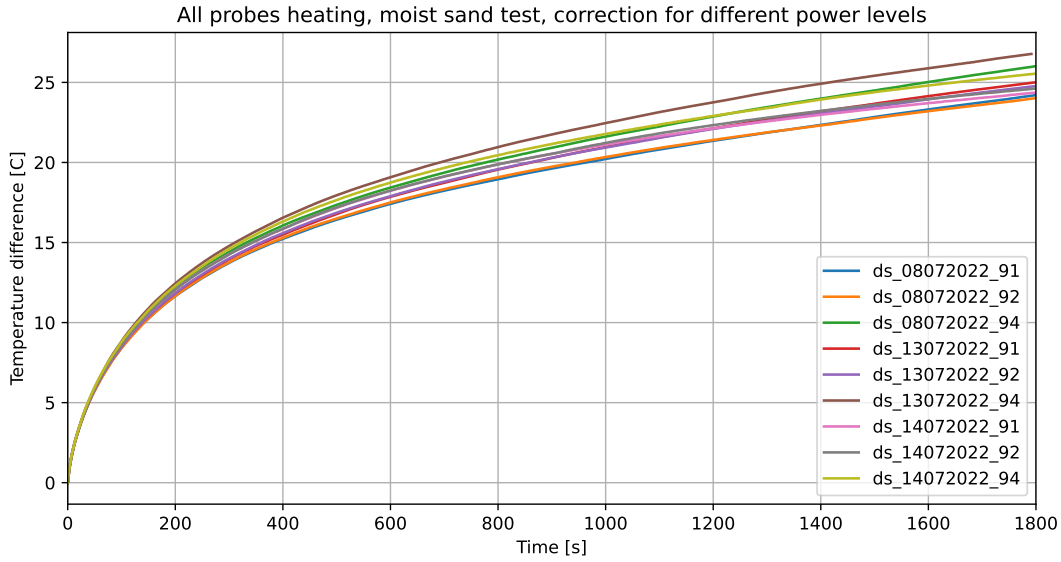


Figure 5.1.: Temperature difference (y-axis) over time (x-axis) for all moist sand tests. The temperature difference is normalized for a power level of 20 W.

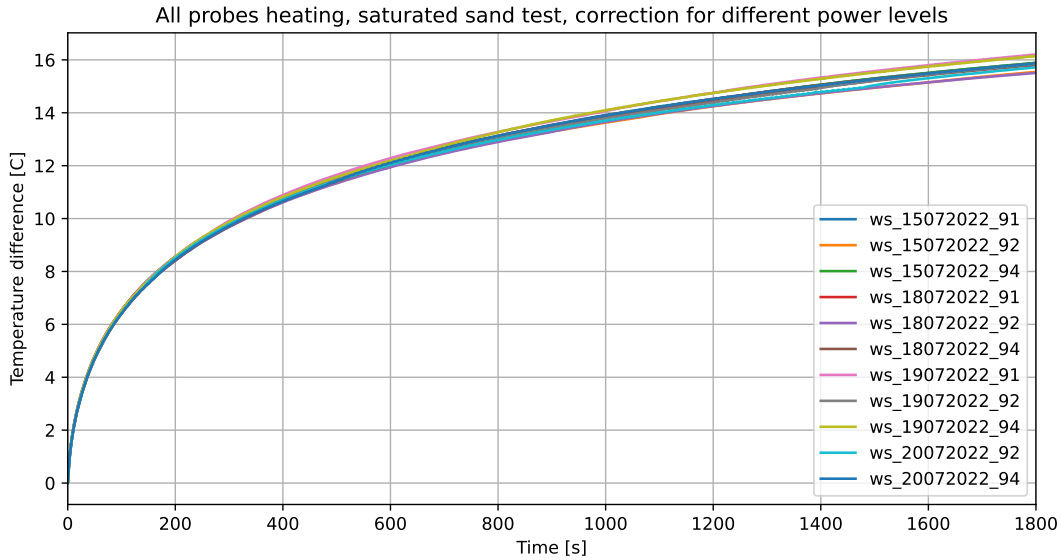


Figure 5.2.: Temperature difference (y-axis) over time (x-axis) for all saturated sand tests. The temperature difference is normalized for a power level of 20 W.

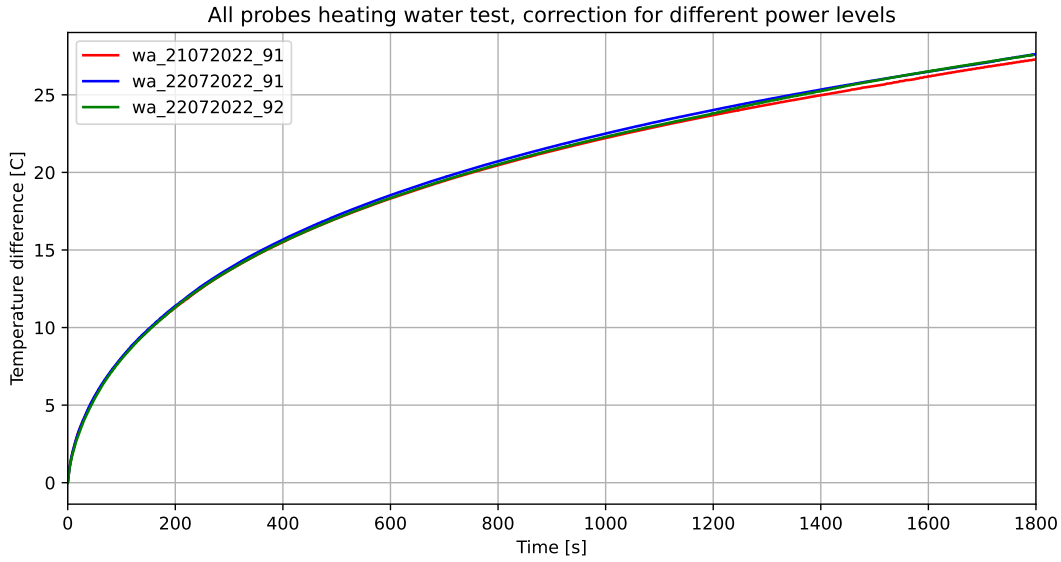


Figure 5.3.: Temperature difference (y-axis) over time (x-axis) for all water tests. The temperature difference is normalized for a power level of 20 W.

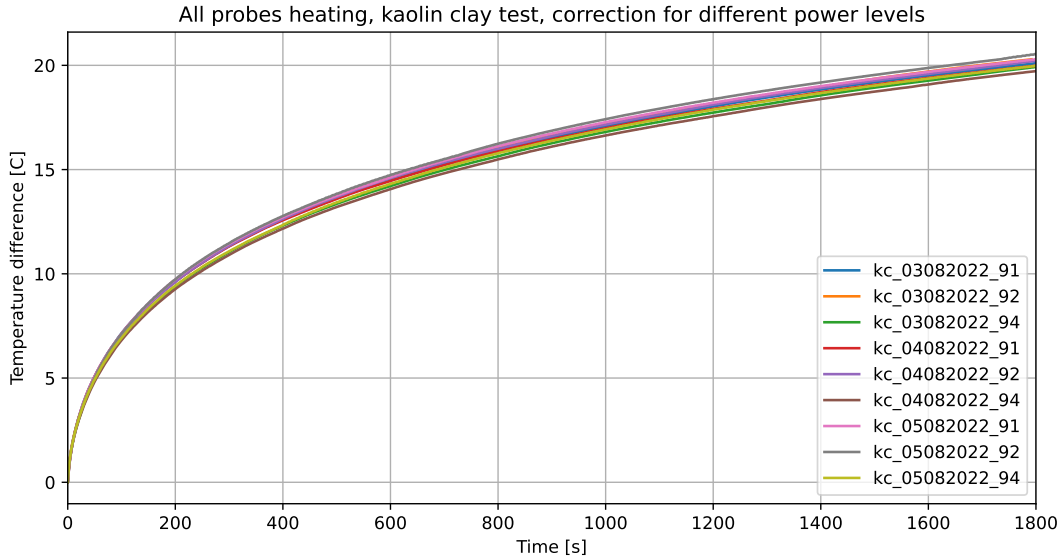


Figure 5.4.: Temperature difference (y-axis) over time (x-axis) for all kaolin clay tests. The temperature difference is normalized for a power level of 20 W.

### 5.3.1. Repeatability

For the water tests, the tests were shown to be repeatable (Figure 5.3). As the water-agar mixture is homogeneous, different tests in the same homogeneous material led to the same result independent on the probe used. For the saturated sand and kaolin clay tests (Figure 5.3 & 5.4) the results had more deviation, as these materials were less uniform and local saturation and density differences were possibly present between tests. For the moist sand tests, a larger spread between the results was observed (Figure 5.2). Local differences in both the density and the water content were possibly present in the moist sand, influencing the thermal properties of the soil.

## 5.4. Conclusion

Laboratory tests with three HF-CPT prototypes were performed in four different materials: moist sand, saturated sand, kaolin clay and a water-agar mixture. In order to have an estimate of the thermal values of the materials, multiple laboratory tests were performed with other methods: single thermal needle probe tests, dual thermal needle probe tests, hot disk tests and density measurements. These reference material tests gave a valid estimation of the range of thermal properties of the reference materials. Next to the reference material tests, 32 tests with the HF-CPT test probes were performed. These tests were proven to be repeatable, as tests in different casts with the same material resulted in similar measurements.

# 6. Analysis of forward models

Is this section, the first research question is answered:

*Which forward model is suitable for the interpretation of the heat flow cone penetration test data?*

In order to answer this research question, three different forward models that can be used for the prediction HF-CPT thermal response were analysed. The forward model must be able to predict the thermal response reasonably well for the complete range of thermal properties found in offshore soils. The forward models analysed in this chapter were:

- Numerical solution found with finite element modelling.
- Analytical solution of the asymmetric heat conduction equation (Equation 2.10).
- Semi-analytical solution of interpolating a g-function from numerical analysis.

## 6.1. Numerical model

The first forward model that was analysed is the usage of a numerical model to predict the thermal response of the HF-CPT. In this thesis, a preliminary COMSOL model was made to predict the thermal response of the HF-CPT. This model consists of a simplified version of the geometry of the HF-CPT, and a uniform soil layer. The model was simplified to decrease runtime. In a later stage of the thesis, a more detailed COMSOL model was developed with the exact dimensions of the HF-CPT. This section details the preliminary COMSOL model. Next to this, it is analysed if the COMSOL model is a suitable forward model by comparing the numerical results to the laboratory test results.

### 6.1.1. Geometry

The preliminary model of the HF-CPT was made in COMSOL Multiphysics version 5.6. The model is 2D axisymmetric and has heat conduction as the only heat transfer mechanism. The cross section of the preliminary COMSOL model is shown in Figure 6.1. The material properties used are displayed in Table 6.1. The soil and the probe had the same initial temperature of 282.15 K. The outer boundaries of the model were set to a Dirichlet boundary condition with the same fixed temperature of 282.15 K. Inside the probe a boundary heat source was present at the interface of the inner heating cylinder and the air insulation. This boundary heat source had a constant heat rate over time, of which the rate can be varied for different tests.

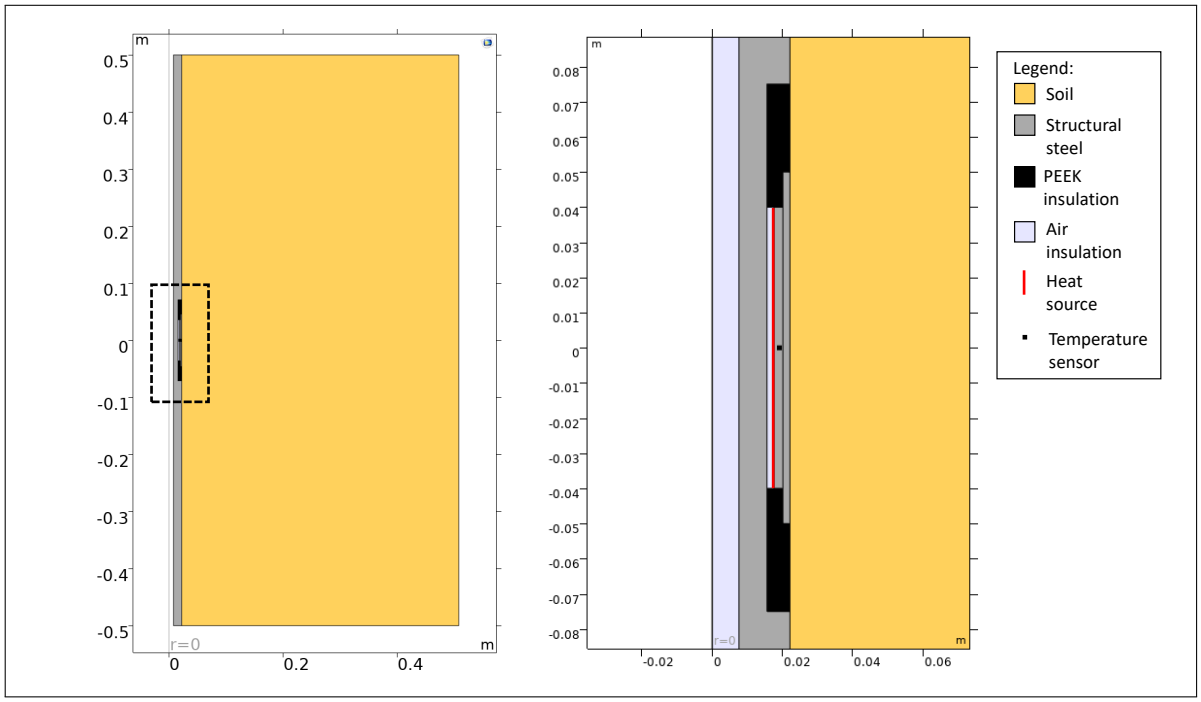


Figure 6.1.: Cross section of the preliminary COMSOL model. This model is based on a simplified geometry of the heat flow cone penetration test with a uniform soil. Left picture shows the entire model. Right picture shows the inset around the heating element.

Table 6.1.: Thermal properties of the materials used in the preliminary COMSOL model.

| | Thermal conductivity [W/(mK)] | Volumetric heat capacity [MJ/(m$^3$K)] |
|---|---|---|
| Structural steel | 44.50 | 3.73 |
| PEEK | 0.25 | 1.40 |
| Air | 0.03 | 0.01 |

A sensitivity analysis on the preliminary model was performed to find the optimal mesh size and tolerance of the model (Appendix B). An absolute tolerance of 0.00001 and a mesh size containing 3031 domain elements were determined to be suitable.

### 6.1.2. Final mesh

The final mesh used in the preliminary COMSOL model is shown in Figure 6.2. The elements of the mesh are more refined around the HF-CPT heating element. This is because this is the area where the most influence on the soil due to the heating occurs. .

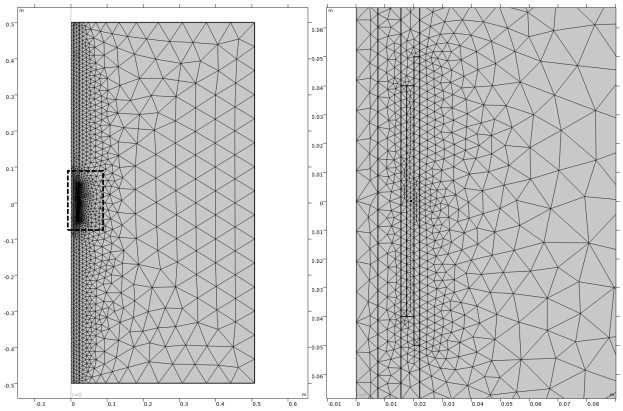

Figure 6.2.: Final mesh size of the preliminary COMSOL model.

### 6.1.3. Comparison preliminary COMSOL model to laboratory tests

To examine the potential of using a numerical solution as a forward model, the preliminary COMSOL model was compared to the laboratory test results. It was chosen to use the water tests as a basis for comparison, as the water-agar mixture has proven to be uniform and the thermal properties of the material were known. When comparing the water laboratory test results to the results gained with the preliminary COMSOL model, the COMSOL model underestimated the heating of the probe (Figure 6.3).

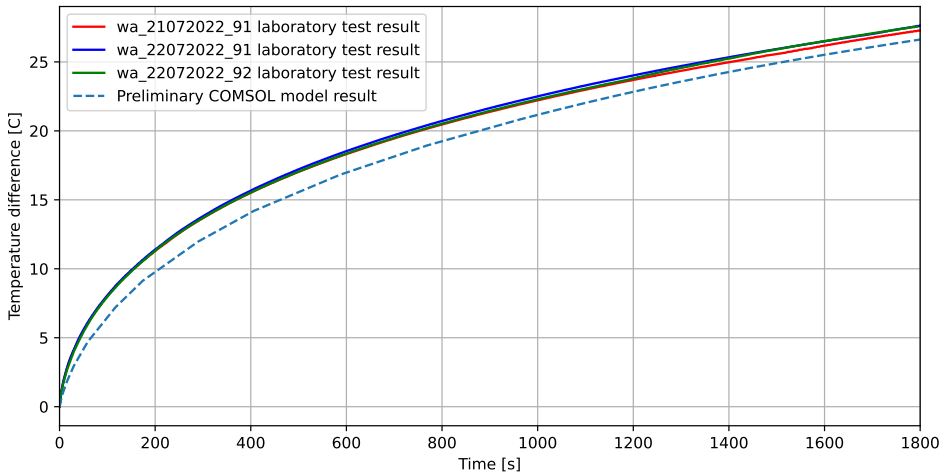


Figure 6.3.: Comparison of the preliminary COMSOL model (blue striped line) to the laboratory test results of the water test normalized for a power level of 20 W (solid lines) with the time on the x-axis and the temperature difference on the y-axis.

### 6.1.4. Conclusion

A preliminary COMSOL model was constructed in order to test the potential of using a numerical solution as forward model to predict the behaviour of the HF-CPT probe. This model used a simplified geometry of the probe. When comparing the results of the preliminary COMSOL model to the water laboratory tests, an underestimation of the heating of the probe of the preliminary model was found. In order to accurately predict the thermal behaviour of the probe using a numerical solution as a forward model, the COMSOL model can be further improved.

## 6.2. Analytical solution

The second forward model that was examined is the usage of an analytical solution of the asymmetric heat conduction equation. Three analytical solutions of the one-dimensional axisymmetric heat conduction equation (Equation 2.10) were compared to the laboratory test with the HF-CPT and the preliminary COMSOL model described in Section 6.1. The solutions considered were:

- The solution for an infinite line heat source (Equation 2.15).
- The solution for a hollow infinite cylindrical heat source (Equation 2.21).
- The solution for a solid infinite cylindrical heat source (Equation 2.22).

### 6.2.1. Comparison analytical solutions to laboratory test results

Similar to the analysis shown in Section 6.1.3, the results of the analytical solutions were compared to the laboratory test results of the water tests. The results of the preliminary COMSOL model were included in the comparison as a reference. No analytical solution provided accurately predicted the thermal response of the probe found in the laboratory test results (Figure 6.4).

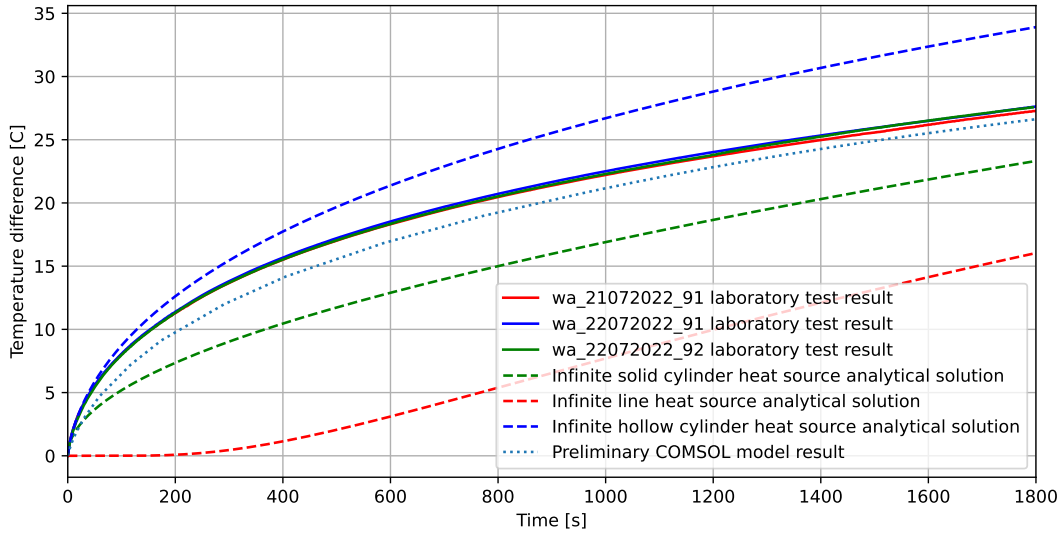


Figure 6.4.: Comparison of three analytical solutions of the axisymmetric heat conduction equation (striped lines) to the laboratory test results of the water test normalized for a power level of 20 W (solid lines) and the preliminary COMSOL model (blue dotted line) with the time on the x-axis and the temperature difference on the y-axis. For both the COMSOL model and the analytical solutions, the known thermal properties of water are used as the input (k=0.6 W/(mK), C=4.14 MJ/($m^3$K)).

### 6.2.2. Heater length parametric study

To determine if the heater length is the cause for the analytical solutions to not align with the preliminary COMSOL model, a parametric study to determine the influence of the heater length was performed. The different heater lengths that are tested are shown in Table 6.3. The other input parameters used for the analysis are shown in table 6.2. For a larger heater length, the solution showed more alignment with the infinite cylindrical heat source solutions (Figure 6.5). This because the heat that is generated in a longer heating element mainly flows trough the soil in radial direction at the height of the temperature senor (Figure 6.6a), making it possible to use the one-dimensional axisymmetric heat conduction equation to approximate the temperature rise in the probe. For a shorter

heating element, heat also flows trough the soil in the perpendicular axial direction at the height of the temperature senor (Figure 6.6b), making a one-dimensional approach not suitable.

For the longest tested heater length of 0.5 meters, the solution of the COMSOL model was between the analytical solutions of the hollow and solid infinite cylindrical heat source model. This can be explained as the inside of the HF-CPT heater consists of a combination of PEEK, stainless steel and air, while the solid and hollow infinite cylindrical heat source model assume that the cylindrical heater is filled with soil and air respectively. Thus, neither analytical solution correctly simulates the temperature behaviour occurring in the inside of the probe for a short time period.

Table 6.2.: The input parameters used in comparing the preliminary COMSOL model to three analytical solutions of the one-dimensional axisymmetric heat conduction equation.

| | |
|---|---|
| Total test duration [s] | 3600 |
| Heater radius [m] | 0.022 |
| Heater power per meter [W/m] | 200 |
| Thermal conductivity soil [W/(mK)] | 2.5 |
| Volumetric heat capacity soil [MJ/(m$^3$K)] | 2.75 |

Table 6.3.: Heater lengths that are examined in the parametric study.

| Heater length [m] | $r_b/H$ [-] |
|---|---|
| $\infty$ | 0 |
| 0.5 | 0.044 |
| 0.4 | 0.055 |
| 0.3 | 0.073 |
| 0.2 | 0.110 |
| 0.1 | 0.220 |

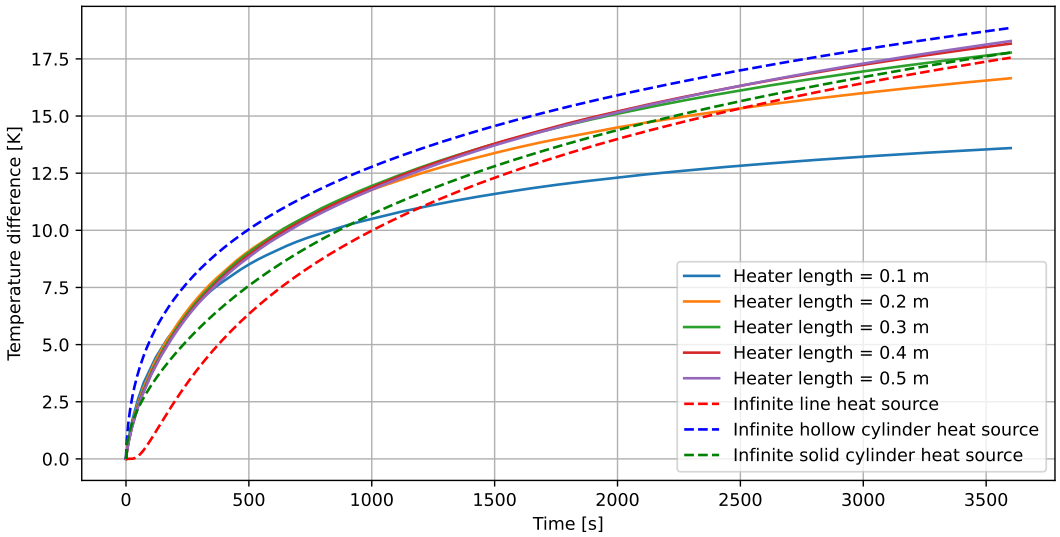


Figure 6.5.: Comparison of the preliminary COMSOL model (solid lines) to three analytical solutions of the one-dimensional axisymmetric heat conduction equation (striped lines) for a varying heater length with the time on the x-axis and the temperature difference on the y-axis.

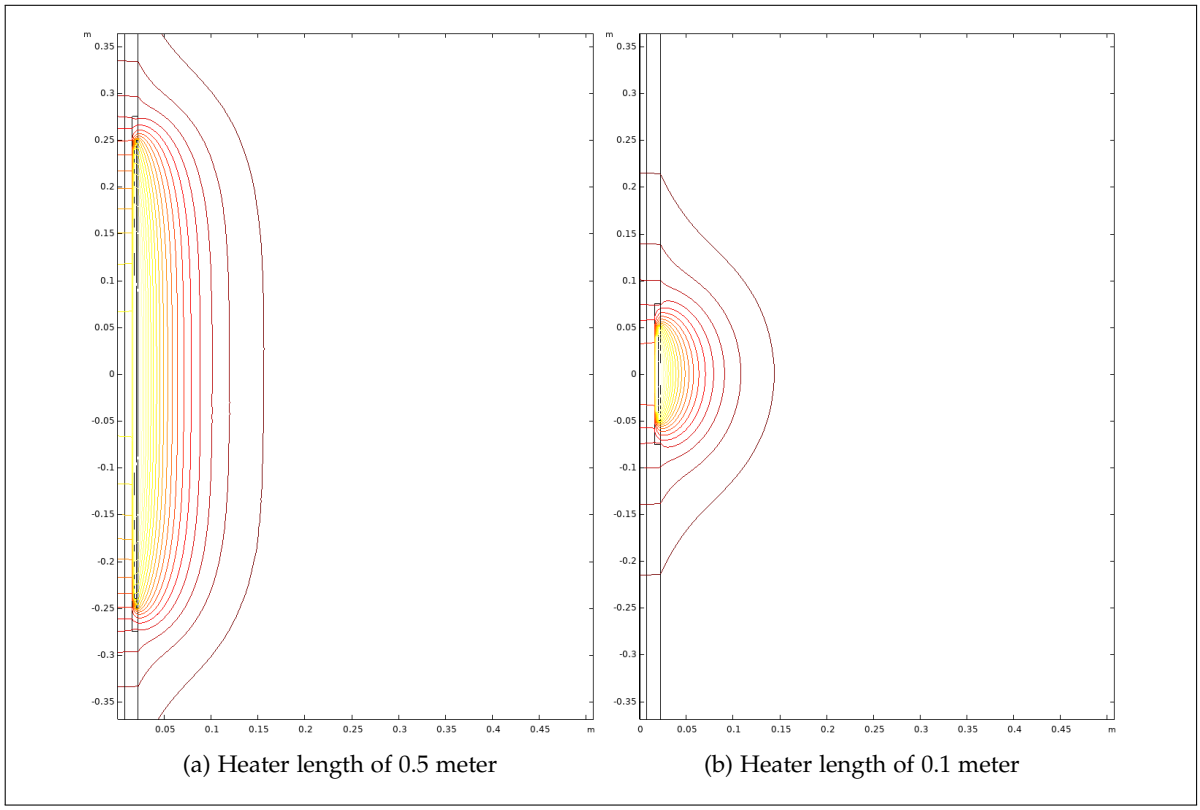

(a) Heater length of 0.5 meter

(b) Heater length of 0.1 meter

Figure 6.6.: Isothermal contours of the COMSOL model for two different heater lengths. The isothermal contours parallel to the heater in the middle of the heating element in figure a indicate a heat flow at the temperature sensor height mostly though the radial direction. The curved isothermal contours in the middle of the heating element in figure b indicate a heat flow at the temperature sensor height in both the radial as the axial direction.

### 6.2.3. Conclusion

There is no solution of the one-dimensional axisymmetric heat conduction that accurately predicts the heat transfer of the heat flow cone penetrometer. This is due to two reasons:

- Due to the short length of the heating element, the heat flow trough the soil at the temperature sensor height is not only in the radial direction, but also in the the perpendicular axial direction. Because of this, the one-dimensional axisymmetric heat conduction equation does not accurately predict the heat transfer mechanism occurring in the soil.
- The inside of the HF-CPT probe is complex as it contains multiple materials with specific dimensions. This affects the heat flow inside the probe. The analytical solutions considered in this section either assume a cylinder filled with air or soil, making accurate simulation of the HF-CPT for a short time period impossible.

## 6.3. G-Function

The third forward solution that was analysed is the usage of a g-function derived from numerical simulation. In this section, an analysis was performed to examine if an interpolation of a single g-function with the dimensionless parameters of the normalized temperature (Equation 2.23) and the Fourier number (Equation 2.24) is possible (Equation 2.25). In this case, the g-function has a similar form as used by Bernier (2001), Man et al. (2010) and Loveridge and Powrie (2013) (Equation 2.26).

### 6.3.1. Parametric study

Three parametric studies were performed to examine if it is possible to interpolate a single g-function based on the normalized temperature and the Fourier number (Equation 2.25). For each parametric study, the preliminary COMSOL model was run multiple times, changing a single parameter while keeping the rest of the parameters constant. The same initial parameters were used as in Section 6.2.2 (Table 6.2).

#### Heater power

The first parameter that was examined is the heater power. The heater power level used in testing is not yet a fixed value and finding a g-function independent on the heater power adds flexibility to the testing procedure. The amount of power used for the tests in this study are shown in Table 6.4.

Table 6.4.: Heater power levels that are examined in the parametric study.

| Heater power [W] | Heat release per length [W/m] |
|---|---|
| 60 | 600 |
| 50 | 500 |
| 40 | 400 |
| 30 | 300 |
| 20 | 200 |
| 10 | 100 |

A higher power level resulted in a larger temperature difference (Figure 6.7a). This difference was cancelled out when normalizing the temperature difference according to Equation 2.25 (Figure 6.7b). Therefore, this dimensionless axis system is suitable for accounting for the effect of different power levels on the HF-CPT COMSOL model.

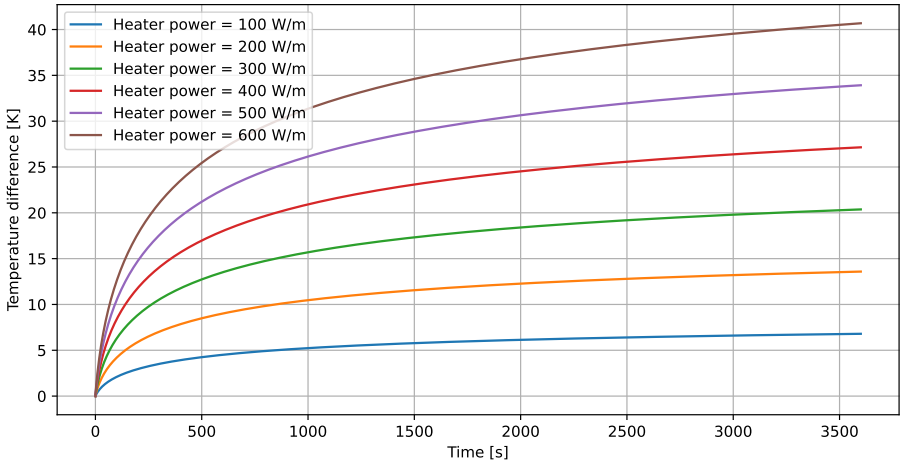


(a) Temperature (y-axis) plotted against time (x-axis).

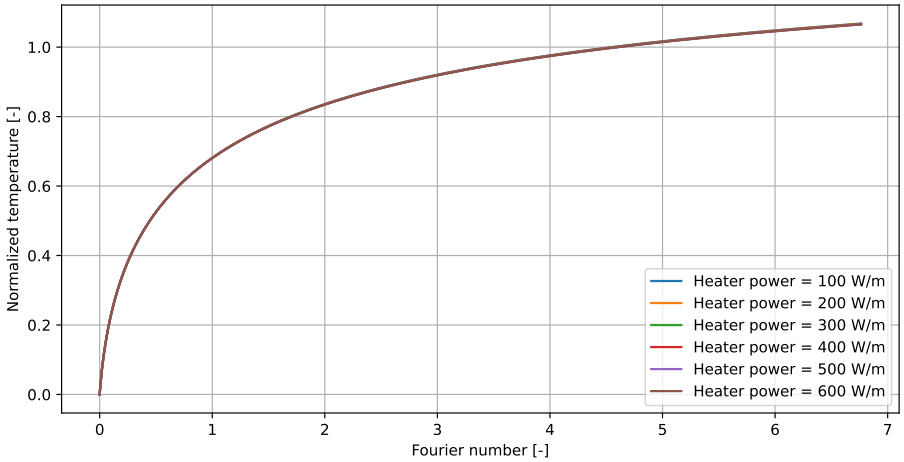


(b) Normalized temperature (y-axis) plotted against the Fourier number (x-axis).

Figure 6.7.: COMSOL result for various heater power levels.

### Thermal conductivity

The main goal of the HF-CPT is to find the thermal conductivity of the soil. The g-function developed to find the thermal conductivity must be suitable for the complete range of soil thermal conductivity values that are found in offshore soils. The range of values used for the parametric study is shown in Table 6.5.

Table 6.5.: Values of soil thermal conductivity that are examined in the parametric study.

| Thermal conductivity [W/(mK)] | Thermal diffusivity [$m^2/s$] |
|---|---|
| 0.5 | $0.18*10^{-6}$ |
| 1.0 | $0.36*10^{-6}$ |
| 1.5 | $0.55*10^{-6}$ |
| 2.0 | $0.73*10^{-6}$ |
| 2.5 | $0.91*10^{-6}$ |
| 3.0 | $1.09*10^{-6}$ |
| 3.5 | $1.27*10^{-6}$ |
| 4.0 | $1.45*10^{-6}$ |
| 4.5 | $1.64*10^{-6}$ |

A lower thermal conductivity value led to a higher temperature difference (Figure 6.8a). A lower thermal conductivity results in a lower heat flow through trough the soil and thus more heat to stay within the probe. Plotting the data in a dimensionless axis system according to Equation 2.25 did not result in alignment of the data (Figure 6.8b). This means that finding a single g-function with Equation 2.25 for this range of thermal conductivity values is impossible. The Fourier number and normalized temperature do not give acceptable results for the preliminary COMSOL model because of the limited length of the heater. When conducting the same study for a heater with an infinite length, the test results did align for the dimensionless axis system (Figure 6.9b).

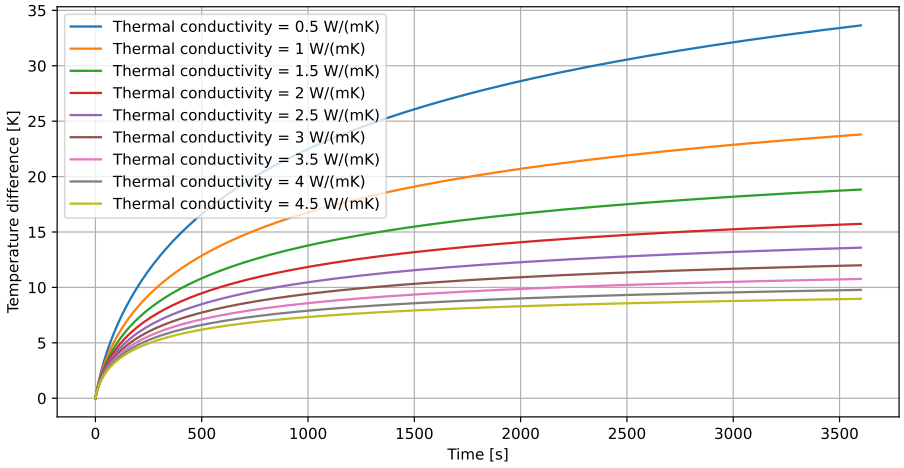


(a) Temperature (y-axis) plotted against time (x-axis).

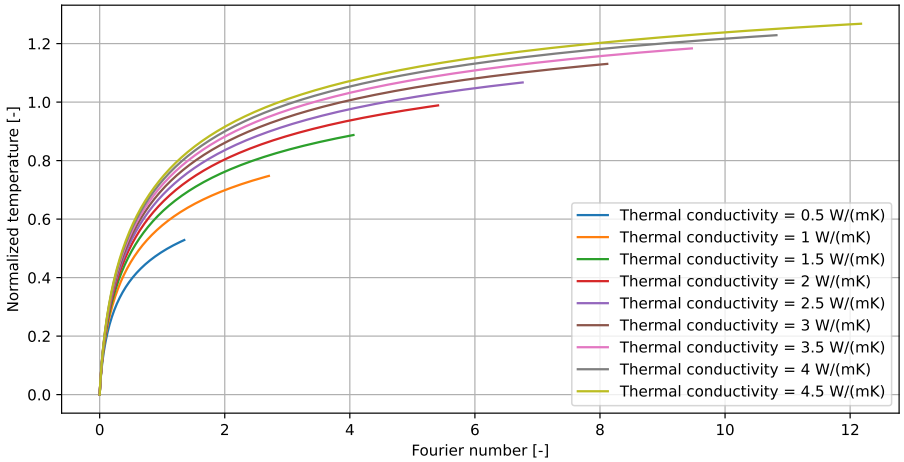


(b) Normalized temperature (y-axis) plotted against the Fourier number (x-axis).

Figure 6.8.: COMSOL result for various soil thermal conductivity values.

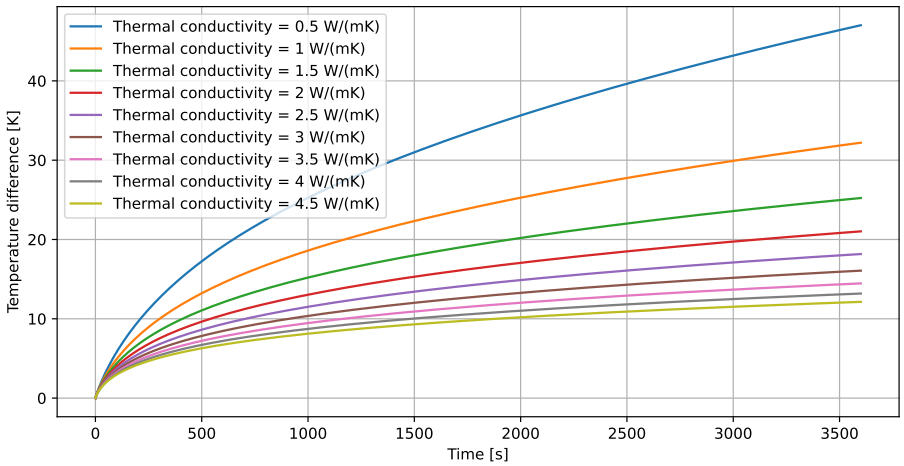


(a) Temperature (y-axis) plotted against time (x-axis).

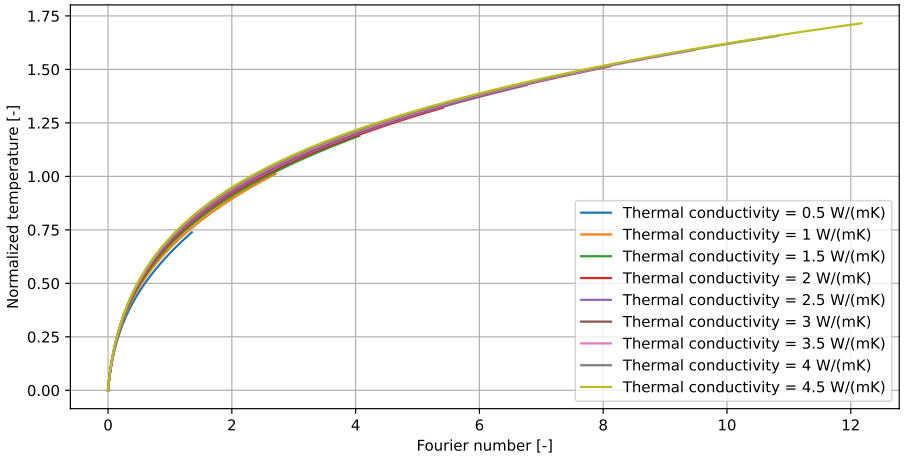


(b) Normalized temperature (y-axis) plotted against the Fourier number (x-axis).

Figure 6.9.: COMSOL result for various soil thermal conductivity values and an infinite heater length.

### Volumetric heat capacity

Similar to the soil thermal conductivity, a range of values that is found for the different types of offshore soils was used for the parametric study on the volumetric heat capacity (Table 6.6).

Table 6.6.: Values of soil volumetric heat capacity that are examined in the parametric study.

| Volumetric Heat Capacity [MJ/(m$^3$K)] | Thermal diffusivity [m$^2$/s] |
|---|---|
| 2.50 | 1.00*10$^{-6}$ |
| 2.75 | 0.91*10$^{-6}$ |
| 3.00 | 0.83*10$^{-6}$ |
| 3.25 | 0.77*10$^{-6}$ |
| 3.50 | 0.71*10$^{-6}$ |
| 3.75 | 0.67*10$^{-6}$ |
| 4.00 | 0.625*10$^{-6}$ |

A higher temperature difference was found for a lower volumetric heat capacity value (Figure 6.10a). For a lower volumetric heat capacity value, less energy is needed to heat up the soil, resulting in more energy to heat up the probe. The influence of the heat capacity on the temperature difference was however relatively small compared to the influence of the thermal conductivity. Similar to Figure 6.7b, the results for the dimensionless axis system seem to align (Figure 6.10b). However, it must be noted that there are some discrepancies between the tests for a shorter time frame (Figure 6.10c). As these discrepancies are limited, this dimensionless axis system is still suitable for accounting for the effect of the heat capacity on the COMSOL model.

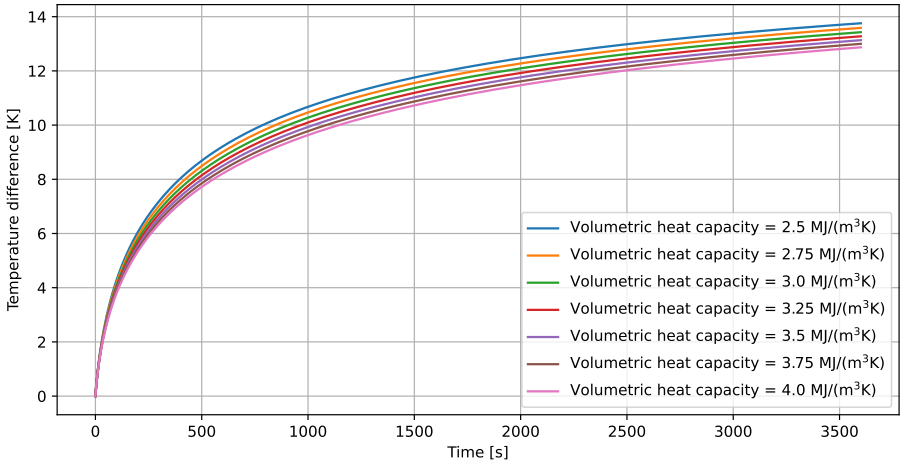


(a) Temperature (y-axis) plotted against time (x-axis).

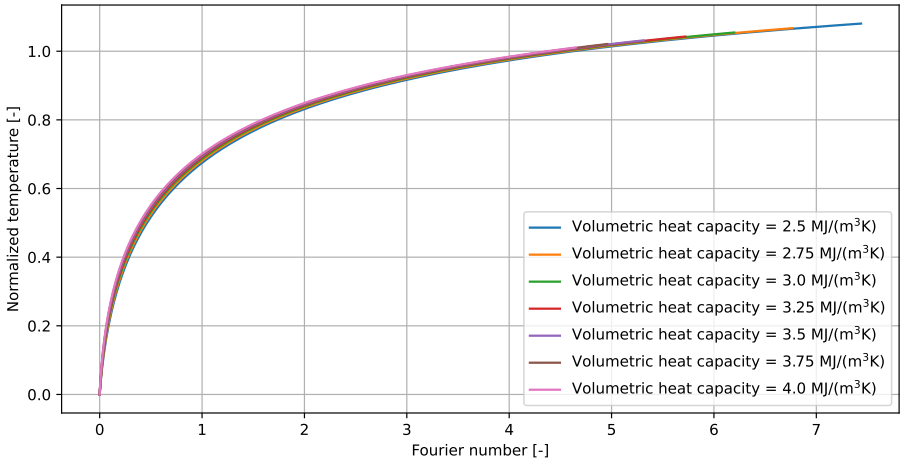


(b) Normalized temperature (y-axis) plotted against the Fourier number (x-axis).

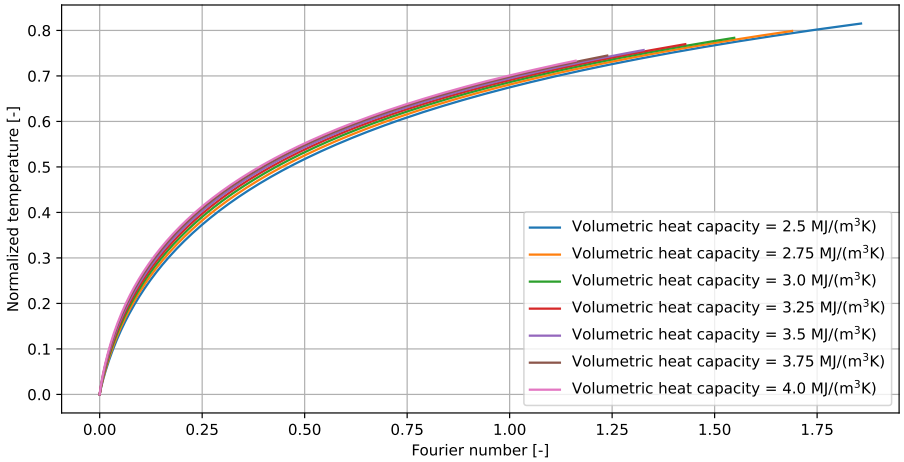


(c) Normalized temperature (y-axis) plotted against the Fourier number (x-axis) for the first 900 seconds of testing.

Figure 6.10.: COMSOL result for various soil volumetric heat capacity values.

#### Conclusion

By comparing the results of the numerical model in the parametric studies using the dimensionless axis system with the Fourier number and normalized temperature, it was determined if a single g-function dependent on these dimensionless parameters can describe this system accurately. For the heater power, this dimensionless axis system showed accurate results, as no difference between tests is observed in this system (Figure 6.7b). For the volumetric heat capacity, the results were also promising, but there are small discrepancies between the tests (Figure 6.10c). However, for the thermal conductivity, the test results did not align on the dimensionless axis system (Figure 6.8b). This makes it impossible to find a single g-function for the dimensionless axis system with the Fourier number and normalized temperature.

### 6.3.2. Other dimensionless systems

As a single g-function did not describe the system accurately for the dimensionless parameters of the Fourier number and normalized temperature, a g-function based on other parameters needs to be found in order to use a g-function for the interpretation of the HF-CPT. The form of g-function derived by Eskilson (1987) (Equation 2.27) is not suitable for this, as the same dependencies on the thermal conductivity are present as in the g-function with the Fourier number (Equation 2.25). A dimensionless parameter which has a new relation of the thermal conductivity that accounts for the differences in test results has to be found in order to use a single g-function to interpret the HF-CPT. A dimensionless number that relates these differences in thermal conductivity to the heater dimension might be possible to find.

## 6.4. Discussion

Three types of forward models were examined in this chapter:

- Numerical solution found with finite element modelling.
- Analytical solution of the asymmetric heat conduction equation (Equation 2.10).
- Semi-analytical solution of interpolating a g-function from numerical analysis.

The three analytical solutions of the asymmetric heat conduction equation considered in section 6.2 did not accurately predict the thermal behaviour of the HF-CPT probe. This is due two reasons. First of all, the analytical solutions assume that the heat generated by the heater solely flows in the radial direction though the soil, while flow in the perpendicular axial direction also occurs in the HF-CPT. Secondly, the inside of the HF-CPT probe is complex, as it contains multiple materials with specific dimensions. An analytical solution is not able to correctly simulate the heat flow inside the probe. Therefore, an analytical solution is not suitable as a forward model to predict the thermal response of the HF-CPT.

The two remaining forward models are both based on numerical solutions. The use of a numerical solution as a forward model, either directly or by interpolating a g-function, showed potential, as the preliminary COMSOL model shows reasonable agreement with the laboratory test results. The COMSOL model can further be improved to more accurately represent the thermal behaviour of the HF-CPT probe.
In the case of using a single g-function as a forward model, this function can directly be used to form an inversion method. For using the numerical solution as a forward method, a method must be constructed that does not require multiple runs of the numerical model to perform the inversion. This method is called the 'direct data inversion method' and is explained in detail in Section 7.1. The direct data inversion method brings several benefits and disadvantages compared to using a g-function for the inversion method.

A benefit of the direct data inversion method compared to using a g-function for the inversion is that no dimensionless parameters are used. As the thermal conductivity and volumetric heat capacity are direct inputs of the COMSOL model, an inversion on this model is performed without using the Fourier number or normalized temperature. Another benefit to the direct data inversion method is that the implementation of such a method is relatively straightforward, while for the g-function suitable dimensionless parameters need to be studied. It is currently uncertain if a single g-function exists for the HF-CPT that accounts for a wide range of thermal conductivity values and which dimensionless parameters correspond to this.

However, if a suitable g-function is found, this method is easier to understand and use in practice than the direct data method. The g-function method only consists of one equation instead of a numerical model, which adds clarity. Next to this, it is a fast method with low storage space due to the fact it is based on a single equation. The direct data inversion can feel as a black box to users and might have a longer run time and be less storage efficient. Another disadvantage is that the direct data method uses a single COMSOL model, which means that it is only suitable for a specific probe geometry. If the geometry of the probe changes, a new COMSOL model must be made and run for the direct data inversion. For the g-function method, it might be possible to find a solution which is independent on the heater dimensions.

## 6.5. Conclusion

The research question described in this section was:

*Which forward model is suitable for the interpretation of the heat flow cone penetration test data?*

Using an analytical solution as a forward model for the interpretation of the HF-CPT was not deemed suitable, as no analytical model was found that can accurately simulate the thermal response of the HF-CPT. Both the numerical method and the g-function method showed potential, as the preliminary COMSOL model showed reasonable agreement with the laboratory test results. The COMSOL model can further be improved to more accurately represent the thermal behaviour of the HF-CPT. However, it is uncertain if it is possible to find single g-function to represent the thermal behaviour of the probe. Therefore, it is chosen to continue with the numerical solution as a forward method. A suitable inversion method which directly uses the numerical solution must be constructed and validated.

# 7. Direct data inversion method

An inversion method was created that uses the numerical COMSOL model as a forward model, called the direct data inversion method. The direct data inversion method needs to give consistent and reliable results for a wide range of thermal properties. The method should also use a relatively short runtime and have a reasonably small storage space, as the goal is to use this method during offshore soil investigation. The method was first tested with numerical data. After this, the method was tested with laboratory test data in order to answer the second research question:

*Can the inversion method combined with the suitable forward model accurately predict the thermal properties of the materials used in laboratory tests with the heat flow cone penetration test?*

## 7.1. Explanation of the numerical inversion method

In this section, the workings of the inversion method is first briefly explained. After this, the construction of the solution space and the inversion method are further detailed.

The goal of the inversion method is to find the soil thermal conductivity and volumetric heat capacity from thermal data generated by the HF-CPT by comparing the data with the HF-CPT COMSOL model. The inversion method finds the thermal conductivity and volumetric heat capacity values for which the COMSOL model has the best match with the input data. As running the COMSOL model is time consuming, the COMSOL model is not directly run during the inversion method. Instead, a solution space is made beforehand that stores the COMSOL results for specific thermal conductivity and volumetric heat capacity values. This solution space is then interpolated to estimate the COMSOL result for a specific thermal conductivity and volumetric heat capacity value. A minimization is performed to find the best match between the raw data and the COMSOL model. A schematic overview of the inverse analysis is shown in Figure 7.1.

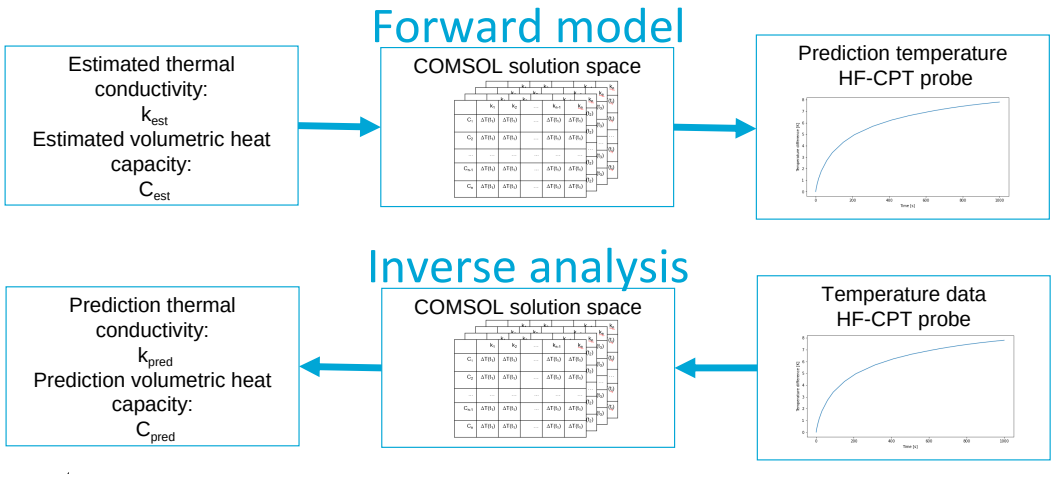


Figure 7.1.: Schematic overview of a forward model (top figure) and an inverse analysis (bottom figure) problem using a the direct data from a COMSOL model.

### 7.1.1. Constructing the solution space

In order to run the inversion method, a solution space must be created that stores a wide range of COMSOL simulations. This solution space is used to perform an 2D linear interpolation to find the temperature difference over time for a specific thermal conductivity and volumetric heat capacity value. This is further explained in Section 7.1.2. There are three factors that influence the size of the solution space:

- The range of thermal conductivity values that is in the solution space [W/(mK)]
- The range of volumetric heat capacity values that is in the solution space [J/(m$^3$K)]
- The range of time points on which the inversion is performed [s]

The size and values of the ranges can be determined by the user of the method. In general, a larger number of values leads to a more accurate match with the COMSOL model. However, increasing the number of values also extends the amount of time needed to construct the solution space and perform the inversion. After the ranges of values are determined, the COMSOL model is run for all different thermal conductivity and volumetric heat capacity values. For example, for 20 different values of thermal conductivity and 20 different values of volumetric heat capacity, the model runs 400 times. For each COMSOL run, the temperature difference is interpolated for each time point on which the inversion is performed. This temperature difference is stored in a three-dimensional array with the thermal conductivity values on the x-axis, the volumetric heat capacity values on the y-axis, and the different time points on the z-axis. A schematic overview of the process of constructing the solution space is shown in Figure 7.2. The solution space is created once per specific COMSOL model. Multiple inversions can be performed with the same solution space.

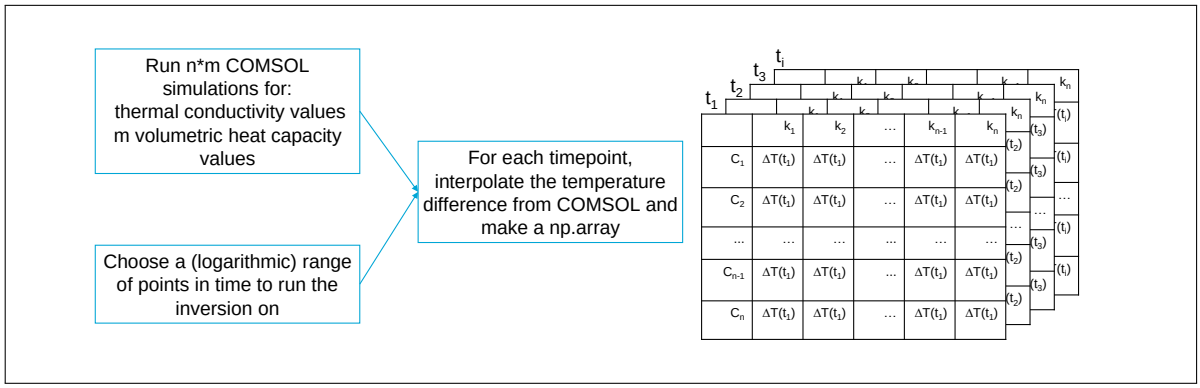


Figure 7.2.: Schematic overview of the process of constructing the solution space.

### 7.1.2. Direct data inversion

The inversion method consists of four different parts that are explained separately. A schematic overview of the inversion method is shown in Figure 7.3.

#### Interpolation of raw data

The data that is analysed by the interpretation method is called the raw data. This data can be generated by the COMSOL model, but the goal is to use test data obtained by the HF-CPT. This data consists of a column of time points and a column of temperature values measured per time point. Before this raw data is inverted, it is adapted to correctly fit the inversion method. In order to achieve this, the temperature column of the raw data is first subtracted by the initial temperature to find the temperature difference. After this is performed, the temperature difference is normalized according

to the power of the test, removing the influence of the power level from the inversion (Equation 7.1).

$$\Delta T_{norm} = \Delta T_{data} * \frac{Q_{ref}}{Q_{data}} \tag{7.1}$$

where

| | |
|---|---|
| $\Delta T_{norm}$ | is the normalized temperature difference [K] |
| $\Delta T_{data}$ | is the temperature difference of the raw data [K] |
| $Q_{ref}$ | is the reference the power level used for normalization, which in this case is equal to the power level for which the solution space is generated [W] |
| $Q_{data}$ | is the power level for which the raw data is generated [W] |

After the raw data is normalized for the power level, the data is linearly interpolated to find the normalized temperature difference for the specific time points for which the inversion is performed. These time points are the same time points as on the z-axis of the solution space.

#### Interpolation of the solution space

The solution space is used to find the temperature difference over time for a specific thermal conductivity and volumetric heat capacity value (Section 7.1.1). This temperature difference is calculated for the time points of the inversion. For each specific time point the solution space is divided in a 2D grid of temperature differences with the thermal conductivity on the x-axis and the volumetric heat capacity on the y-axis (Figure 7.2). This grid is interpolated with a 2D linear interpolator to find the temperature difference of a time point for a specific thermal conductivity and volumetric heat capacity value. This 2D interpolation is performed for all time points in the solution space, finding the temperature difference for a specific thermal conductivity and volumetric heat capacity value.

#### Finding the Root Mean Square Error

The temperature difference of the raw data and the temperature difference found from the solution space for a specific thermal conductivity and volumetric heat capacity value are now compared by taking the Root Mean Square Error (RMSE) of the two solutions (Equation 7.2).

$$RMSE = \sqrt{\sum_{i=1}^{n} \frac{(\Delta \hat{T}(t_i) - \Delta T(t_i))^2}{n}} \tag{7.2}$$

where

| | |
|---|---|
| $\Delta \hat{T}(t_i)$ | is the temperature difference found from the solution space at timepoint $t_i$ [K] |
| $\Delta T(t_i)$ | is the temperature difference of the raw data at timepoint $t_i$, corrected for the power level [K] |
| $n$ | is the total number of timepoints for which the inversion is performed [-] |

The smaller the value of the RMSE is, the better the match is between the raw data and the data generated with the solution space. For example, a RMSE of zero means that the temperature difference for each time point is identical for the raw data and the data generated with the solution space.

### Minimization

A lower value of the RMSE means a better match between the raw data and the data generated from the solution space. For the lowest value of the RMSE, the best match between the two is found. As the data from the solution space is generated for a specific volumetric heat capacity and thermal conductivity value, these two values can be adjusted in order to minimize the RMSE. This calculation is performed by a minimization solver.

With this solver, the thermal conductivity and volumetric heat capacity values are found for which the solution space has the best match with the raw data. The Nelder-Mead method is used as the minimization method, which does not require the calculation of function derivatives and can handle boundaries. The boundaries of the minimization are set to the minimum and maximum values of thermal conductivity and volumetric heat capacity found in the solution space. A first estimation of the thermal conductivity and volumetric heat capacity is provided as initial value of the minimization.

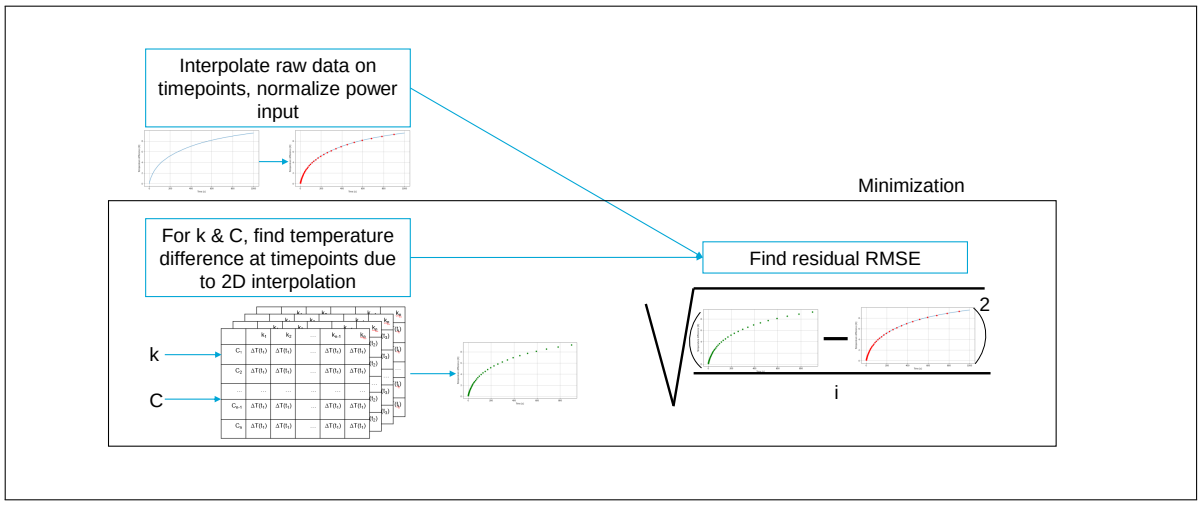


Figure 7.3.: Schematic overview of the inversion method.

## 7.2. Testing the inversion method with numerical data

To verify if the inversion method works as expected, the method was tested with data generated from the preliminary COMSOL model (Section 6.1) as the raw data input. Note that this is the same model for which the solution space is generated, so a perfect match between the raw data and the solution space can theoretically be found. The solution space was generated for the following values:

- 20 linearly spaced thermal conductivity values from 0.5 to 4.5 W/(mK)
- 20 linearly spaced volumetric heat capacity values from 1.5 to 4.0 MJ/(m$^3$K)
- 50 logarithmically spaced time points from 1 to 900 s
- A power level of 20 W

Three tests were executed with the inversion method. The input and outcome of the three tests are shown in Table 7.1. The first estimation of the thermal values was the same for all tests: a thermal conductivity of 2.0 W/(mK) and a volumetric heat capacity of 3.0 MJ/(m$^3$K). The inversion method returned values of the thermal conductivity and volumetric heat capacity that were in agreement with the input values, with a maximum relative error of 0.2% and 1.4% found between the values, respectively. The optimisation path of the inversion method is visualised in Figure 7.4.

Table 7.1.: Input and results of the model tests with the inversion method.

| | Test 1 | Test 2 | Test 3 |
|---|---|---|---|
| Input power [W] | 20 | 20 | 18 |
| Input thermal conductivity [W/(mK)] | 2.7500 | 1.1400 | 3.5000 |
| Found thermal conductivity [W/(mK)] | 2.7512 | 1.1404 | 3.4929 |
| Relative error thermal conductivity [-] | 0.0005 | 0.0004 | 0.0020 |
| Input volumetric heat capacity [W/(m$^3$K)] | 3.3000 | 3.7500 | 2.7000 |
| Found volumetric heat capacity [W/(m$^3$K)] | 3.3031 | 3.7523 | 2.7369 |
| Relative error volumetric heat capacity [-] | 0.0010 | 0.0006 | 0.0137 |

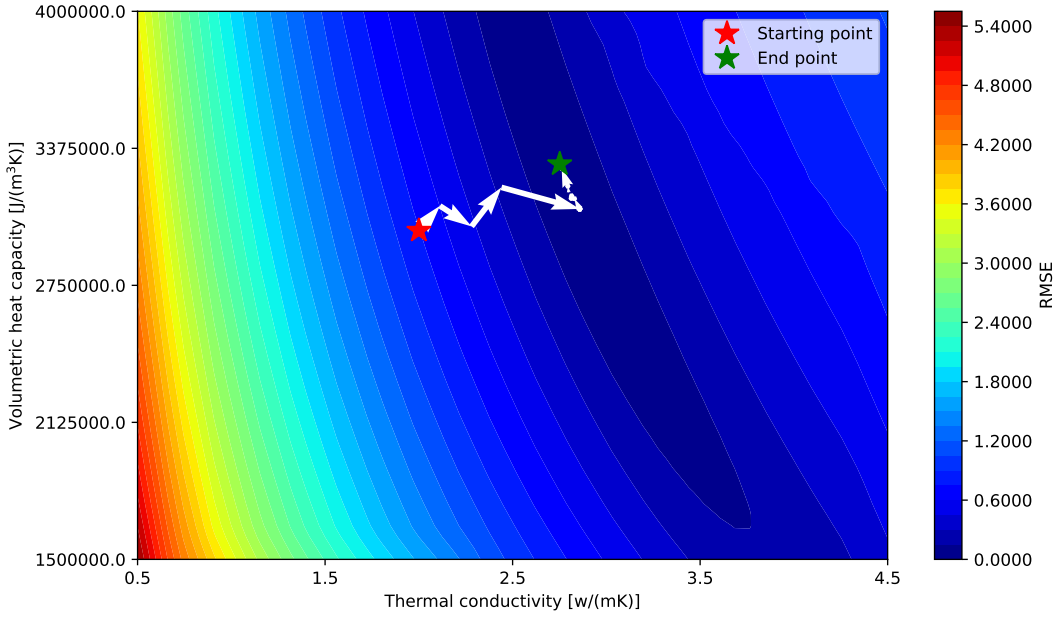


Figure 7.4.: Optimisation path of the inversion method for model test 1, with a thermal conductivity of 2.75 W/(mK) and a volumetric heat capacity of 3.3 MJ/(m$^3$K). The RSME found for this test is shown for the solution space with the thermal conductivity values on the x-axis and the volumetric heat capacity values on the y-axis.

In Figure 7.4, the RMSE is visualised for the raw data of test 1 and the solution space for various thermal values. The value of thermal conductivity affects the RMSE more than the value of the volumetric heat capacity. This is because the thermal conductivity has a higher influence on the thermal response of the probe than the volumetric heat capacity, as in shown by Figure 6.8a & 6.10a.

### 7.2.1. Initial values

To test the robustness of the method, the effect of the starting value of the model was examined. Model test 1 was run for four different initial values (Table 7.2). The results of this analysis are shown in Figure 7.5. The same result was found for all tests, thus the starting value of the inversion method is independent from the end value found.

Table 7.2.: Initial values used for analysing test 1.

| Testname | Thermal conductivity [W/(mK)] | Volumetric Heat Capacity [MJ/(m$^3$K)] |
|---|---|---|
| Test 1.1 | 1.5 | 2.125 |
| Test 1.2 | 1.5 | 3.375 |
| Test 1.3 | 3.5 | 3.375 |
| Test 1.4 | 3.5 | 2.125 |

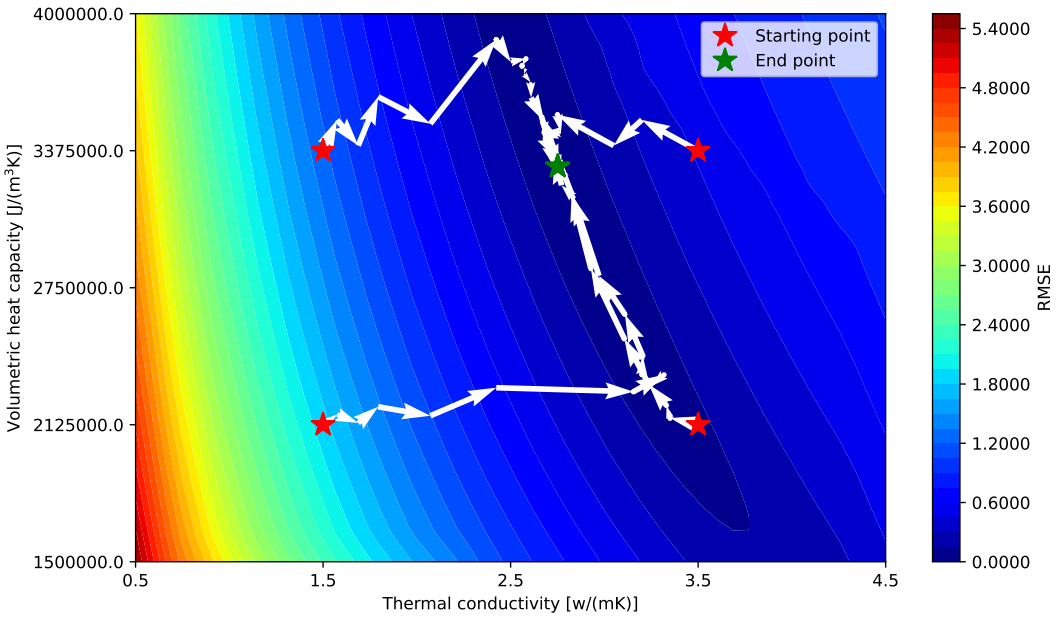


Figure 7.5.: Optimisation path of the inversion method for model test 1, with four different initial thermal property values. The RSME found for this test is shown for the solution space with the thermal conductivity values on the x-axis and the volumetric heat capacity values on the y-axis. The starting values of the tests are shown in Table 7.2.

### 7.2.2. Run time and storage

To find out if the inversion is suitable for offshore side investigation, it is important to know the run time and storage space required of the inversion method. The run time of a single test is less then 0.2 seconds, which is sufficiently fast. The total data required for the inversion method and solution space files is 168 kB, which is also sufficiently low for practical use of the method.

### 7.2.3. Conclusion

The inversion method shows potential for being suitable for the interpretation of the heat flow cone penetration test. The method found the correct values of the volumetric heat capacity and thermal conductivity within a 2% accuracy range when using data generated by the COMSOL model. The runtime of the method is short and the storage space of the method is low. However, the inversion method was only tested with the same COMSOL model as for which the data in the solution space is generated. This means that it is possible for the inversion method to find a perfect match between the input data and the data generated from the solution space. For real test data, the COMSOL model and the input data likely do not match perfectly. To verify the method, an analysis with the HF-CPT laboratory test data is needed to examine how the inversion method handles possible discrepancies between the COMSOL model and the data obtained by measurement with the HF-CPT.

## 7.3. Testing the inversion method with laboratory test data

### 7.3.1. Improvement forward model

Before the inversion method was validated with laboratory test data, a new COMSOL model was generated which uses the precise geometry of the test probe. This model accurately predicts the behaviour of the test probe and is a improvement compared to the preliminary COMSOL model (Figure 7.6). The mesh of the COMSOL model is shown in Figure 7.7.

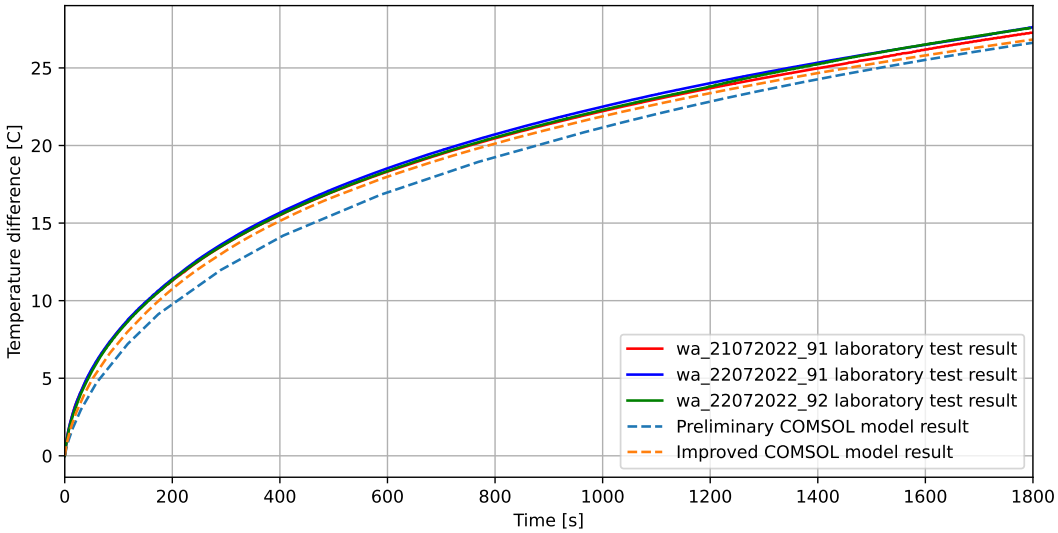


Figure 7.6.: Comparison of the preliminary and improved COMSOL model (striped lines) to the laboratory test results of the water test normalized for a power level of 20 W (solid lines) with the time on the x-axis and the temperature difference on the y-axis. For both the COMSOL models, the known thermal properties of water are used as the input (k=0.6 W/(mK), C=4.14 MJ/($m^3$K)).

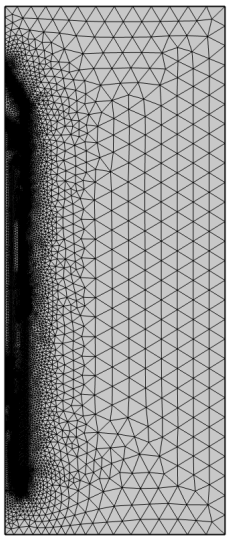

Figure 7.7.: Mesh of the HF-CPT COMSOL model used for the generation of the solution space of the inversion.

### 7.3.2. Construction solution space

To validate the inversion method, the laboratory test results were interpreted with the inversion method. The solution space of the inversion method was generated for the following values:

- 20 linearly spaced thermal conductivity values from 0.5 to 4.5 W/(mK)
- 20 linearly spaced volumetric heat capacity values from 1.0 to 4.0 MJ/(m$^3$K)
- 50 logarithmically spaced time points from 1 to 900 s
- A power level of 20 W

### 7.3.3. Results of the inversion to find the thermal conductivity and volumetric heat capacity

A comparable trend was found for all laboratory tests when analysing the test data with the inversion method. In Figure 7.8, the results of the inversion method on a laboratory test with water as a reference material are shown. The stating point of the inversion (the red star in Figure 7.8) was chosen at the known thermal property values of water, which are a thermal conductivity of 0.598 W/(mK) and a volumetric heat capacity of 4.14 MJ/(m$^3$K). After running the method, this point was not found as the optimal solution. A point was found with a significantly lower volumetric heat capacity and a slightly higher thermal conductivity where the RMSE had the lowest value. This trend of finding a significantly lower heat capacity outside the expected range was found when analysing all data from the laboratory tests.

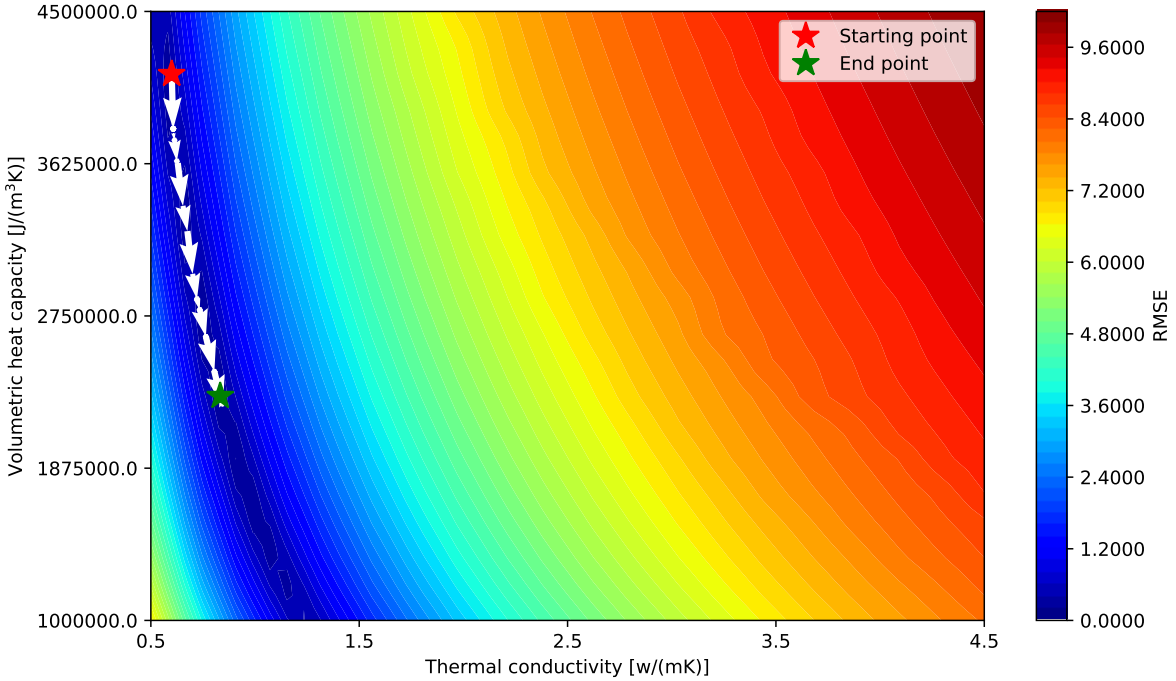


Figure 7.8.: Inversion method results of water test wa_21072022_91 with the initial estimation of k=0.598 W/(mK) and C=4.14 MJ/(m$^3$K), which are the known thermal properties of water. The RSME found for this test is shown for the solution space with the thermal conductivity values on the x-axis and the volumetric heat capacity values on the y-axis.

When comparing the results of the water test with the result generated by the solution space for the starting point of the inversion method, a close resemblance to the laboratory test data was found

(Figure 7.9a). However, at the endpoint of the inversion method, a slightly better resemblance to the laboratory test data was found (Figure 7.9b). The following can be concluded:

- The inversion method works as expected. The thermal property values for which the COMSOL model and the laboratory test results have the smallest mean square error was found.
- Due to discrepancy between the COMSOL model and the laboratory test results, the inversion algorithm found thermal property values outside of the expected range.
- The inversion method showed to be highly sensitive for the volumetric heat capacity. Small discrepancies between the COMSOL model and the laboratory test results led to mayor differences in the found volumetric heat capacity. This is due to the limited effect of the volumetric heat capacity on the temperature difference, mainly influencing the starting phase of the heating.

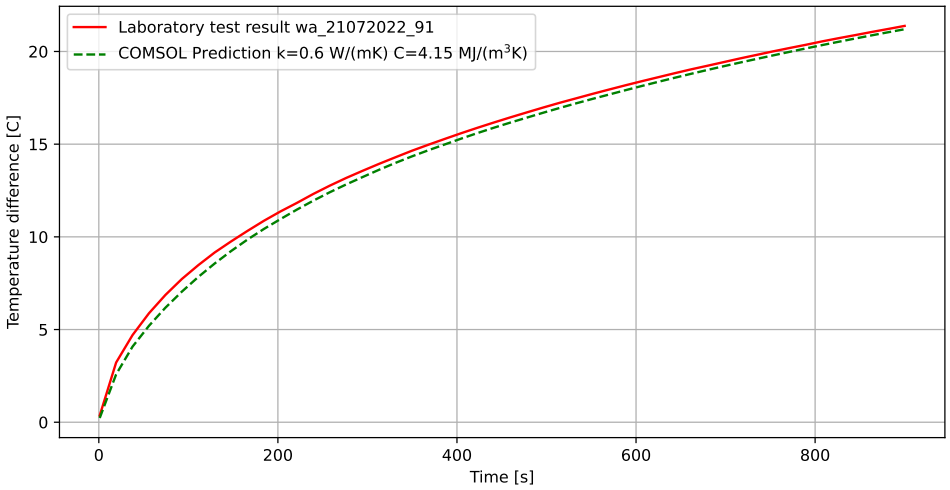


(a) Water laboratory test result (red solid line) compared with the inversion begin point result (green striped line), which is the COMSOL simulation for the expected thermal property values of water. The temperature difference, normalized for a power level of 20 W, is shown on the y-axis, the time is shown on the x-axis.

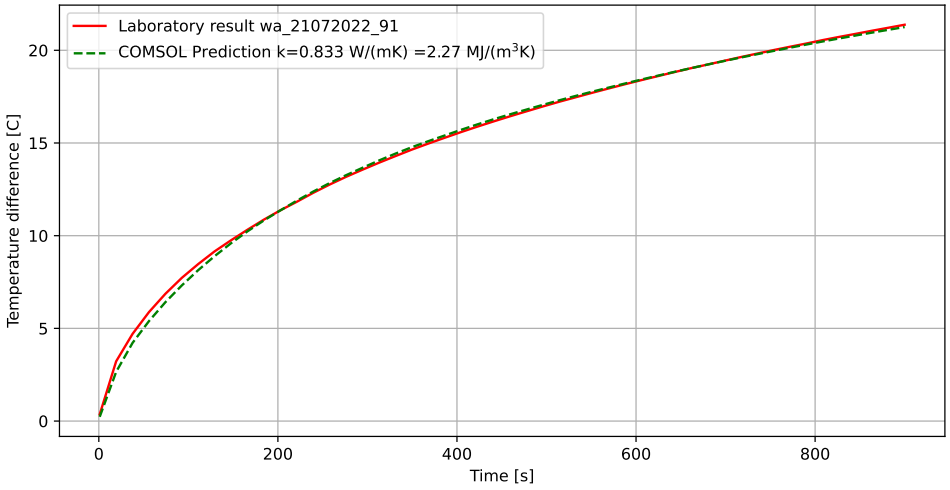


(b) Water laboratory test result (red solid line) compared with the inversion end point result (green striped line), which is the COMSOL simulation for found thermal property values of water. The temperature difference, normalized for a power level of 20 W, is shown on the y-axis, the time is shown on the x-axis.

Figure 7.9.: Comparison of the laboratory test result and the generated result by the inversion algorithm.

### 7.3.4. Volumetric heat capacity prediction

When using the HF-CPT in an offshore environment, new uncertainties affect the test results, for example due to soil disturbance. As the inversion method has proven to be sensitive in finding the

expected volumetric heat capacity, these uncertainties could strongly affect the results of the inversion method. However, this issue can be mitigated by using an estimation of the volumetric heat capacity in the inversion method. Vardon and Peuchen (2020) proposed a correlation relating the normalized cone resistance and normalized friction ratio, which are standard values found when performing a CPT, to the volumetric heat capacity of the soil. This information can be used in the inversion method in two separate ways.

- Fixing the volumetric heat capacity value. The predicted volumetric heat capacity value is used as an input to the inversion method beforehand. Then the inversion method is only performed to find the thermal conductivity.
- Regularization of the inversion method. An error function is added to the inversion method that penalizes the minimization solver for found volumetric heat capacity values that do not align with the predicted value. The further the found value is from the expected value, the more penalty is added.

Both these strategies were considered in the thesis. First an analysis of the results fixing the volumetric heat capacity was conducted. Secondly, an explanation and analysis of the regularization of the inversion method was described.

### 7.3.5. Inversion with fixed volumetric heat capacity value

Is this section, the laboratory tests were inverted with a fixed volumetric heat capacity value. The fixed volumetric heat capacity values were estimated based on the results of the in-situ laboratory dual thermal needle probe and hot disk tests (Table 5.1) in combination with the estimated volumetric heat capacity from the densities of the soil (Table 5.2). The results of the inversion with a fixed volumetric heat capacity value are shown in Appendix C.1. The average values of the inversion method and thermal needle probe test is shown in Table 7.3.

Table 7.3.: Results of the inversion method with a fixed volumetric heat capacity value without thermal contact resistance.

| Soil type | Fixed volumetric heat capacity value [MJ/(m$^3$K)] | Average thermal conductivity inversion method [W/(mk)] | Average thermal conductivity single needle probe test [W/(mk)] | Relative error [-] |
|---|---|---|---|---|
| Moist sand | 1.30 | 1.1278 | 1.1051 | 0.021 |
| Saturated sand | 2.84 | 1.8427 | 2.0826 | 0.117 |
| Kaolin Clay | 3.36 | 1.1550 | 1.3314 | 0.132 |
| Water | 1.14 | 0.5680 | 0.5980 | 0.050 |

The variation between values found on tests with the same material is similar to the variation of single thermal needle probe test results. However, apart from the moist sand test, the average thermal conductivity found with the inversion method was consistently lower than the average found with the single thermal needle probe test. This is due to discrepancies between the COMSOL model prediction and the laboratory test results. The COMSOL model under-predicts the amount of temperature that is generated in the probe, especially during the first five minutes of heating.

### 7.3.6. Thermal contact resistance

A possible reason for the underestimation of the amount of temperature generated in the probe by the COMSOL model is the lack of thermal contact resistance in the model. In the COMSOL model, all interfaces between two materials have perfect conductance. In real life, the interface between two materials is a complex three-dimensional system with microscopic air gaps that influence the conductance of the material (Cooper et al., 1969). This can be approximated by defining a thermal contact resistance layer between materials. The inner and outer heating cylinder of the HF-CPT are pressed together with thermal paste in between the interface of the materials. This could result in

the conductance between the cylinders being not ideal and the inner cylinder warming up more. A thermal contact resistance layer is added to the COMSOL model at the interface of the inner and outer cylinder of the probe to simulate this behaviour (Figure 7.10). An analysis was performed to examine if adding thermal contact resistance results in a more reliable outcome when using the inversion method with the fixed volumetric heat capacity.

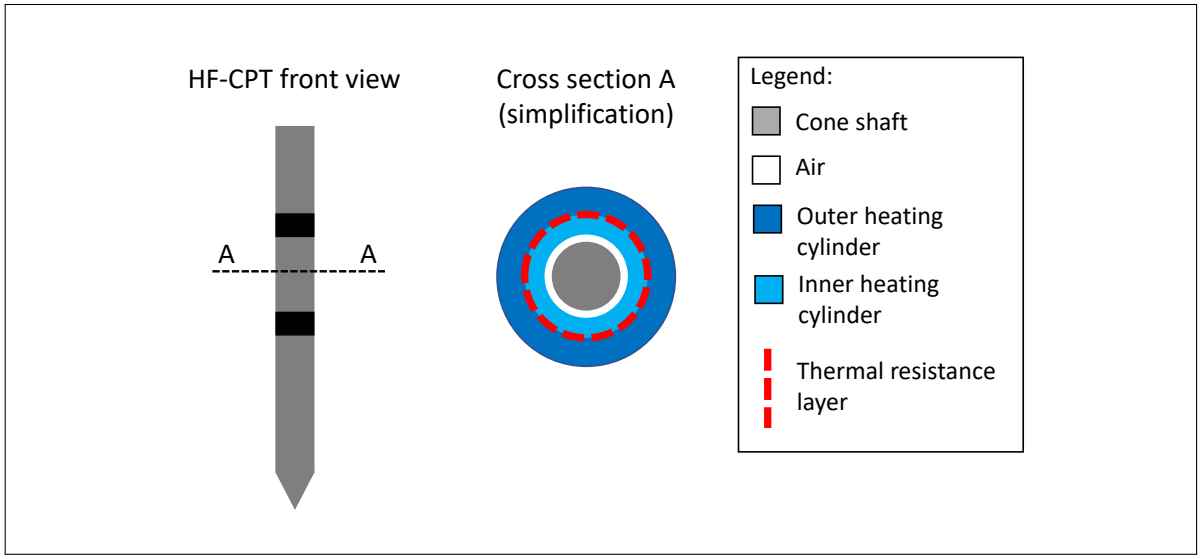


Figure 7.10.: Schematic overview of the location of the thermal resistance layer in the COMSOL model. For clarity, the thickness of the cylinders is not to scale.

#### Contact resistance study with water and saturated sand test

First, a parametric study was conducted to find out which values of thermal contact resistance led to representative results. To decrease processing time, the parametric study was only performed on the water and saturated sand tests. First, a single water and single saturated sand test were compared to the COMSOL simulation with the expected thermal properties and a range of thermal contact resistance values. The saturated sand and water showed the best match with the COMSOL simulation with a thermal resistance between 0.00005 $m^2K/W$ and 0.0002 $m^2K/W$ (Figure 7.11).

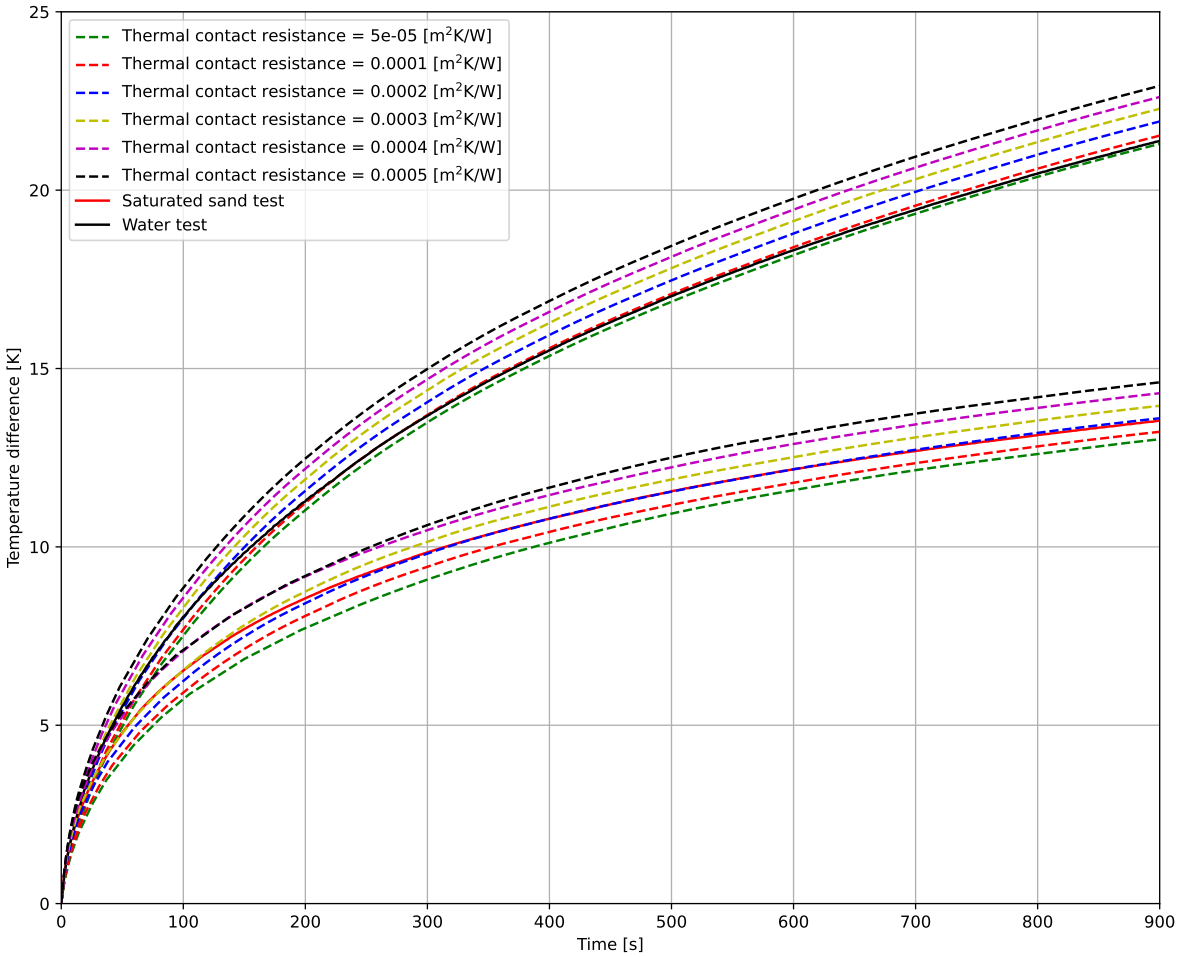


Figure 7.11.: Comparison between the laboratory test results of a water and saturated sand test (solid lines) and the COMSOL model with a range of contact resistance values (striped lines), with the temperature difference, normalized for a power level of 20 W, on the y-axis, and the time on the x-axis.

After this, the influence of the addition of the thermal contact resistance on the results of the inversion with a fixed volumetric heat capacity value for the water and saturated sand test was determined. For this, four different values were chosen that are within the expected range shown in Figure 7.11: 0.00005, 0.0001, 0.00015 and 0.0002 $m^2K/W$. A thermal contact resistance of 0.0001 $m^2K/W$ resulted in a relative error of less then 5% compared to the average thermal needle probe results for both tests (Figure 7.12). This value was chosen to run the full inversion with all soil types on.

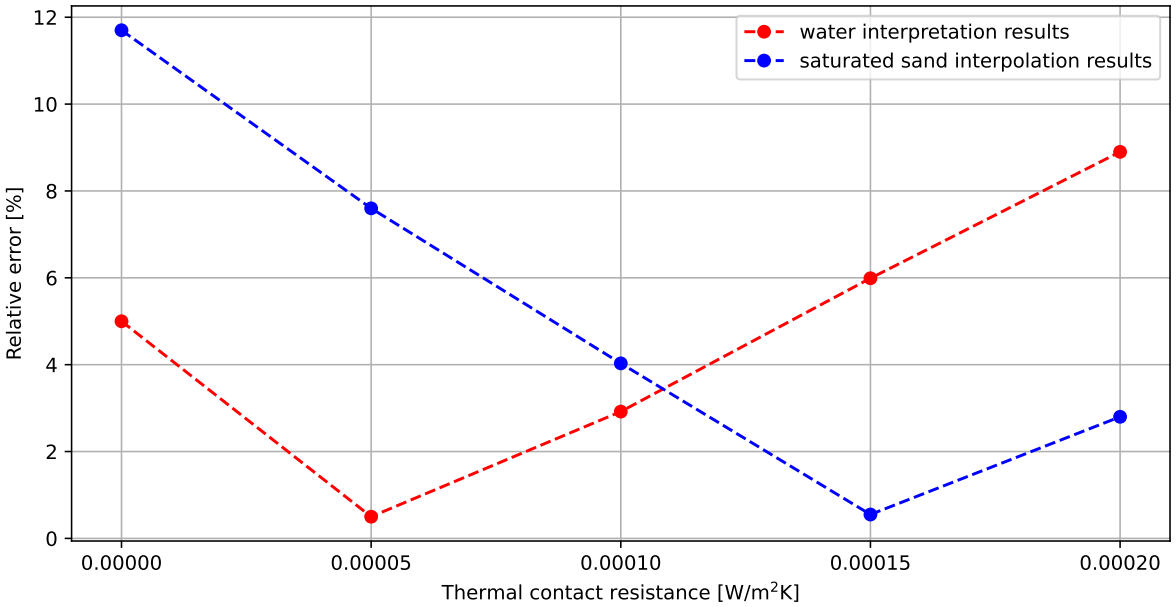


Figure 7.12.: Relative error found with the inversion over the thermal conductivity for a range of thermal resistance values for the water (red striped line with dots) and saturated sand (blue striped line with dots) tests, with the relative error on the x-axis and the thermal contact resistance on the y-axis.

#### Inversion with a thermal contact resistance of 0.0001 $m^2K/W$

The results of the inversion with an added thermal contact resistance of 0.0001 $m^2K/W$ to the COMSOL model is shown in Appendix C.2. The found mean thermal conductivity and relative error compared to the average thermal needle probe results is shown in Table 7.4. A significant improvement was found with the water, kaolin clay and saturated sand test. The relative error for the moist sand test increased.

Table 7.4.: Results of the inversion method with a fixed volumetric heat capacity value and an added thermal contact resistance of 0.0001 $m^2K/W$ between the inner and outer cylinder of the COMSOL simulation.

| Soil type | Fixed volumetric heat capacity value [MJ/($m^3$K)] | Average thermal conductivity inversion method [W/(mK)] | Average thermal conductivity single needle probe test [W/(mK)] | Relative error [-] |
|---|---|---|---|---|
| Moist sand | 1.30 | 1.2066 | 1.1051 | 0.092 |
| Saturated sand | 2.84 | 2.0028 | 2.0826 | 0.040 |
| Kaolin Clay | 3.36 | 1.2559 | 1.3314 | 0.056 |
| Water | 1.14 | 0.6155 | 0.5980 | 0.029 |

### 7.3.7. Regularization of the inversion method

As the volumetric heat capacity value found from either laboratory tests or a correlation always contains uncertainty, fixing the volumetric heat capacity value in the inversion is not desirable. Regularization of the inversion method might be more suitable, as there is less dependency of the predicted volumetric heat capacity value on the results of the inversion method. By regularizing the inversion method, an error function is added to the minimization solver which penalises the inversion method if a different value is found than the expected value. The further the solution is from the expected value, the higher the penalty of the function is. A quadratic loss function is added to the equation

that is minimized in order to achieve this. The quadratic loss function is symmetric in nature which means that no difference in penalty is made for over- or underestimation of the estimated volumetric heat capacity. The function that is minimized then consists of two parts:

- The RMSE function that gives the error between the raw data and the parametric space for specific thermal properties (Section 7.1.2).
- The quadratic error function that penalizes the method when volumetric heat capacity value is found that differs from the expected value.

In order to assure that these two parts have the same relative influence on the minimization solver, independent of the power level and thermal properties of the test, normalizations are performed. The RMSE is divided by the total temperature difference of the raw data to form the Normalized Root Mean Square Error (NRMSE) (Equation 7.3).

$$NRMSE = \frac{RMSE}{\max(\Delta T(t)) - \min(\Delta T(t))} \tag{7.3}$$

where

| | |
|---|---|
| $NRMSE$ | is the normalized root mean square error [-] |
| $RMSE$ | is the root mean square error (Equation 7.2) [-] |
| $\Delta T(t)$ | is the temperature difference of the raw data found for the inversion time points [K] |

All thermal conductivity and volumetric heat capacity values used in the minimization solver are also normalized beforehand, keeping all values within a range from 0 to 1. The minimization function combining the NRMSE and the quadratic penalty function is shown in Equation 7.4.

$$f(k_{norm}, C_{norm}) = NRMSE(k_{norm}, C_{norm}) + W_r \cdot (C_{exp;norm} - C_{norm})^2 \tag{7.4}$$

$$k_{norm} = \frac{k - \min(k_{data})}{\max(k_{data}) - \min(k_{data})} \tag{7.5}$$

$$C_{norm} = \frac{C - \min(C_{data})}{\max(C_{data}) - \min(C_{data})} \tag{7.6}$$

$$C_{norm;exp} = \frac{C_{exp} - \min(C_{data})}{\max(C_{data}) - \min(C_{data})} \tag{7.7}$$

where

| | |
|---|---|
| $f()$ | is the function that is minimized [-] |
| $W_r$ | is the regularization constant, a value from 0 to 1 [-] |
| $k_{data}$ | is the range of thermal conductivity values in the inversion solution space [W/(mK)] |
| $C_{exp}$ | is the expected value of the volumetric heat capacity, found by a CPT correlation or laboratory tests [J/(m$^3$K)] |
| $C_{data}$ | is the range of volumetric heat capacity values in the inversion solution space [J/(m$^3$K)] |

The regularization constant, $W_r$, determines the severity of the penalty added to the minimization. For a value of zero, no penalty for a deviation from the excepted volumetric heat capacity is added, so the inversion is the same as the regular inversion to find the thermal conductivity and the volumetric heat capacity. For a value of 1, the penalty of deviation is high, and the results tend to the results of the inversion method with a fixed volumetric heat capacity value. In a later stage, a penalty function that accounts for the expected thermal conductivity can be added to the method.

#### Results regularization

The effects of the regularization constant were examined by conducting the inversion method for a range of values of the regularization constant from zero to one. A thermal resistance between the inner and outer cylinder, proposed in Section 7.3.6, was added to the COMSOL model used for the inversion. Agreement with the average thermal conductivity values of the inversion method and the thermal needle probe values was found when using a regularization constant of 0.2 and larger for the saturated sand, kaolin clay and water tests (Figure 7.13).

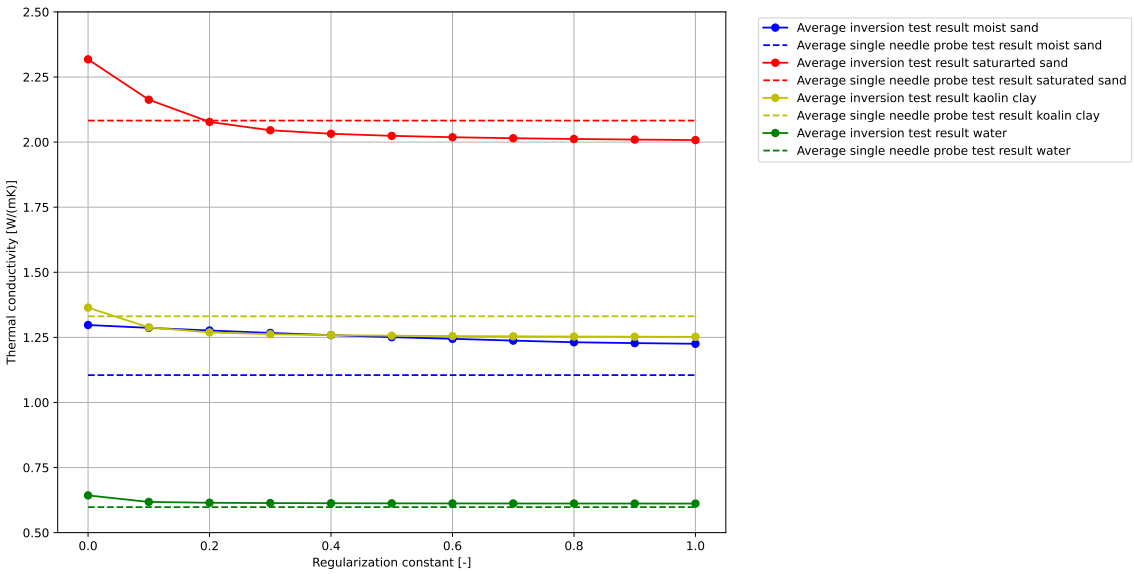


(a) Found thermal conductivity values of the inversion (y-axis) over the regularization constant (x-axis). The striped lines are the average thermal conductivity values found per material by the single needle probe test.

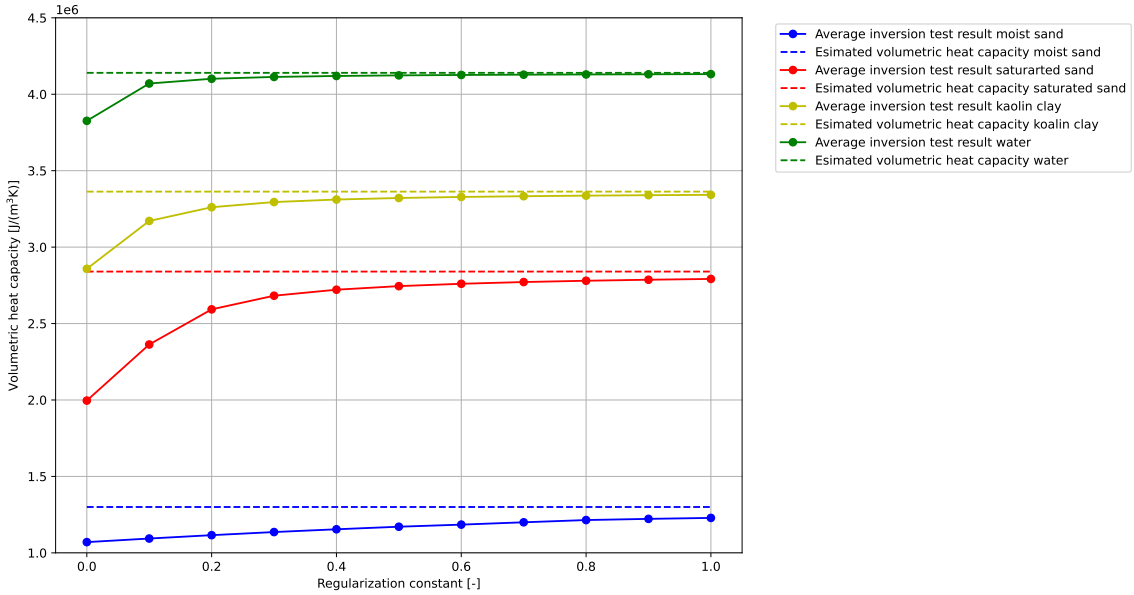


(b) Found volumetric heat capacity values of the inversion (y-axis) over the regularization constant (x-axis). The striped lines are the estimated volumetric heat capacity values used in the inversion penalty function.

Figure 7.13.: Effects of the regularization constant on the results of the inversion method. Eleven values of the regularization constant in a linear range from zero to one are tested.

To minimize the influence that the estimated volumetric heat capacity has on the inversion results, a regularization constant of 0.2 is proposed. The solution space of the regularized inversion method with a regularization constant of 0.2 and an added thermal resistance of 0.0001 $m^2K/W$ for a water test is visualised in Figure 7.14. The results of the regularized inversion method for all material tests are shown in Table 7.5 and are visualised in Appendix C.3. The average values found for the saturated

sand, kaolin clay and water tests were within 5% relative error from the found values of the single thermal needle probe test. The relative error of the moist sand test increased compared to the results with a fixed volumetric heat capacity value.

Table 7.5.: Results of the inversion method with an added thermal contact resistance of 0.0001 $m^2K/W$ between the inner and outer cylinder of the COMSOL simulation and an added penalty function for the estimated volumetric heat capacity with a regularization constant of 0.2.

| Soil type | Estimated volumetric heat capacity value [MJ/($m^3$K)] | Average thermal conductivity inversion method [W/(mK)] | Average thermal conductivity single needle probe test [W/(mK)] | Relative error [-] |
|---|---|---|---|---|
| Moist sand | 1.30 | 1.2782 | 1.1051 | 0.157 |
| Saturated sand | 2.84 | 2.0795 | 2.0826 | 0.004 |
| Kaolin Clay | 3.36 | 1.2765 | 1.3314 | 0.041 |
| Water | 1.14 | 0.6200 | 0.5980 | 0.037 |

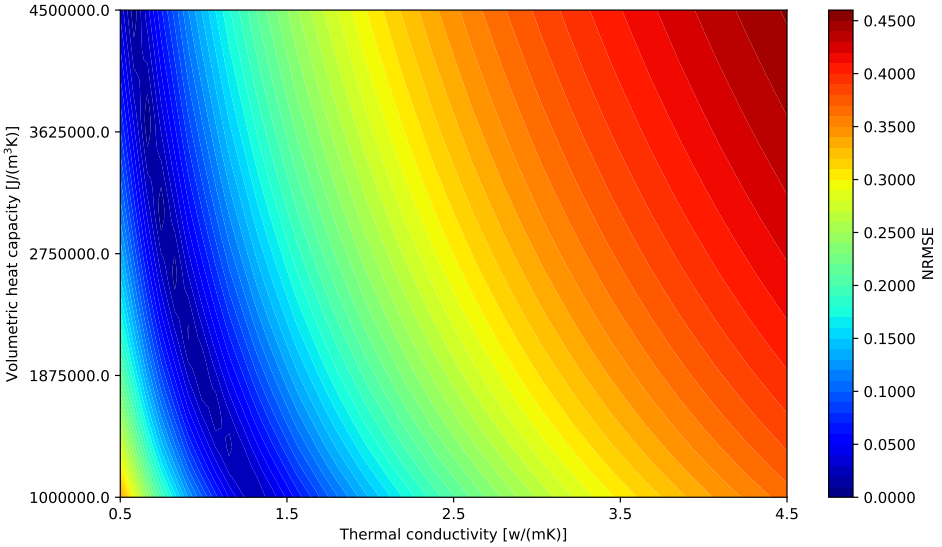


(a) Normalized root mean square error found for test wa_21072022_91.

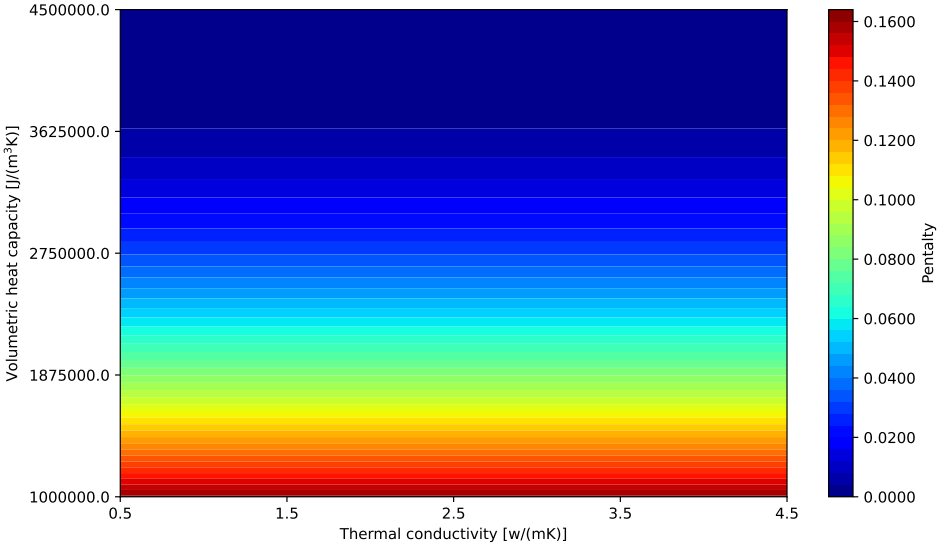


(b) Penalty function for a estimated volumetric heat capacity value of 4.14 MJ/($m^3$K) and a regularization constant of 0.2.

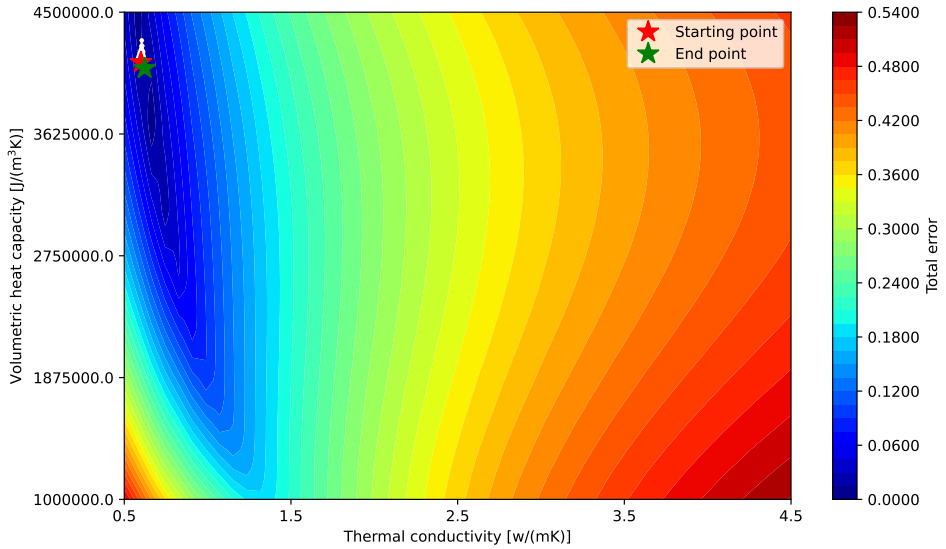


(c) Total error found shown for the solution space. This gained by adding the penalty function (b) to the NRMSE (a).

Figure 7.14.: Visualization of the minimization solver of the regularized inversion method for water test wa_21072022_91 with the thermal conductivity values on the x-axis and the volumetric heat capacity values on the y-axis.

### 7.3.8. Sensitivity estimated volumetric heat capacity value

#### Sensitivity analysis estimated volumetric heat capacity on all test results

As the inversion method with a fixed volumetric heat capacity value as well as the regularized inversion method are dependent on the estimated volumetric heat capacity value, it is important to examine the dependency of this value on the results. Estimating the volumetric heat capacity in the field with laboratory tests or a CPT correlation is prone to errors, thus a low dependency is preferred. A sensitivity analysis was performed by changing the estimated volumetric heat capacity by 10% and analysing the difference in the found average thermal conductivity value. This analysis was performed for the inversion method with a fixed volumetric heat capacity value and the regularized inversion method with a regularization constant of 0.2 on all laboratory test results. Both of these methods contained the thermal resistance of 0.0001 $m^2K/W$ added between the inner and outer cylinder of the COMSOL model. For the saturated sand, kaolin clay and water tests the regularized inversion method was slightly less dependent on the estimated volumetric heat capacity value compared to the inversion method with a fixed volumetric heat capacity value (Figure 7.15). For the moist sand test, a significantly smaller dependency on the estimated volumetric heat capacity value was found for the regularized compared to the fixed inversion. The small dependency for the moist sand test can be explained by two factors:

- The estimated volumetric heat capacity and found volumetric heat capacity for the regular inversion were relatively close for the moist sand test (Figure 7.13b). This means that the penalty function had a lower relative impact on the minimization solver.
- Due to larger discrepancies between the COMSOL model and the raw data of the moist sand test, the found NRMSE was relatively high. This means that the minimization solver was more affected by minimizing the NRMSE and the effect of the penalty function on the minimization was less.

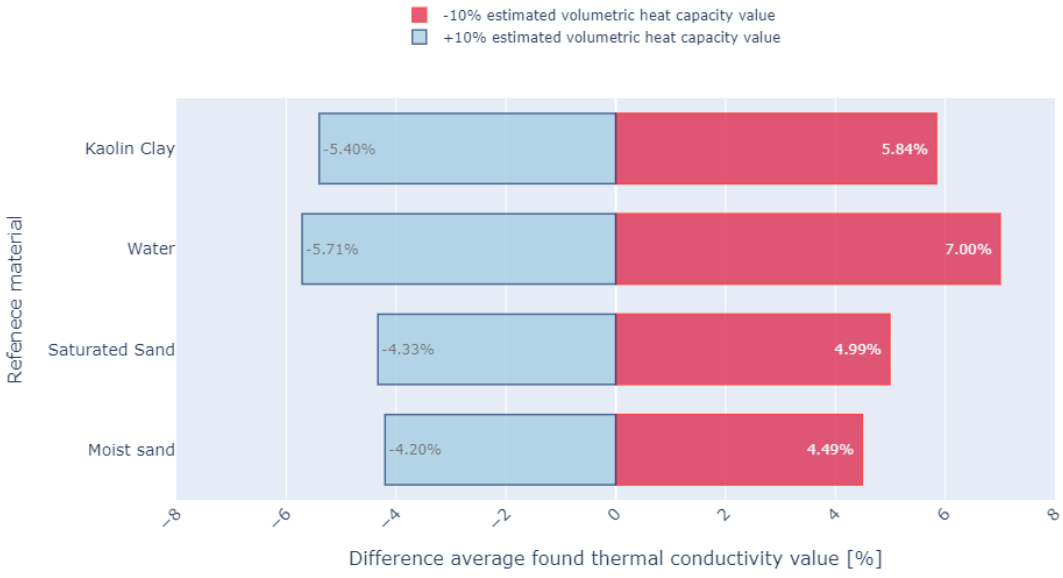


(a) Inversion with a fixed volumetric heat capacity value.

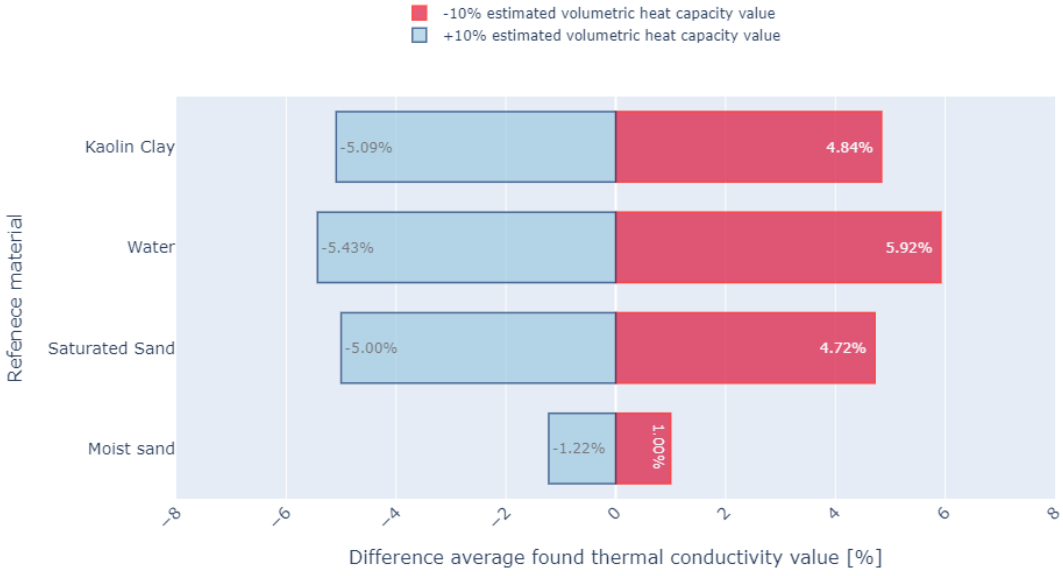


(b) Regularized inversion with a regularization constant of 0.2

Figure 7.15.: Sensitivity analysis on the estimated volumetric heat capacity value. The value used in the inversion method is changed by 10%. The difference in the average found thermal conductivity value is shown.

### Sensitivity analysis estimated volumetric heat capacity offshore soils

The main goal of the HF-CPT, is to find the thermal conductivity of offshore soils. Therefore, the influence of the estimated volumetric heat capacity is further examined for offshore soils specifically. Two materials tested in the laboratory represent an offshore soil type, namely saturated sand and

kaolin clay. For offshore sand/clay mixtures, the typical range of volumetric heat capacity values lays between 2.7 and 3.5 MJ/(m$^3$K) (Figure 2, Vardon and Peuchen (2020)). To study the influence of the volumetric heat capacity on offshore soils, the inversion method was performed with estimated volumetric heat capacity values covering this entire range. The regularized inversion method with a regularization constant of 0.2 was used in this study, as this method showed best agreement with the single thermal needle probe tests and has proven to be less dependent on the estimated volumetric heat capacity value. The maximum relative error found between the average single thermal needle probe tests and inversion results is 11% for the entire range of typical offshore soil volumetric heat capacity values of sand/clay mixtures (Figure 7.16). The relative error found over the estimated volumetric heat capacity shows a linear trend of $\sim$ 1.5% per 0.1 MJ/(m$^3$K). If no prediction of the estimated volumetric heat capacity value in the method is used, it is advised to use a median offshore volumetric heat capacity value of 3.1 MJ/(m$^3$K) as input of the method. In this way, the maximum relative error found would theoretically be $\sim$ 6% for offshore sand/clay mixtures. This is an agreeable relative error compared to other offshore thermal conductivity tests, thus the inversion method still gives acceptable results for offshore sand/clay mixtures without using a prediction of the estimated volumetric heat capacity value. However, significant improvements to the results of the method are found if an accurate estimated volumetric heat capacity value is used. For soils containing a significant amount of organic material, the range of expected volumetric heat capacity values is wider, and more care should be taken in providing an accurate estimated volumetric heat capacity value.

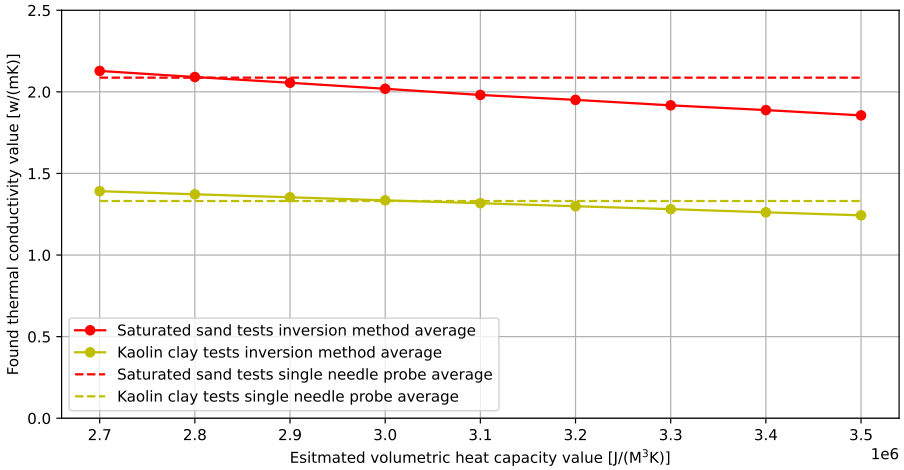


(a) Found thermal conductivity values of the inversion method (y-axis) over the estimated volumetric heat capacity value (x-axis). The striped lines are the average thermal conductivity values found per material by the single needle probe test.

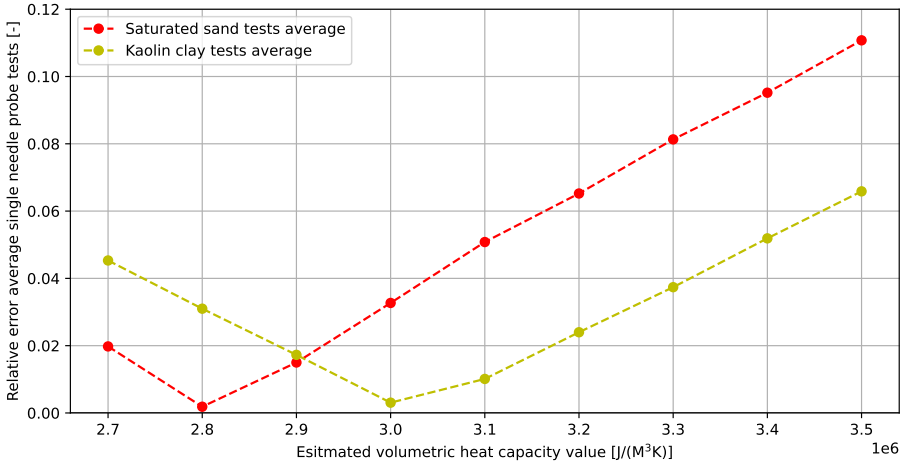


(b) Relative error between the found thermal connectivity values of the inversion method and the single needle probe tests (y-axis) over the estimated volumetric heat capacity value (x-axis).

Figure 7.16.: Sensitivity analysis on the estimated volumetric heat capacity value on offshore soils. The values of estimated volumetric heat capacity used lay in the typical range of offshore sand/clay mixtures.

### 7.3.9. Test time inversion

An objective of the test with the HF-CPT is that the test is performed in a relatively short time. The influence of the test duration on the inversion method results was examined. This examination was performed with the regularized inversion method with a regularization constant of 0.2 and an added thermal resistance of 0.0001 $m^2K/W$. The inversion time range was changed in equal steps of 100 seconds to have a test duration from 100 until 1500 seconds. 30 timepoints that are linearly spaced were used for each inversion test. For a test duration of 600 seconds, agreement was found with the average thermal needle probe values of the saturated sand, kaolin clay and water tests (Figure 7.17b,

7.17c and 7.17d). For an 800 second or longer test time, the results of these tests did not significantly differ.

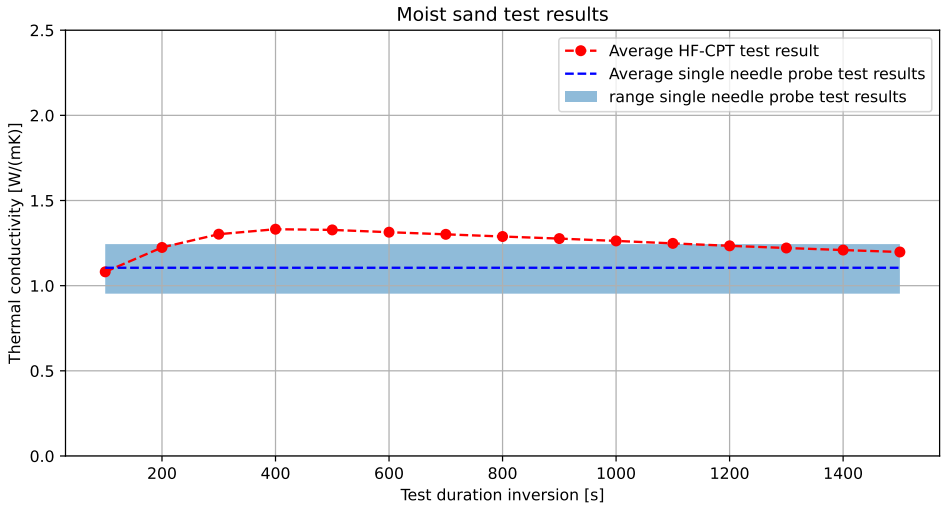


(a) Moist sand test results.

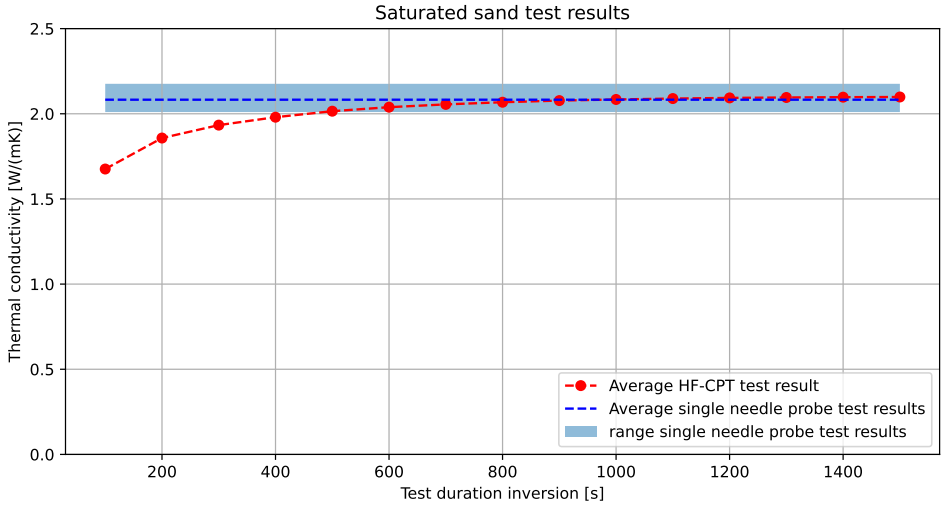


(b) Saturated sand test results.

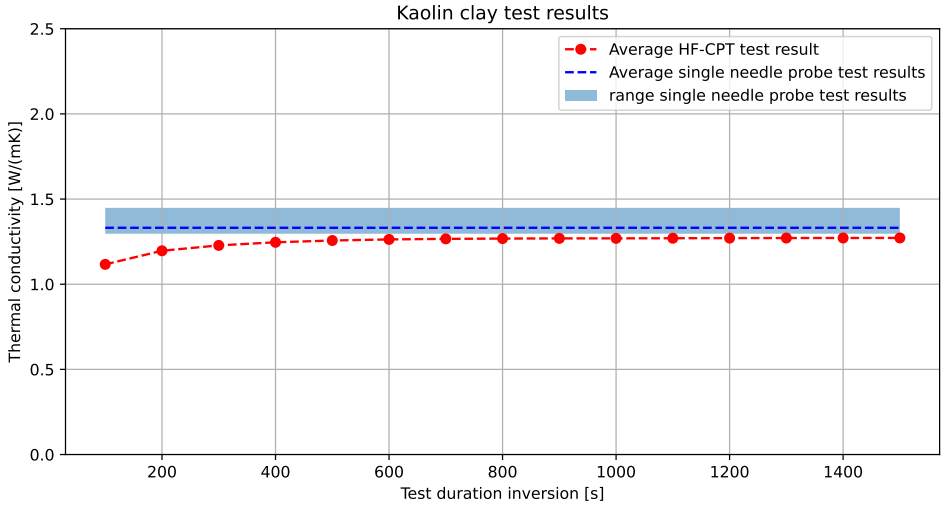


(c) Kaolin clay test results.

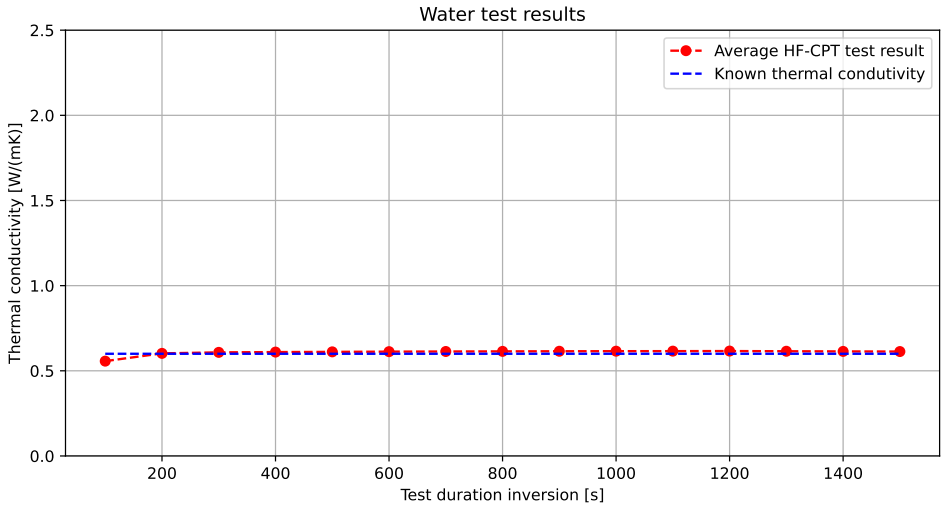


(d) Water test results.

Figure 7.17.: Regularized inversion results with a regularization constant of 0.2 for the laboratory tests for different time durations per reference material. 30 timepoints that are linearly spaced are used for each inversion test. 0.001 $m^2K/W$ thermal resistance is added to the COMSOL model used to generate the solution space. The thermal conductivity is shown on the y-axis, the test duration of the inversion is shown on the x-axis. The red striped line with dots is the average value found for the inversion method. The blue striped line is the average thermal needle probe test result. The blue box indicated the range of values found with the thermal needle probe test.

The minimum test time of 600 seconds is relatively fast when compared to similar methods that predict the in-situ thermal conductivity. For an both the T-CPT test (Section 2.3) and the in-situ thermal needle probe test (Section 2.4) a test duration of around 900 seconds is required (Fugro, 2021). For interpretation method of both the T-CPT and the thermal needle probe test, the log-linear gradient of temperature against the natural logarithm of time ($\ln(t)$) is used for the derivation of the thermal conductivity. For a heating test, this is only reached after a long timescale, which is defined as (Section 2.4.2):

$$t > \frac{5Cr^2}{k} \tag{7.8}$$

Due to the relatively large diameter of the HF-CPT, this timescale will only be reached after a test duration for over one hour for high conductive offshore soils. Therefore, it can be concluded that using the log-linear gradient of temperature against $\ln(t)$ for the interpretation of the HF-CPT is significantly more time consuming compared to the proposed interpretation method. It also needs to be noted that with the current geometry of the HF-CPT, taking the log-linear gradient of temperature against $\ln(t)$ does not result in accurate results due to the heat flow though the soil not only flowing in the radial direction (Section 6.2).

## 7.4. Discussion

An inversion method was constructed that uses a numerical finite element forward model. This method performed well when tested with data generated by the preliminary COMSOL model. The runtime of the method is short and the storage space of the method is low. To verify the method, an analysis with the HF-CPT laboratory test data was performed.

The tests with the test probes were interpreted with the following inversion methods:

- The 'regular' inversion method to find both the thermal conductivity and the volumetric heat capacity (Section 7.3.3)
- The inversion method with a fixed volumetric heat capacity value (Section 7.3.5)
- The inversion method with a fixed volumetric heat capacity value and an added thermal resistance of 0.001 $m^2K/W$ between the inner and outer cylinder of the heating element (Section 7.3.6)
- The regularized inversion method with a regularization constant of 0.2 and an added thermal resistance of 0.001 $m^2K/W$ between the inner and outer cylinder of the heating element (Section 7.3.7)

The result of these inversion methods were compared to the results of the reference material tests (Table 5.1). However, caution must be taken when comparing these results because of the following reasons.

The reference material tests do not determine the thermal properties with a complete accuracy, but also contain a certain measurement error. Next to this, the reference material tests only examined a small part of the material. All reference tests were performed within in the top 5 cm of the material. The middle of the heating element of the test probe, where the temperature sensors were located, was at a deeper level of 20 cm from the top of the material. Local differences in the reference materials, for example differences in density or saturation, could lead to a differences of the thermal properties throughout the sample. This could result in a deviation of the reference tests results compared to the test probe results.

The material most prone to this effect is the moist sand, as this has proven to be the least uniform material (Section 5.3.1). As this soil was neither completely saturated nor completely dry, local saturation differences were likely present is the sample. Although the top of the samples was covered with film, evaporation can result in the saturation of the material being lower at the top of the sample. ASTM (2014) states that redistribution of water due to thermal or hydraulic gradients could lead to significant error in the thermal needle tests. Another factor that could influence the moist sand tests is the presence of convection throughout the sample. Mondal et al. (2018) reported that the heat-transfer mechanism occurring in dry sand is not only conductive behaviour, but also convective heat-transfer takes place. This could lead to discrepancies between the COMSOL model used to construct the solution space and the test probe temperature data, influencing the found value of the inversion.

For the saturated sand tests, the soil was flooded and a fully saturated sample was not guaranteed. Microscopic air bubbles can be present in the soil, influencing the heat transfer throughout the soil. For the kaolin clay, small air gaps can be present in the material due to the layered build up of the material, also influencing the heat transfer of the soil.

The COMSOL model used to construct the solution space of the inversion method assumed perfect conductance between the soil and the probe. When constructing the samples, care is taken to ensure good contact between the probe and the sample. However, contact resistance between the soil and probe can still occur, influencing the heat transfer.

For these reasons, the true thermal values of the materials tests that should be found with test probe remain unknown. The in-situ reference material tests form a reasonable basis for comparison, but due to the limited soil volume tested and measurement error of both methods, a perfect match between the test probe inversion method results and the reference material tests is not likely. However, due to the high number of reference tests performed per material, a valid estimation can be made for the expected range of thermal properties of the reference materials. For the tests with water, a more precise estimation of the thermal properties can be used, as this material has proven to be uniform (Section 5.3.1) and is widely used for calibration of thermal needle probe tests (ASTM, 2014).

For the 'regular' inversion method to find both the thermal conductivity and the volumetric heat capacity, the found thermal properties were outside the expected range based on the reference material tests. This was the most severe for the volumetric heat capacity values. This was caused by discrepancy between the COMSOL model used for the inversion and the laboratory test results. Due to the limited effect of the volumetric heat capacity on the temperature difference found, a small discrepancy leads to a large difference in the found volumetric heat capacity. This sensitivity of the inversion method for the volumetric heat capacity value is not desirable, as for offshore testing, uncertainties of the tests lead to an unreliable estimation of the thermal properties.

To overcome this issue, three inversion methods that use an estimated value of the volumetric heat capacity as input of the inversion were proposed. For the water, saturated sand and kaolin clay tests, the best agreement with the reference material tests was found for regularized inversion method with a regularization constant of 0.2 and an added thermal resistance of 0.001 $m^2K/W$ between the inner and outer cylinder of the heating element. For the moist sand test, the values found for this inversion method did not align with the results of the reference material tests. This could be caused by the non-uniformity of the material, with local saturation differences affecting the results. A disadvantage of this inversion method is the influence of the estimated volumetric heat capacity on the inversion results. For offshore soils, a 0.1 $MJ/(m^3K)$ difference in the estimated volumetric heat capacity value resulted in a difference in the found thermal conductivity value of $\sim$ 1.5%. However, as the range of expected volumetric heat capacity values for offshore soils is relatively small, the method was still found to be reliable. Because of the agreement with the reference material tests of the water, saturated sand and kaolin clay tests, and the dependence on the estimated volumetric heat capacity being relatively small due to the narrow range of expected volumetric heat capacity values of offshore soils, the inversion method with a regularization constant of 0.2 and an added thermal resistance of 0.001 $m^2K/W$ between the inner and outer cylinder of the heating element is proposed for the interpretation of the HF-CPT test data.

## 7.5. Conclusion

The third research question is:

*Can the inversion method combined with the suitable forward model accurately predict the thermal properties of the materials used in laboratory tests with the heat flow cone penetrometer?*

The 'regular' inversion method to find both the volumetric heat capacity and thermal conductivity could not accurately predict the thermal properties of the materials used in laboratory tests as this inversion method proved to be highly sensitive for the volumetric heat capacity. Small discrepancies between the laboratory test results and the COMSOL model used to generate the solution space of the inversion method led to large differences of the volumetric heat capacity.

In order to overcome this issue, multiple inversion methods were examined that used an estimated value of the volumetric heat capacity as an input. For offshore testing, an estimation of volumetric heat capacity can be correlated from CPT measurements (Vardon & Peuchen, 2020). A regularized inversion method with a regularization constant of 0.2 and an added thermal resistance of 0.0001

$m^2K/W$ between the inner and outer cylinder of the heating element is proposed for the interpretation of the HF-CPT data. This method showed excellent agreement with the reference material tests of the saturated sand, kaolin clay and water tests. For the moist sand test, a discrepancy between this method and the reference material test was observed. However, this can partially be accounted by the fact that the material is heterogeneous throughout the sample, and the reference material tests were performed at a different height then the height of the heating element of the test probe. The estimated volumetric heat capacity is of influence on the results of the inversion method. However, as the range of expected volumetric heat capacity values for offshore soils is relatively small, the method was still found to be reliable. A benefit of the inversion method is that already an agreement with the saturated sand, kaolin clay and water reference material tests was found for a test duration of 600 seconds. This is significantly fast when compared to other in-situ tests to find the thermal conductivity of the soil.

# 8. Practical design considerations

The inversion method was successfully validated with the laboratory tests. However, before the test procedure for offshore side investigation with the HF-CPT can be determined, some practical design questions need to be considered. The final research question is:

*Which practical design conditions need to be addressed before the test procedure of an offshore heat flow cone penetration test can be determined?*

The following two key design considerations were addressed in this chapter:

- Heating of the probe due to soil friction
- Probing depth

## 8.1. Heating of the probe due to soil friction

The inversion method assumes the soil and probe to be at the same temperature before testing. For the laboratory tests, this assumption was valid, as the test setups were constructed in a climate room at least 24 hours before the start of the test. For offshore tests this assumption has not been proven to be correct.

When the probe penetrates the soil, the cone heats up due to soil friction. Both the cone tip resistance and the sleeve friction induce this effect. It is currently unknown how much the heating element of the HF-CPT heats up due to this phenomenon, as no field test are performed with the HF-CPT. Berthet (2019) assumed the heating of the probe due to sleeve friction to be negligible compared to the cone tip resistance. In addition, it was assumed that the heat transfer between the cone tip and the rest of the penetrometer is limited. If this assumption is correct, the effect of the heating due to the soil friction is limited for the heating element of the HF-CPT. However, no research is available that validates this assumption. A study was performed to examine the effect on the inversion method of a temperature difference between the probe and the soil before testing.

### 8.1.1. No initial cooling period

First, the effect of a temperature difference between the probe and the soil was examined when the heating of the probe is started as soon as the HF-CPT is stopped, without an initial waiting period for the probe to cool down. The COMSOL model was run for different initial temperature differences between the probe and the soil of 0 to 10 K. The probe had a higher temperature than the soil. The thermal response of the probe is visualised in Appendix D. For large temperature differences, a drop in temperature occurred in the probe before the temperature increased (Figure D.1). As the soil has a lower temperature than the probe, the probe is cooled by the soil. For large temperature differences, this effect is initially larger than the effect of the probe heating up due to the heater, hence the initial temperature drop. Due to this behaviour, the inversion method did not perform well if a temperature difference is present between the probe and the soil and no initial cooling period is performed during testing, as the found values of the inversion were at the boundary of the solution space.

### 8.1.2. Cooling period parametric study

Adding cooling time before heating up the probe led to better results. A study was performed to examine the effect of adding an initial cooling time before the probe is heated. A cooling time from 100 to 400 seconds was analysed. The thermal response of the probe for a cooling period of 300 seconds is visualised in Appendix D. When performing the inversion method with the temperature difference found from the start of the heating, a shorter cooling period and a larger initial temperature difference led to a larger relative error in the found thermal conductivity value (Figure 8.1).

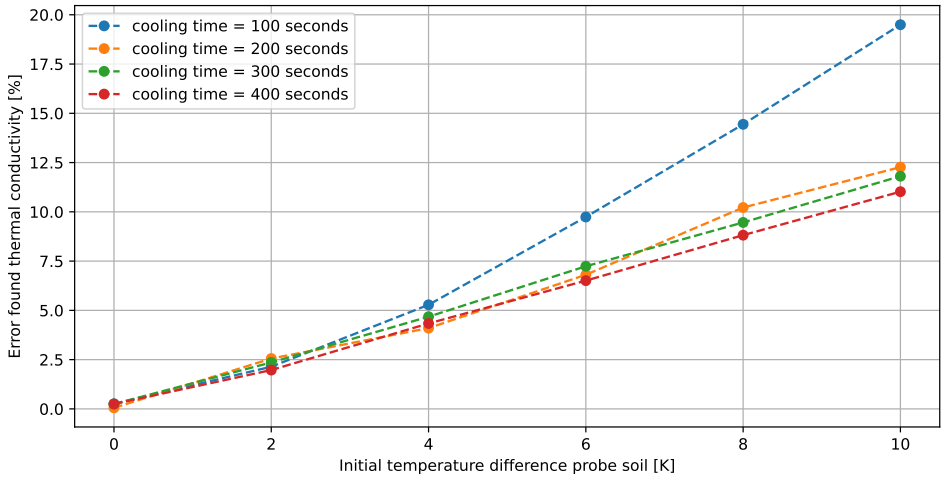


Figure 8.1.: The relative error found for the inversion method (y-axis) over the initial temperature difference between the probe and the soil (x-axis) with the COMSOL model as the raw data with initial cooling periods from 100 to 400 seconds. The thermal properties of the soil used in the COMSOL model represent the expected thermal properties of saturated sand. The heater power level is 20 W.

### 8.1.3. Heater power parametric study

Next to the cooling time duration, the amount of power used also influences the accuracy of the inversion method when the probe and the soil do not have the same initial temperature. A parametric study was performed with various heater power levels and an initial cooling time of 300 seconds. This study showed that more accurate results are found when the heater power used for the test increased (Figure 8.2).

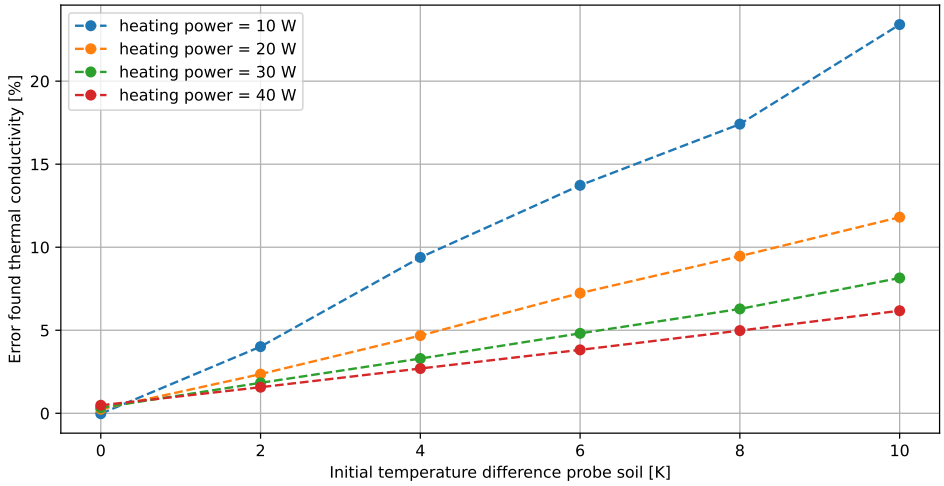


Figure 8.2.: The relative error found for the inversion method (y-axis) over the initial temperature difference between the probe and the soil (x-axis) with the COMSOL model as the raw data with various heater power levels from 10 to 40 W. The thermal properties of the soil used in the COMSOL model represent the expected thermal properties of saturated sand. A initial cooling period of 300 seconds is simulated during the test.

### 8.1.4. Conclusion

When a temperature difference was present between the soil and the probe at the beginning of testing and no initial cooling time has been taken, the inversion method did not give reliable results. However, there are two factors that can improve the accuracy of the method. First, an initial cooling time was added to the test. The longer the duration of the cooling was, the more accurate the method got. However, extending the total test duration for a large amount of time is not preferable, as the goal is to have a relatively fast testing duration. Secondly, the heater power of the test was adjusted. For a higher heater power, more accurate results were found when having an initial cooling time of 300 seconds. If more information is found on the expected temperature difference of the test, the test procedure can be adjusted accordingly based on the results of the parametric studies presented in this section.

### 8.1.5. Alternative solutions

In both the cooling time and the heater power parametric study, the relative error found with the inversion method increased as the initial temperature difference between the soil and the probe got larger. It is possible that the temperature difference between the probe and the soil is deemed too large to give reliable results. In this case, there are two alternative solutions possible to still successfully use the HF-CPT.

The first solution is extending the distance between the cone of the CPT and the heating element of the HF-CPT. Is is expected that the heating element is less affected by the heating due to soil friction the further the probe is from the cone tip. However, due to practical design considerations, for example due to a limitation in installation height of the probe, this might not be preferable for offshore testing.

The second solution is combining a HF-CPT with a T-CPT (Section 2.3) during a single offshore test. In this case, the T-CPT can be conducted if the soil friction causes the cone to heat up significantly, while the HF-CPT can be used when there is less heat generated by the soil friction. The cone must heat

up approximately 3 degrees before a T-CPT test can be performed (Vardon et al., 2018). It is expected that the heating of the cone tip, where the T-CPT temperature sensor is located, is larger compared to the heating of the HF-CPT heating element. Therefore, a HF-CPT test is suitable when the heating of the cone is insufficient for a T-CPT test.

## 8.2. Probing depth

An important design consideration is how much soil volume is tested during a single test. This can be expressed as the probing depth. The probing depth is the maximum radial distance from the heater of the probe for which the soil is affected by the heating of the probe. For a thermal needle probe, the probing depth can be estimated with the following equation (Hütter & Kömle, 2012):

$$P_d = \sqrt{6.7 D t_{test}} \tag{8.1}$$

where

$P_d$ is the probing depth [m]
$D$ is the thermal diffusivity of the soil ($\frac{k}{C}$) [$m^2/s$]
$t_{test}$ is total test duration [s]

As the HF-CPT can not be accurately simulated by the analytical solution of the line heat source due to the two-dimensional heat flow and the complex inside of the probe (Section 6.2), Equation 8.1 can not be used to estimate the probing depth of the HF-CPT. The probing depth can however be estimated by visually inspecting the reach of the isothermal contours of the COMSOL model simulation. A study was performed where this is examined for three different thermal diffusivity values: $0.3*10^{-6}$, $0.8*10^{-6}$ and $1.3*10^{-6}$ $m^2/s$. These values were chosen, as they lay in the typical range of offshore soils. The highest value of thermal diffusivity is typical for a dense sand, while the lowest value is representative for a soft clay. A chart was made which related the probing depth to the test duration for the three thermal diffusivity values (Figure 8.3). From this chart, an estimation of the minimum test duration in order to reach a certain probing depth can be made.

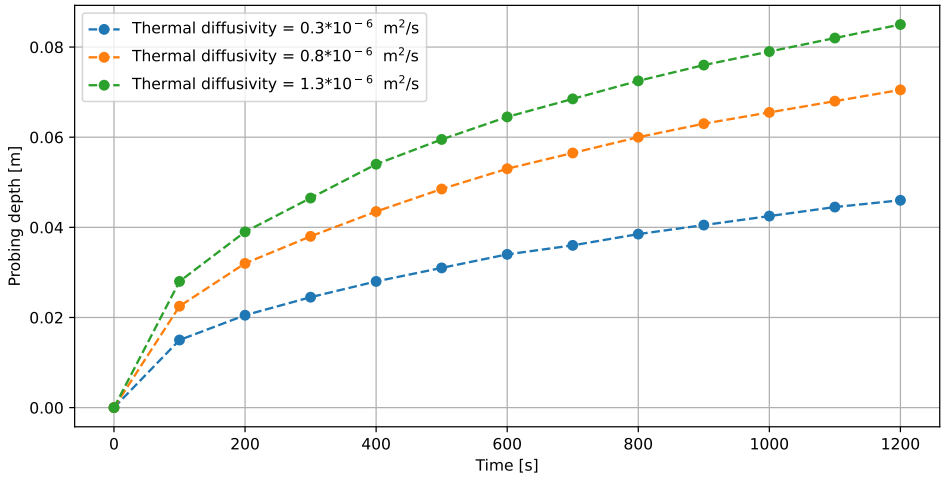


Figure 8.3.: The total test duration (x-axis) over the probing depth (y-axis) found by visually expecting the isothermal contours of the COMSOL model for a thermal diffusivity of $0.3*10^{-6}$, $0.8*10^{-6}$ and $1.3*10^{-6}$ $m^2/s$.

## 8.3. Final advice testing procedure

With the conducted studies, a final advice on the testing procedure of the HF-CPT is given. Three aspects of the test procedure are considered: the heater power of the test, the test duration and the possibility to perform a cooling test.

### 8.3.1. Heater Power

Due to practical considerations, it is beneficial to use the least amount of power needed to conduct a successful test. Because differences in heater power levels can be normalized (Section 5.3), there is some flexibility in choosing a heater power level of the test. However, there are two factors that influence the amount of power needed for a test:

- The power level has to be large enough that there is a measurable increase in temperature in the probe. To find the minimum power level for which there is a measurable increase in temperature in the probe, field tests can be performed with different power levels. The decrease in accuracy due to a lower power level can than be analysed.
- Based on the quantity of the initial temperature difference between the probe and the soil due to soil friction, the power level can be increased in order to get more reliable results (Section 8.1.3).

### 8.3.2. Test duration

As offshore soil investigation is relatively expensive, the test duration must be as short as possible. However, there are three factors that limit the minimum testing time.

- It was found that in order for the inversion method to perform well, a test of at least 600 seconds needs to be conducted (Section 7.3.9). If the forward model is improved to have a better match with the short-term thermal response of the HF-CPT, the minimum test duration could theoretically be shortened.
- A longer test duration increases the probing depth of the test (Section 8.2). If it is important to reach a specific probing depth during testing, the time needed to reach this probing depth might limit the minimum testing time. The time needed to reach a certain probing depth for three different thermal diffusivity values can be estimated from Figure 8.3.
- If the probe heats up due to the soil friction, an initial cooling period might be needed in order to get reliable results. This increases the total test duration. HF-CPT field tests need to be conducted in order to obtain knowledge about the amount of heating that the HF-CPT experiences due to soil friction.

### 8.3.3. Cooling test

The focus of this thesis was on performing a heating test with the HF-CPT. A cooling test can also be performed with the HF-CPT. When adapting the forward model to model a cooling test, the same inversion method can be used to interpret the data. A cooling test can be used in the test procedure in the following ways:

- Add a cooling test after the heating test of the HF-CPT is performed. The expectation is that this increases the accuracy of the tests, minimizing the effect of temperature drift similar to a thermal needle probe test (ASTM, 2014). However, adding a cooling test extends the total testing duration, which is not beneficial for offshore testing.

- Only perform a cooling test with the HF-CPT. During penetration of the soil, the heater of the HF-CPT can be activated. When the penetration is stopped, the heater is turned off, only performing a thermal dissipation test. This testing procedure has the benefit of not having an issue with the probe heating up due to the soil friction, as a temperature difference between the probe and the soil is required for the test to work. In order to examine the potential of this testing procedure, laboratory or field test data of the HF-CPT using this testing procedure is needed.

## 8.4. Conclusion

The final research question was:

*Which practical design conditions need to be addressed before the test procedure of an offshore heat flow cone penetration test can be determined?*

Two key design considerations were addressed in this chapter. First, the influence of the probe heating up due to the soil fiction was examined. If the soil heats up due to soil friction, the inversion method is not able to give accurate results. However, the testing procedure can be adapted in the following two ways to improve the accuracy of the method:

- An initial cooling period can be added to the test. The longer the cooling period is, the less the influence is of the initial temperature difference on the inversion method results.
- A higher power level can be used for the test. When an initial cooling period is added to the test, the inversion method results further improve when the power level of the test is increased.

If the temperature increase of the probe due to soil friction is deemed too high to give reliable results, the distance between the heating element of the HF-CPT and the cone tip can be increased. Next to this, the HF-CPT can be combined with a T-CPT in order to be able to test soils that cause a large temperature increase of the heating element of the HF-CPT.

The second design consideration examined was the probing depth achieved by a HF-CPT test. The probing depth is dependent on the test duration and the thermal diffusivity of the soil. A chart was constructed where the probing depth over the test duration is showed for three different thermal diffusivity values (Figure 8.3). If a specific probing depth is required, this could limit the minimum test duration of a HF-CPT test.

With the analysis performed in this chapter, a test procedure for offshore side investigation with the HF-CPT cannot yet be determined. The amount of heat generated on the heating element of the HF-CPT by the penetration of the probe must be analysed by performing field tests with the HF-CPT. Next to this, an analysis is needed examining the potential of a conducting a cooling test with the HF-CPT. However, a first advice on the testing procedure was given based on the analysis of design considerations presented in this chapter.

# 9. Discussion

Laboratory tests were performed with the HF-CPT in the climate room of the Delft University of Technology. In total, 32 tests with a test probe were performed in four different reference materials: moist sand, saturated sand, kaolin clay and a water-agar mixture. The water-agar mixture is a homogeneous material and widely used as a calibration material (ASTM, 2014). As similar results were found in the water-agar tests for different probes and different casts, it can be concluded that the tests are repeatable. For the other materials tested a larger discrepancy between test results was observed, with the moist sand test having the largest variance. This can be accounted to the fact that the materials are not homogeneous. Density and water content differences were likely present in the soil, which influenced the thermal properties of the soil.

To obtain information about the expected range of the thermal properties of the materials used in the laboratory, reference material tests were performed. These tests included single thermal needle probe tests, dual thermal needle probe tests, hot disk tests and density measurements. All tests were performed in the same cast as the tests with the HF-CPT test probe. It is important to note that the reference material tests do not give a completely accurate prediction of the tests, as these tests unavoidably contain measurement errors. Next to this, the tests only examined a small faction of the soil. Local density or water content differences in the materials could have affected the results of the reference material tests. Especially the moist sand test was prone to this, as it has proven to be a highly heterogeneous material. However, due to the high number of reference tests performed per material, a valid estimation can be made for the expected range of thermal properties of the reference materials.

In order to construct an interpretation method, a suitable forward model needed to be found. The forward model should be able to predict the thermal response of the probe for a wide range of thermal properties of the soil. The following three types of forward models were tested in this thesis:

- Numerical solution found with finite element modelling.
- Analytical solution of the asymmetric heat conduction equation (Equation 2.10).
- Semi-analytical solution of interpolating a g-function from numerical analysis.

No analytical solution of the asymmetric heat conduction equation was found that was suitable to use as a forward model. This is due two reasons. First, the heat transfer process in the soil is not one-dimensional due to the relatively short length compared to the diameter of the heating element. Secondly, the inside of the HF-CPT probe is complex as it contains multiple materials with specific dimensions. An analytical solution was not able to simulate the heat flow inside the probe to a reasonable accuracy. A forward model based on a numerical solution, either by directly using a numerical model or by interpolation a single g-function from the numerical results, showed potential, as the numerical COMSOL model developed in the thesis showed reasonable accuracy with the HF-CPT laboratory tests. Interpolating a single g-function from the numerical results has proven to be complicated, as a study needs to be performed to find new dimensionless parameters that could be used in the function. It is currently unknown if it is possible to find a single g-function that can accurately predict the thermal response of the HF-CPT. Therefore, it was chosen to use the numerical solution as forward model.

The chosen forward model, which is a numerical COMSOL model, was used in an inverse analysis. A direct data inversion method was constructed. This method had a short runtime and low storage space. When using data generated by the COMSOL model, the inversion method performed well, finding the correct values of the volumetric heat capacity and thermal conductivity within 2%

accuracy.

To verify the inversion method, the method was tested with the laboratory test data. The predicted volumetric heat capacity values were, however, outside the expected range of values found from the reference material tests. This was due discrepancies between the forward model prediction and the laboratory test results. The inversion method has proven to be highly sensitive in finding the volumetric heat capacity, as small discrepancies between the COMSOL model prediction and the laboratory test results led to large deviations in the found volumetric heat capacity value. For offshore testing, the sensitivity of the inversion method for the volumetric heat capacity value is undesirable. This is because offshore tests contain uncertainties that affect the test results, for example due to soil disturbance during testing, leading to an unreliable estimation of the thermal properties.

In order to improve the inversion method, the method was adapted to include an estimation of the volumetric heat capacity as an input of the method. For the laboratory tests, the volumetric heat capacity was estimated by the reference material tests. For offshore testing, the volumetric heat capacity can be estimated by CPT correlations proposed by Vardon and Peuchen (2020). It needs to be noted that both the reference material tests and the CPT correlations do not predict the volumetric heat capacity to a complete accuracy, as errors and uncertainties during measurement are unavoidable. However, the methods do give an estimation of the volumetric heat capacity of the materials.

The following three inversion methods that include an estimation of the volumetric heat capacity as an input were tested in the thesis:

- The inversion method with a fixed volumetric heat capacity value
- The inversion method with a fixed volumetric heat capacity value and an added thermal resistance of 0.001 $m^2K/W$ between the inner and outer cylinder of the heating element
- The regularized inversion method with a regularization constant of 0.2 and an added thermal resistance of 0.001 $m^2K/W$ between the inner and outer cylinder of the heating element

For the saturated sand, kaolin clay and water test results, the best agreement with the reference material test was found for the regularized inversion method with a regularization constant of 0.2 and an added thermal resistance of 0.001 $m^2K/W$ between the inner and outer cylinder of the heating element (maximum relative error compared to thermal needle probe results of 4.1%). For the moist sand test, the values found for this inversion method did not align with the results of the reference material tests. This could be caused by the non-uniformity of the material, for example by the water content being lower at the top of the material compared to deeper in the material.

A disadvantage of this inversion method is the influence of the estimated volumetric heat capacity on the inversion results, as for offshore soils a 0.1 $MJ/(m^3K)$ difference in the estimated volumetric heat capacity value resulted in a difference in the found thermal conductivity value of $\sim 1.5\%$. However, as the range of expected volumetric heat capacity values for offshore soils is relatively small, the method was still found to be reliable. An advantage of the inversion method is that already an excellent agreement with the saturated sand, kaolin clay and water reference material tests was found for a test duration of 600 seconds. This is significantly fast when compared to other in-situ tests to find the thermal conductivity of the soil.

The effects of the heating of the probe due to soil friction was examined. It was found that if the probe is heated by the soil fiction, accuracy of the method decreased. However, an initial waiting time and a higher heater power can be added to the method to increase the accuracy. No study is conducted that examines the amount temperature increase of the probe due to soil fiction. When more information is found on the heating of the probe, the test procedure can be adapted for this effect.

A study on the probing depth of the HF-CPT was performed by visually inspecting the isothermal heat contours of the COMSOL model. It was found that the probing depth increases for a larger testing duration. If a specific probing depth is required, this could limit the minimum test duration

of a HF-CPT test required. However, this study only gives a rough estimation of these values, and a more thorough analysis is needed to validate the results.

# 10. Conclusion

The main research question of the thesis was:

*What is a suitable method to interpret the thermal conductivity of offshore soils from heat flow cone penetration test data?*

In order to answer the main research question, three research questions were answered in the thesis. The first research question answered was:

*Which forward model is suitable for the interpretation of the heat flow cone penetration test data?*

No analytical solution was found that could accurately simulate the thermal response of the HF-CPT. Using a numerical solution, either by directly using a numerical model or by interpolation a single g-function from the numerical results, was deemed suitable, as a numerical COMSOL model developed in the thesis was able to simulate the thermal response of the HF-CPT to a reasonable accuracy. Constructing a single g-function from numerical analysis has proven to be difficult, as no suitable dimensionless parameters that could be used for the interpolation of the function were found. Therefore, a numerical forward model, constructed in COMSOL Multiphysics, was chosen as the forward model for the interpretation of the heat flow cone penetrometer data. This forward model was used in an inverse analysis to construct an inversion method.

The second research question was:

*Can the inversion method combined with the suitable forward model accurately predict the thermal properties of the materials used in laboratory tests with the heat flow cone penetration test?*

The inversion method to find both the volumetric heat capacity and thermal conductivity could not accurately predict the predict the thermal properties of the materials used in the laboratory tests. The method has proven to be sensitive in finding the correct volumetric heat capacity, with small discrepancies between the COMSOL model and the laboratory test results leading to large deviations in the found volumetric heat capacity value. The inversion method was improved by adapting the forward model and adding a regularization based on the estimated volumetric heat capacity value. The regularized inversion method with a regularization constant of 0.2 and an added thermal resistance of 0.001 $m^2K/W$ between the inner and outer cylinder of the heating element showed agreement with the reference material tests of the saturated sand, kaolin clay and water tests. For the moist sand test, the values found for this inversion method did not align with the results of the reference material tests. This could be caused by the non-uniformity of the material. The regularized inversion method with a regularization constant of 0.2 and an added thermal resistance of 0.001 $m^2K/W$ between the inner and outer cylinder of the heating element accurately predicted the thermal properties of the materials of the saturated sand, kaolin clay and water tests.

The third research question was:

*Which practical design conditions need to be addressed before the test procedure of an offshore heat flow cone penetration test can be determined?*

Two key design considerations were addressed in this paper. The heating of the probe due to soil friction and the probing depth of the test. It was found that if the probe is heated by the soil fiction, an initial waiting time and a higher heater power can be added to the method to increase the accuracy. It was also found that probing depth is dependent on the test duration, and if a specific probing depth is required, this might limit the minimum test duration. The offshore design procedure of the HF-CPT can further be detailed with information gained from field tests, specifically with information on the heating of the probe due to soil friction and the potential of a conducting a cooling test.

Considering these three research questions, the main research question is answered:

*Which method is suitable for the interpretation of the thermal conductivity of offshore soils from heat flow cone penetration test data?*

A suitable method to interpret the thermal conductivity of offshore soils from heat flow cone penetration test data is a direct data inversion, using a numerical forward model. A COMSOL Multiphysics model was constructed that simulated the thermal behaviour of the HF-CPT. This model was used in an inverse analysis to create a direct data inversion method. This method was validated with laboratory tests performed at the Delft University of Technology. For the regularized inversion method with a regularization constant of 0.2 and an added thermal resistance of 0.001 $m^2K/W$ between the inner and outer cylinder of the heating element, excellent agreement was found with the reference material tests of the saturated sand, kaolin clay and water tests. The method was able to find agreement for these tests for a test duration of at least 600 seconds. This is significantly fast when compared to other in-situ tests to find the thermal conductivity of the soil. For the moist sand tests, the values found for this inversion method did not align with the results of the reference material tests. This, however, could be caused by the non-uniformity of the material. The inversion method is suitable for offshore testing, as it has a short runtime and a low storage space. A first step in determining the offshore test procedure was taken by analysing the effect of the heating of the probe due to soil friction and the acquired probing depth of the test. The offshore design procedure of the HF-CPT can further be detailed with information gained from field tests, specifically with information on the heating of the probe due to soil friction and the potential of a conducting a cooling test. With the interpretation method presented in this thesis, the HF-CPT can become a successful new in-situ test to determine the thermal conductivity of offshore soils. This way, the thesis contributes to the implementation of geothermal energy solutions and offshore cable routes for wind farms.

# 11. Recommendations

## 11.1. Perform field tests

The laboratory tests performed with the HF-CPT were in a controlled environment and without penetrating the soil. In order to gain insight in the behaviour of the probe when it is in an uncontrolled and the HF-CPT does penetrate the soil, field tests can be performed. It can be examined whether the inversion method still performs well when the test is performed in an uncontrolled environment. When testing the HF-CPT in the field, information can also be gained on how much the probe heats up due to soil friction in different soil conditions. Next to this, it is possible to simulate a cooling test with pre-heating in the field, in order to examine the potential of this test procedure.

## 11.2. Improve forward model

The forward model can further be improved. The current COMSOL model already gives a relatively accurate prediction of the thermal behaviour of the HF-CPT. However, if a more accurate representation of the behaviour of the HF-CPT can be simulated with the model, the inversion method might find accurate results for a shorter test duration. To improve the COMSOL model, more detailed information is needed on the thermal behaviour of the HF-CPT. This information can be gained by conducting tests in materials where the thermal properties are known to a high amount of accuracy, similar to the water-agar tests. These test results can then be compared to the COMSOL results, and the COMSOL model can be adapted to more accurately predict the thermal behaviour of the HF-CPT.

## 11.3. Improve regularization

The regularization of the inversion method is currently based on the quadratic loss function. This function does not utilise the expected error of the estimated volumetric heat capacity measurement, but instead uses a empirically determined parameter of the regularization constant to determine the weight of the penalty. An error function that relates to the expected error distribution of the estimated volumetric heat capacity value can be added to the inversion method.

## 11.4. Analyse soil disturbance due to penetration

When the HF-CPT penetrates the soil, the soil around the cone disturbs. This affects the soil properties, including the density, stress state and porosity of the soil. A change in these parameters also affects the thermal properties of the soil. A study can be performed to gain insight in the disturbance of the soil due to penetration. A layer of disturbed soil can be modelled in COMSOL. This way, it is possible to examine the effects of the soil disturbance on the inversion method results.

## 11.5. Examine cooling tests

Adding a cooling to the test procedure might improve the results of the inversion method. When pre-heating the cone, a cooling test can also be performed instead of a heating test (Section 8.3.3). When adapting the forward model to model a cooling test, the same inversion method can be used to interpret the data. An analysis is needed to examine the possibility of using a cooling test. It is important to know if the inversion method still performs well for a cooling test, and if the test procedure can be improved by either adding a cooling test after a heating test, or only performing a cooling test.

## 11.6. Integral approach geo-data

The current interpretation method uses data gained from other geotechnical tests, namely the estimated volumetric heat capacity value correlated form CPT data. There is more potential of combining geo-data in order to further improve the interpretation method. It can be valuable to examine the possibilities to further integrate the available geological, geophysical and geotechnical data into the interpretation method to further improve the accuracy of the method.

# Bibliography


Akrouch, G. A., Briaud, J.-L., Sanchez, M., & Yilmaz, R. (2016). Thermal cone test to determine soil thermal properties. *Journal of Geotechnical and Geoenvironmental Engineering*, *142*, 04015085. https://doi.org/10.1061/(asce)gt.1943-5606.0001353

ASTM. (2014). D5334 14: Standard test method for determination of thermal conductivity of soil and soft rock by thermal needle probe procedure.

Bernier, M. (2001). Ground-coupled heat pump system simulation. *ASHRAE Transactions*, *107*, 605–616.

Berthet, K. (2019). The thermal cone penetration test potentials in soil investigation. *Master Thesis TU Delft*. Retrieved October 4, 2022, from https://repository.tudelft.nl/islandora/object/uuid%3A11fb392c-75db-4a61-9555-eccb8879b440

Carslaw, S., & Jaeger, J. C. (1959). *Conduction of heat in solids* (2nd ed.). Clarendon Press.

Cimmino, M., Bernier, M., & Adams, F. (2013). A contribution towards the determination of g-functions using the finite line source. *Applied Thermal Engineering*, *51*, 401–412. https://doi.org/10.1016/j.applthermaleng.2012.07.044

Cooper, M., Mikic, B., & Yovanovich, M. (1969). Thermal contact conductance. *International Journal of Heat and Mass Transfer*, *12*, 279–300. https://doi.org/10.1016/0017-9310(69)90011-8

de Vries, G. T., & Usbeck, R. (2018). The development of "push-heat", a combined CPT-testing/thermal conductivity measurement system. *Cone Penetration Testing 2018 – Hicks, Pisanò & Peuchen (Eds)*, 689–693.

Eskilson, P. (1987). *Thermal analysis of heat extraction boreholes*. Grahns Boktryckeri Ab.

Farouki, O. T. (1986). *Thermal properties of soils*. Trans Tech Publications.

Fugro. (2021). In situ thermal testing. *FNLM-GEO-APP-060*.

Hartmann, A., & Villinger, H. (2002). Inversion of marine heat flow measurements by expansion of the temperature decay function. *Geophysical Journal International*, *148*, 628–636. https://doi.org/10.1046/j.1365-246x.2002.01600.x

Hütter, E. S., & Kömle, N. I. (2012). Performance of thermal conductivity probes for planetary applications. *Geoscientific Instrumentation, Methods and Data Systems*, *1*, 53–75. https://doi.org/10.5194/gi-1-53-2012

Lines, S., Williams, D. J., & Galindo-Torres, S. A. (2017). Determination of thermal conductivity of soil using standard cone penetration test. *Energy Procedia*, *118*, 172–178. https://doi.org/10.1016/j.egypro.2017.07.036

Liu, X., Congress, S. S. C., Cai, G., Liu, L., Liu, S., Puppala, A. J., & Zhang, W. (2022). Development and validation of a method to predict the soil thermal conductivity using thermal piezocone penetration testing (T-CPTU). *Canadian Geotechnical Journal*, *59*, 510–525. https://doi.org/10.1139/cgj-2021-0034

Loveridge, F., & Powrie, W. (2013). Temperature response functions (g-functions) for single pile heat exchangers. *Energy*, *57*, 554–564. https://doi.org/10.1016/j.energy.2013.04.060

Maglic, K. D., Cezairliyan, A., & Peletsky, V. E. (1992). *Compendium of thermophysical property measurement methods / vol. 2, recommended measurement techniques and practices.* Plenum Press, Cop.

Man, Y., Yang, H., Diao, N., Liu, J., & Fang, Z. (2010). A new model and analytical solutions for borehole and pile ground heat exchangers. *International Journal of Heat and Mass Transfer*, *53*, 2593–2601. https://doi.org/10.1016/j.ijheatmasstransfer.2010.03.001

METER Group. (2018). Tempos manual.

METER Group. (2021). Tempos tech specs. *METER group [image]*. Retrieved October 11, 2022, from https://www.metergroup.com/en/meter-environment/products/tempos/tempos-tech-specs

Mo, P. Q., Gao, L., Yu, H. S., Tao, X. L., & Ma, Q. Z. (2022). Physical and numerical modelling of T-CPT for mechanisms of penetration and heat transfer. *Cone Penetration Testing 2022 – Gottardi & Tonni (eds)*, 577–583. https://doi.org/10.1201/9781003308829-83

Mo, P. Q., Ma, D. Y., Zhu, Q. Y., & Hu, Y. C. (2021). Interpretation of heating and cooling data from thermal cone penetration test using a 1D numerical model and a PSO algorithm. *Computers and Geotechnics*, *130*, 103908. https://doi.org/10.1016/j.compgeo.2020.103908

Mondal, S., Dangayach, S., & Singh, D. N. (2018). Establishing heat-transfer mechanisms in dry sands. *International Journal of Geomechanics*, *18*, 06017024. https://doi.org/10.1061/(asce)gm.1943-5622.0001083

Murali, M. (2015). Characterization of soft clays and the response of soil-foundation system for offshore applications. *Doctor of Philosophy Dissertation Texas A&M University*.

Rees, S. (2016). *Advances in ground-source heat pump systems*. Woodhead Publishing.

Shiozawa, S., & Campbell, G. S. (1990). Soil thermal conductivity. *Remote Sensing Reviews*, *5*, 301–310. https://doi.org/10.1080/02757259009532137

Vardon, P. J., & Peuchen, J. (2020). CPT correlations for thermal properties of soils. *Acta Geotechnica*, *16*, 635–646. https://doi.org/10.1007/s11440-020-01027-2

Vardon, P. J., Baltoukas, D., & Peuchen, J. (2018). Thermal cone penetration test (T-CPT). *Cone Penetration Testing 2018 – Hicks, Pisanò & Peuchen (Eds)*, 649–655.

Vardon, P. J., Baltoukas, D., & Peuchen, J. (2019). Interpreting and validating the thermal cone penetration test (T-CPT). *Géotechnique*, *69*, 580–592. https://doi.org/10.1680/jgeot.17.p.214

Zhang, N., & Wang, Z. (2017). Review of soil thermal conductivity and predictive models. *International Journal of Thermal Sciences*, *117*, 172–183. https://doi.org/10.1016/j.ijthermalsci.2017.03.013

# A. Cast dimensions laboratory tests

An analysis on the influence of the cast size on the laboratory tests is performed. This is needed to ensure no boundary effects due to the cast size affect the tests results. Before performing the analysis, the thermal properties of the reference materials were estimated based on literature and experience with previous tests (Table A.1).

Table A.1.: First estimation of the thermal properties of the reference materials.

| Soil type | Thermal conductivity [W/(mK)] | Volumetric heat capacity [J/(m$^3$K)] |
|---|---|---|
| Moist sand | 0.8 | 1.15*10$^6$ |
| Saturated sand | 2.1 | 2.75*10$^6$ |
| Kaolin Clay | 1.6 | 2.86*10$^6$ |
| Water | 0.6 | 4.14*10$^6$ |

In order to examine the effect of the cast size on the laboratory tests, a COMSOL analysis was performed. In this analysis, two different COMSOL models of the HF-CPT were tested. One model has boundaries that are sufficiently far from the probe to ensure no boundary effects are present. The other COMSOL model has its boundaries set to the cast size dimensions. The results of both these models for the four reference materials, using the estimation of thermal properties described in Table A.1, are shown in Figure A.1. It is shown in this figure that no boundary effects were be found in the COMSOL model with the cast dimension boundaries, as the two COMSOL simulations align perfectly. This indicates that the cast size did not influence the measured results with the test probe.

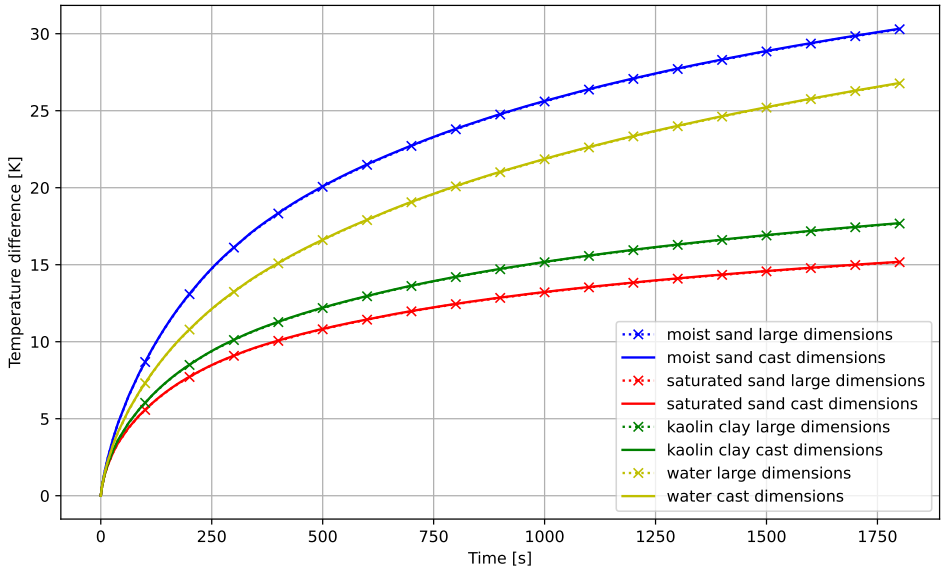


Figure A.1.: Results of two COMSOL models run with the estimated thermal properties of the reference materials (Table A.1). The first model (dotted line with crosses) has boundaries that are sufficiently far from the probe to ensure no boundary effect are present, the second model (solid lines) has boundaries set to the cast dimensions.

# B. Sensitivity analysis preliminary COMSOL model

In order to improve the optimise the preliminary COMSOL model runtime, a sensitivity analysis is performed.

## B.1. Absolute tolerance

The absolute tolerance of the COMSOL model controls the acceptable error of each integration step. For a larger absolute tolerance, the model needs less calculation steps to run the simulation and thus has a faster runtime. A study is conducted on what the maximum absolute tolerance is of the model without influencing the results. For this study, the COMSOL simulation is run multiple times with an range of different absolute tolerance values. Changes are already found from a tight tolerance of 0.001 compared to an extreme tight tolerance of 0.00001 (figure B.1). Because of this, the tolerance of the COMSOL model is set to the absolute tolerance of 0.00001.

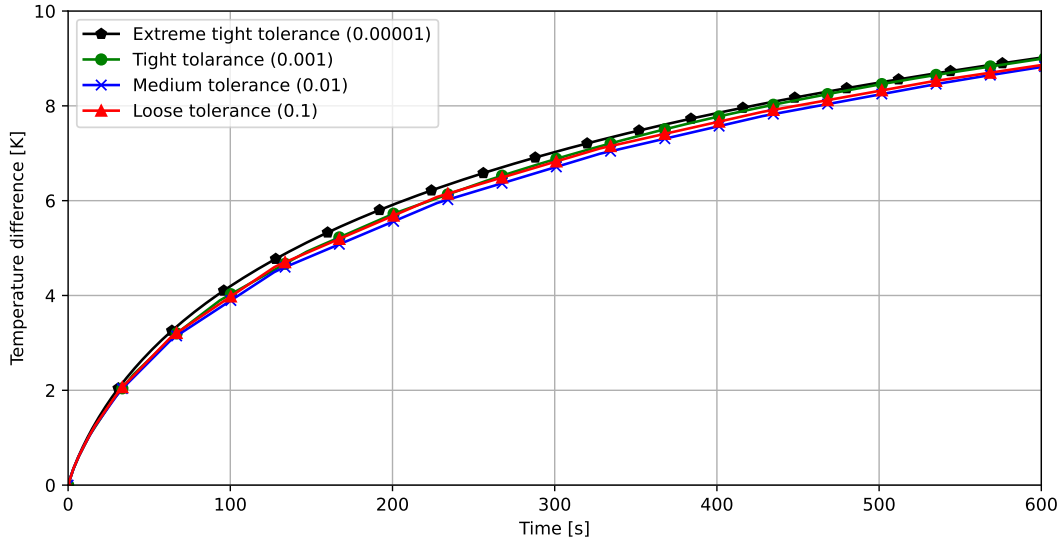


Figure B.1.: Preliminary COMSOL model run with various absolute tolerance values.

## B.2. Mesh size

The amount of elements that the model has influences the accuracy of the model. A higher amount of elements will result in a more accurate result, but will also increase the runtime. Therefore it is desirable that the lowest amount of elements is used, while still maintaining a high accuracy. In order to achieve this, a study is conducted to examine the influence of changing the mesh size. With a 'Normal' mesh of 3031 domain elements, the least amount of elements is found while still keeping the model accurate (figure B.2).

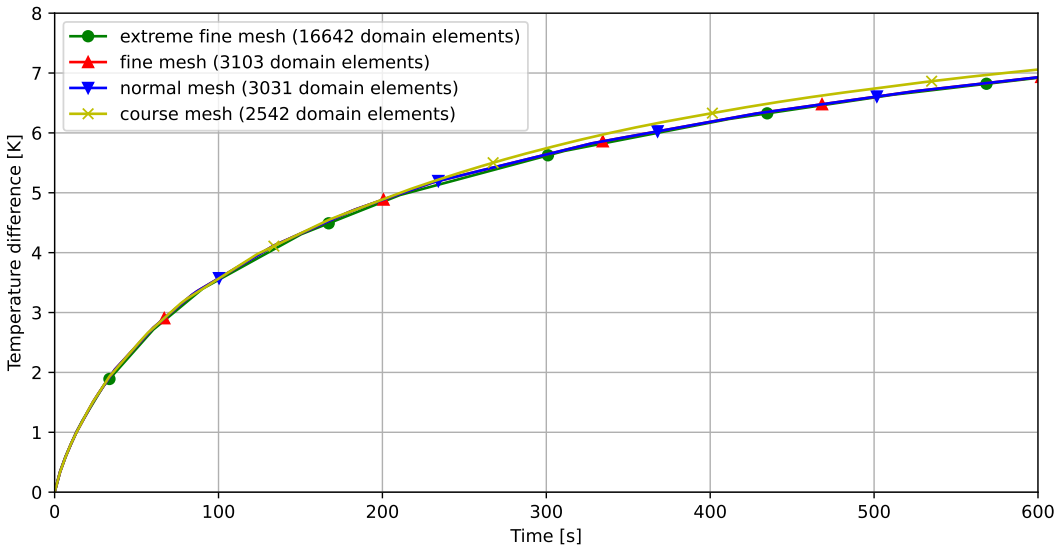


Figure B.2.: Preliminary COMSOL model run with various mesh sizes.

# C. Figures interpretation heat flow cone penetration test results

## C.1. Inversion results fixed volumetric heat capacity value (section 7.3.5)

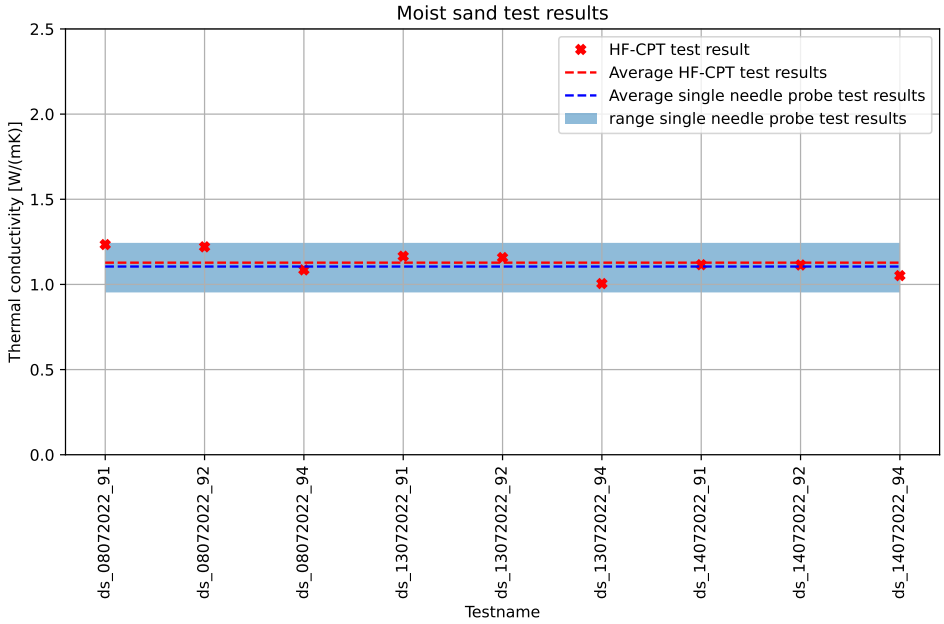


Figure C.1.: Inversion method results of the moist sand tests compared to the results of the in situ single thermal needle probe laboratory tests.

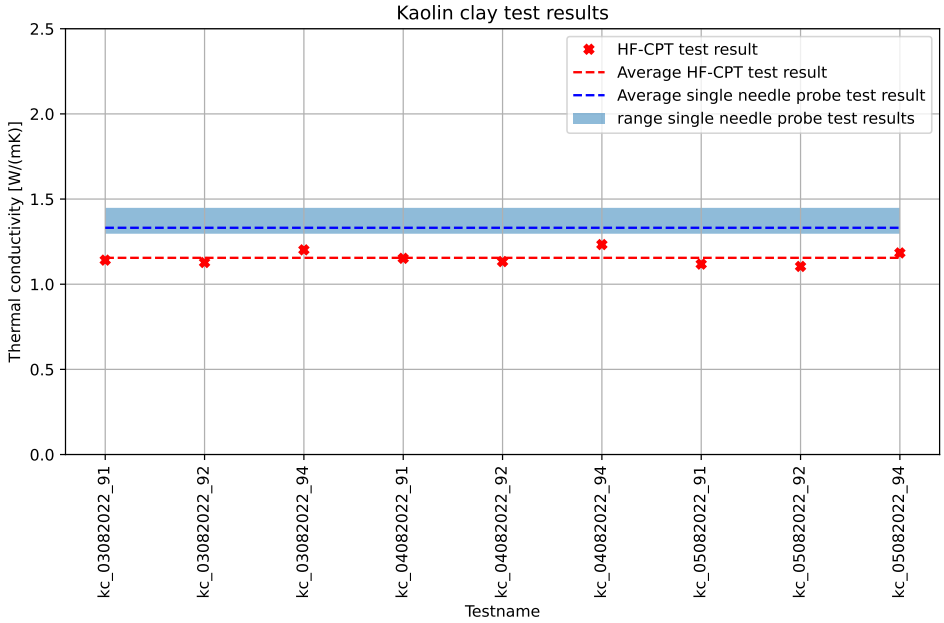


Figure C.2.: Inversion method results of the kaolin clay tests compared to the results of the in situ single thermal needle probe laboratory tests.

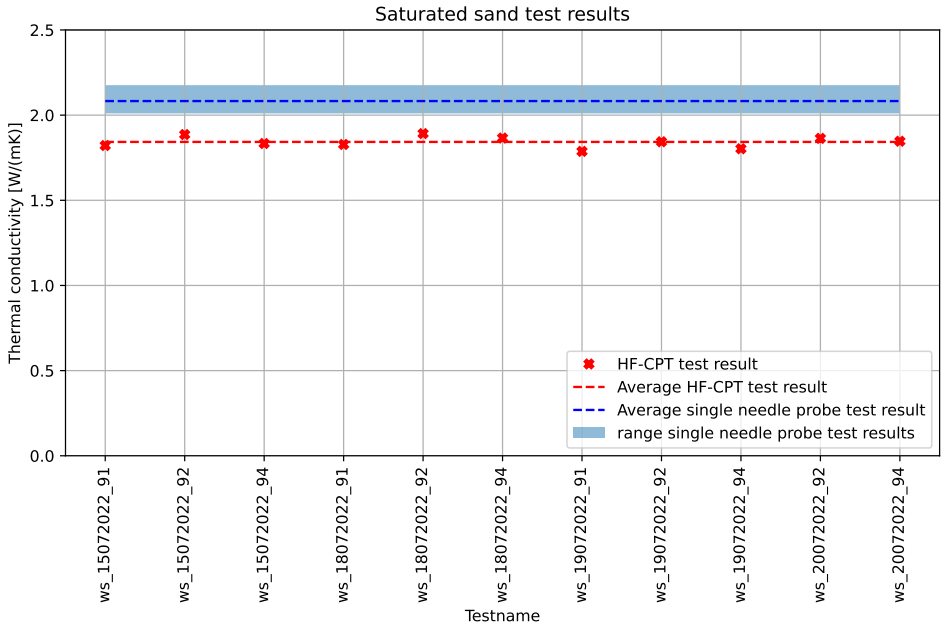


Figure C.3.: Inversion method results of the saturated sand tests compared to the results of the in situ single thermal needle probe laboratory tests.

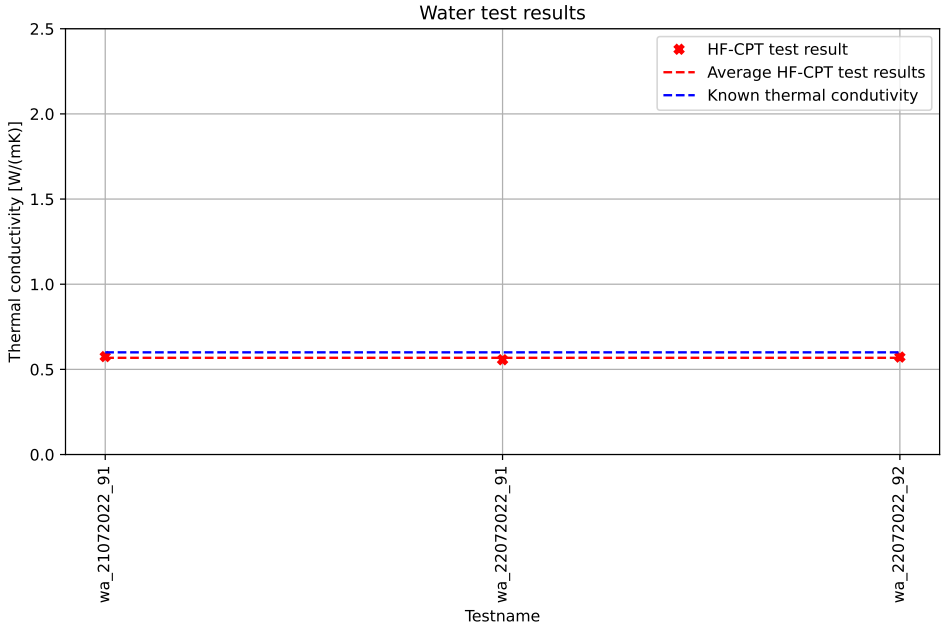


Figure C.4.: Inversion method results of the water tests compared to the results of the in situ single thermal needle probe laboratory tests.

## C.2. Inversion results fixed the volumetric heat capacity value and an added thermal resistance of 0.0001 $m^2K/W$ (section 7.3.6)

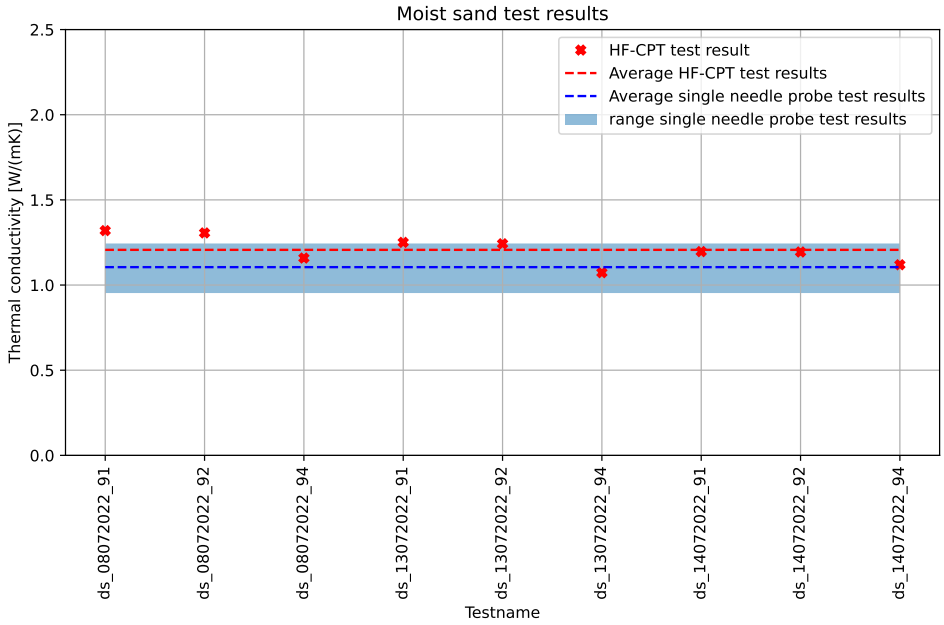


Figure C.5.: Inversion method results of the moist sand tests compared to the results of the in situ single thermal needle probe laboratory tests, the COMSOL simulation has an added thermal resistance of 0.0001 $m^2K/W$ between the inner and outer cylinder.

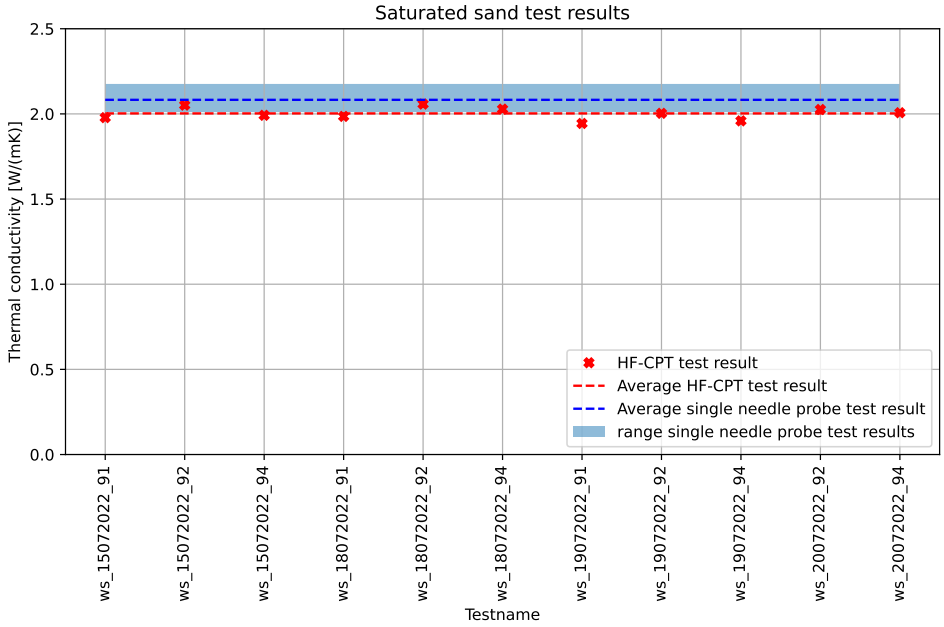


Figure C.6.: Inversion method results of the saturated sand tests compared to the results of the in situ single thermal needle probe laboratory tests, the COMSOL simulation has an added thermal resistance of 0.0001 $m^2K/W$ between the inner and outer cylinder.

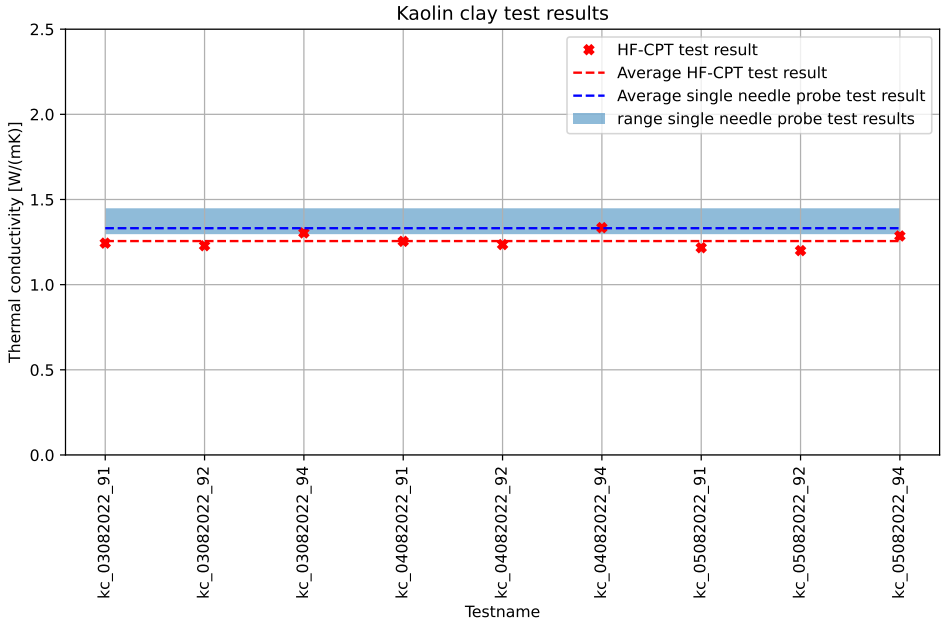


Figure C.7.: Inversion method results of the kaolin clay tests compared to the results of the in situ single thermal needle probe laboratory tests, the COMSOL simulation has an added thermal resistance of 0.0001 $m^2K/W$ between the inner and outer cylinder.

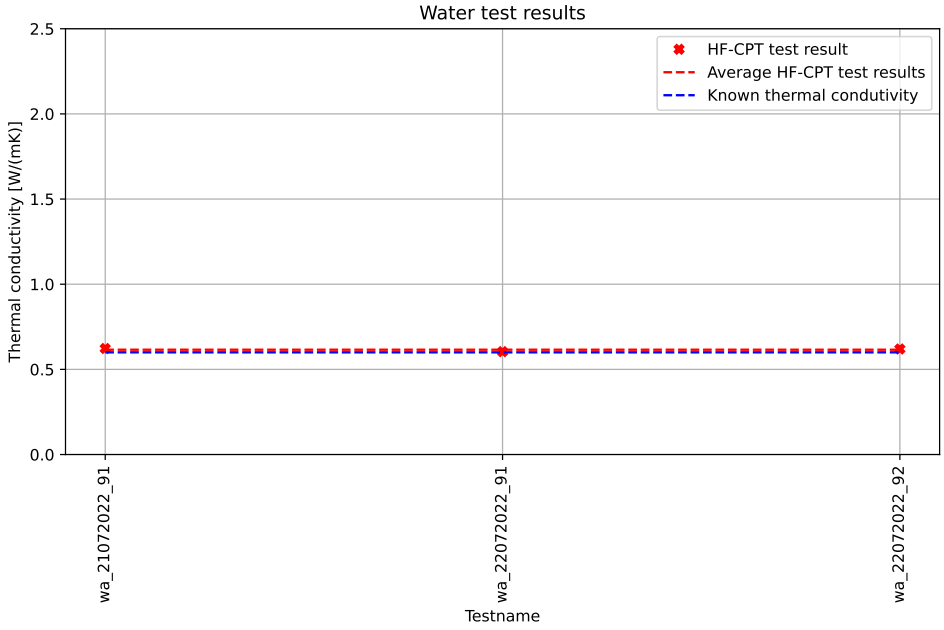


Figure C.8.: Inversion method results of the water tests compared to the results of the in situ single thermal needle probe laboratory tests, the COMSOL simulation has an added thermal resistance of 0.0001 $m^2K/W$ between the inner and outer cylinder.

## C.3. Regularized inversion results with a regularization constant of 0.2 and an added thermal resistance of 0.0001 $m^2K/W$ (section 7.3.7)

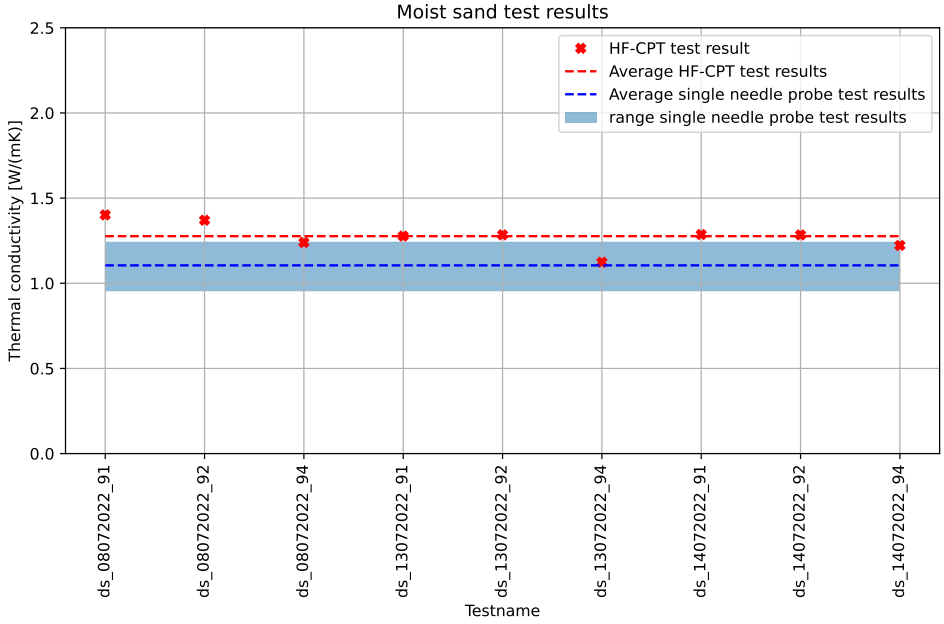


Figure C.9.: Inversion method results of the moist sand tests compared to the results of the in situ single thermal needle probe laboratory tests. The COMSOL simulation has an added thermal resistance of 0.0001 $m^2K/W$ between the inner and outer cylinder. The inversion method has an added penalty function for the estimated volumetric heat capacity with a regularization constant of 0.2.

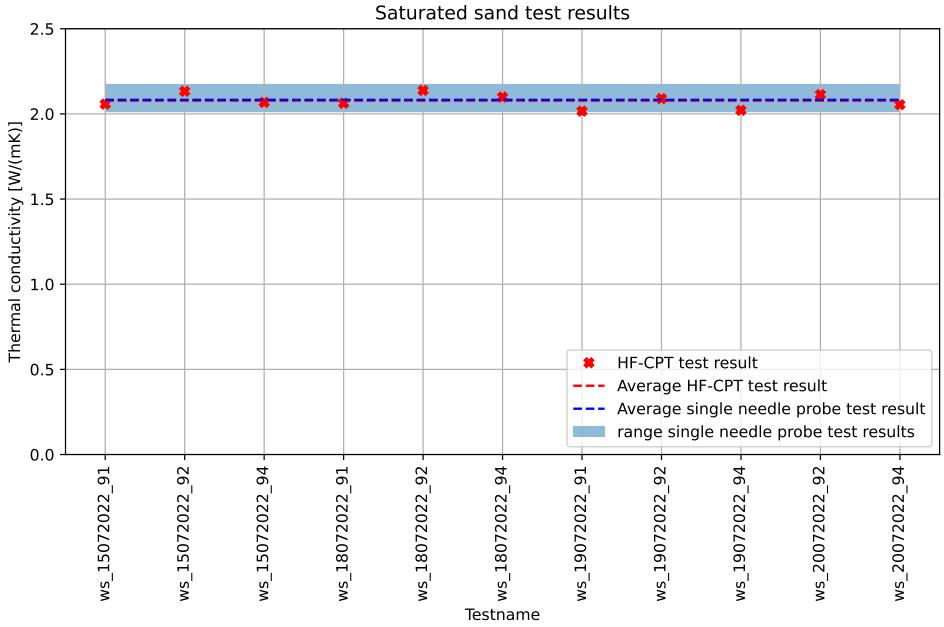


Figure C.10.: Inversion method results of the saturated sand tests compared to the results of the in situ single thermal needle probe laboratory tests. The COMSOL simulation has an added thermal resistance of 0.0001 $m^2K/W$ between the inner and outer cylinder. The inversion method has an added penalty function for the estimated volumetric heat capacity with a regularization constant of 0.2.

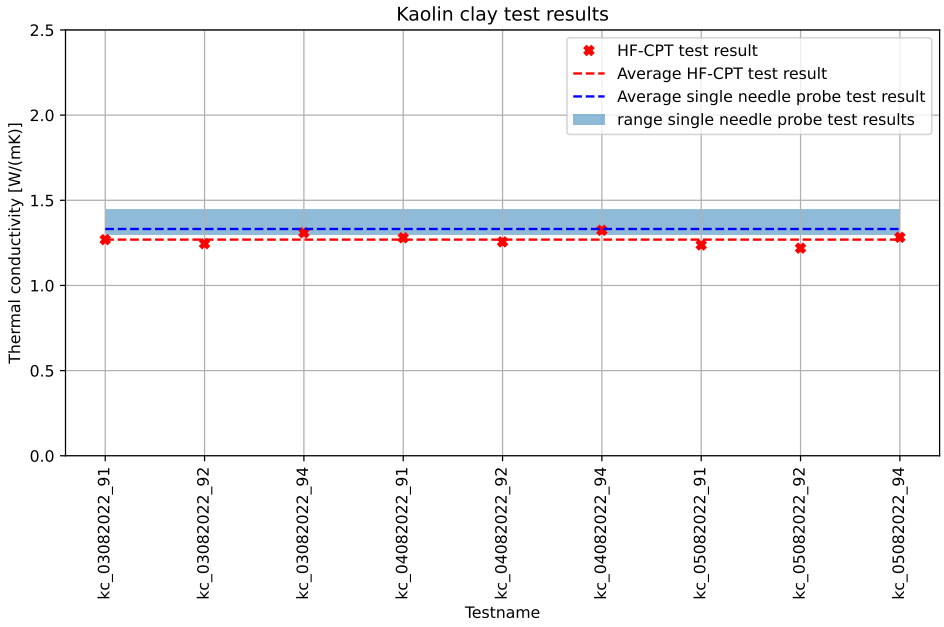


Figure C.11.: Inversion method results of the kaolin clay tests compared to the results of the in situ single thermal needle probe laboratory tests. The COMSOL simulation has an added thermal resistance of 0.0001 $m^2K/W$ between the inner and outer cylinder. The inversion method has an added penalty function for the estimated volumetric heat capacity with a regularization constant of 0.2.

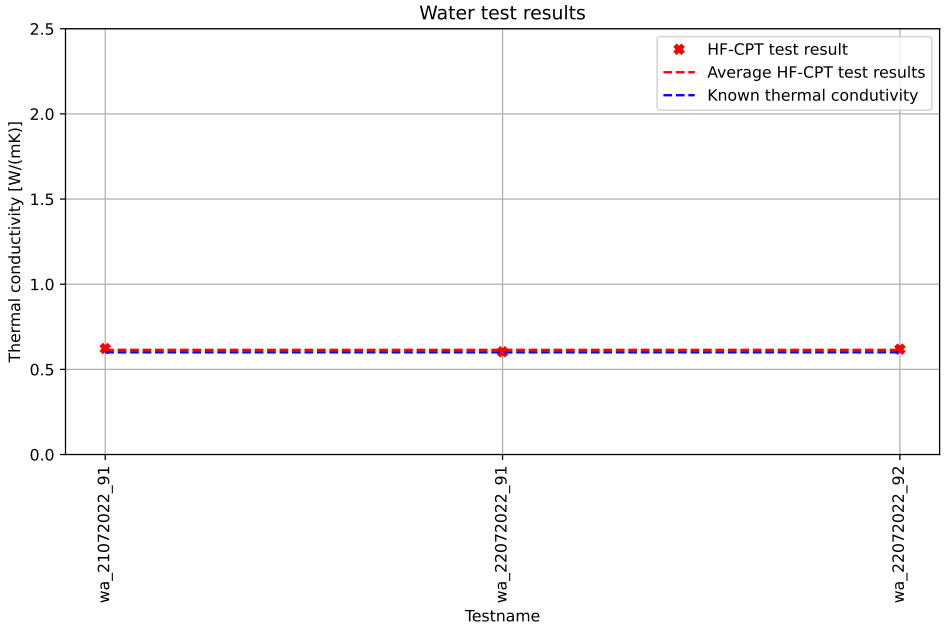


Figure C.12.: Inversion method results of the water tests compared to the results of the in situ single thermal needle probe laboratory tests. The COMSOL simulation has an added thermal resistance of 0.0001 $m^2K/W$ between the inner and outer cylinder. The inversion method has an added penalty function for the estimated volumetric heat capacity with a regularization constant of 0.2.

# D. Figures probe heating parametric study

## D.1. No initial cooling period, heater power level of 20 W

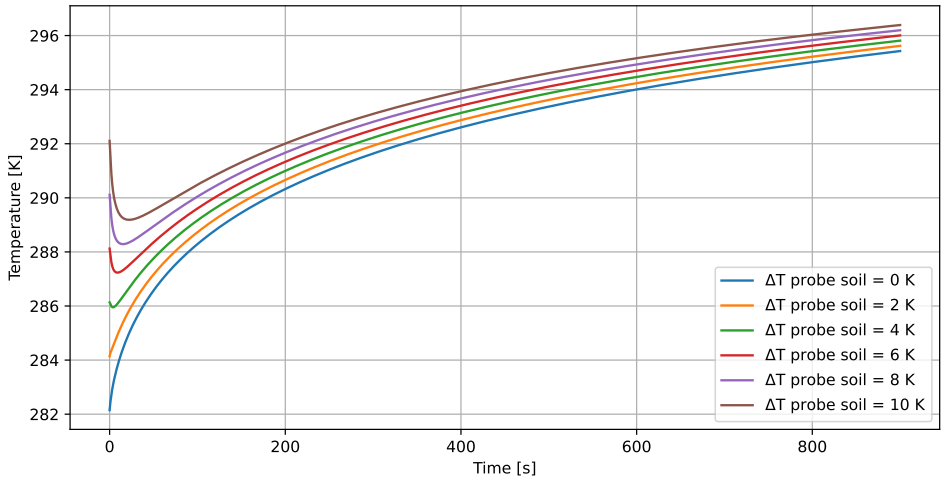


Figure D.1.: Time (x-axis) over temperature (y-axis) found by the COMSOL model with a temperature difference between the probe and the soil of 0 to 10 K. The probe has a higher temperature than the soil. The thermal properties of the soil represent the expected thermal properties of saturated sand. The heater power level is 20 W.

## D.2. 300 second initial cooling period, heater power level of 20 W

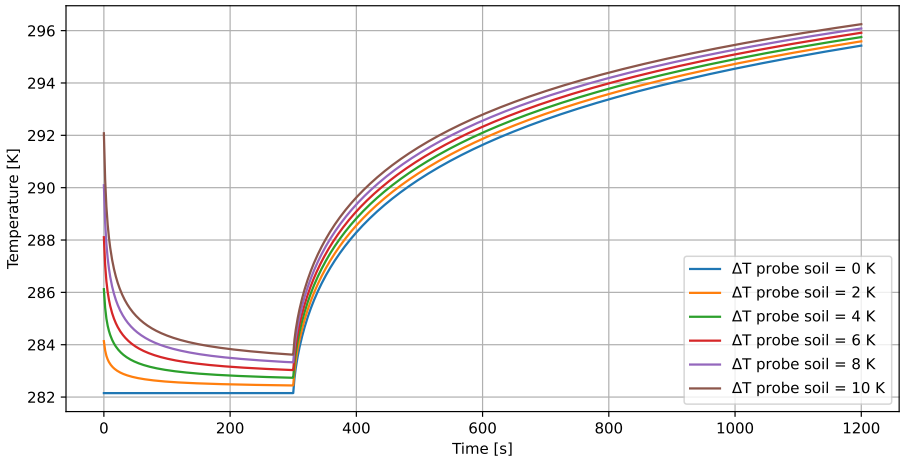


(a) Temperature (x-axis) over time (y-axis) for the complete test duration.

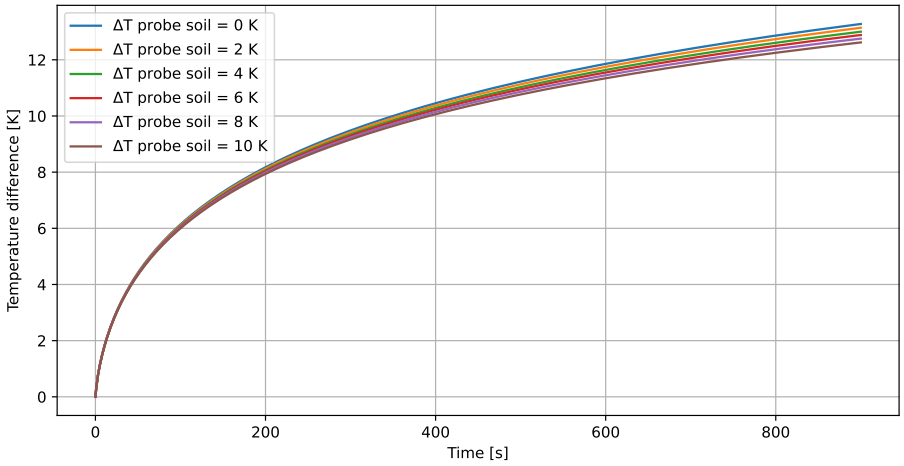


(b) Temperature difference (x-axis) over time (y-axis) from the start of the heating.

Figure D.2.: Results found by the COMSOL model with a temperature difference between the probe and the soil of 0 to 10 K. The probe has a higher temperature than the soil. A initial cooling period of 300 seconds is taken before the probe is heated. The thermal properties of the soil represent the expected thermal properties of saturated sand. The heater power level is 20 W.